# GROWTH, STRUCTURE AND PREDICTION OF THE THERMAL INTERNAL BOUNDARY LAYER

A.C.COMRIE



Dissertation submitted in fulfilment of the requirements towards the Degree of Master of Science in the Department of Environmental and Geographical Science University of Cape Town

1988

This is to declare that this dissertation has not been previously submitted for a degree at any University.

# ABSTRACT

The Thermal Internal Boundary Layer (TIBL) is a dynamic and turbulent mesoscale feature of the coastal atmosphere that forms over the land during conditions of onshore flow. The TIBL develops as an adjustment of the atmospheric boundary layer to the discontinuities of temperature and roughness that occur at the interface between the underlying marine and terrestrial surfaces. The resulting formation of a characteristically convex mixed layer below relatively stable air aloft has serious implications for the dispersion of pollutants in shoreline environments. Although a wide range of research relating to various features of the TIBL may be found in the literature, relatively few broadly-based studies have been performed. This study has employed both airborne and surface measurements to obtain a comprehensive spatial and temporal data set, in order to elucidate aspects of the characteristic structure and behaviour of the TIBL.

TIBL growth was found to follow a diurnal pattern, the initially irregular boundary becoming more uniform during the day as a steady balance between various factors was achieved. The TIBL was associated with a layer of uniform wind speed and direction flowing perpendicular to the coastline, within which warmer temperatures and changes in relative humidity and moisture content were observed. The temperature structure of the onshore flow strongly influenced the intensity of turbulence encountered in the TIBL and the degree of entrainment aloft. Patterns of turbulent properties displayed significant increases in the TIBL, which were relatively abrupt near the surface and more gradual towards the top of the TIBL. Measurements of sensible heat flux revealed strong undulations in TIBL structure due to transitory eddies and thermal upcurrents. Certain theoretically based predictive equations of TIBL height displayed the best overall performance out of eight selected models, and some promise was shown by an empirical formulation. TIBL development was generally complex and irregular within the first few kilometres of the shore, while further inland more regular TIBL formation enabled the relatively accurate observation and prediction of TIBL height.

# CONTENTS

# LIST OF FIGURES

## CHAPTER 1



## CHAPTER 2

CHAPTER 3

## CHAPTER 4

## CHAPTER 5

## CHAPTER 6

# LIST OF TABLES

## CHAPTER 2



## CHAPTER 3



## CHAPTER 4

# ACKNOWLEDGEMENTS

A research project of this nature requires the help of a great many people to be successful, and I am most grateful for the valuable assistance provided by all those who contributed to the research program. I am particularly indebted to the following people for their whole-hearted cooperation and generous help in making this project possible:

- Dr. Cecil Keen for the invaluable guidance, advice and encouragement he has given me as supervisor and mentor. I am most thankful for his help during the inception, experimental stages and final writing of this thesis, both initially from close at hand and later via numerous long-distance telephone calls between here and the USA;

- Bruce Hewitson the project technician, for the design, production and testing of the aircraft instrumentation, and for his friendly advice and much spare time helping with hardware and software required during the project;

- Frikkie Potgieter and his staff at the Koeberg Weather Station for their help with various aspects of the data acquisition and aircraft calibration;

- Theo Stofberg for his help and the use of his farm *Vaatjie* as a base for the acoustic sounder, meteorological tower, surface measurements, pibal tracking and aircraft flyovers;

- Pilots Del Colussi and Andries Van Dijk of Fisantekraal Air Services for their willingness to take off at a moments notice, and for their skilful flying of *ZS-CML*;

- The field staff for all their hard work:
  - Clive Heydenrych and Paul Lee for their help in mobilising the SODAR during the pilot study;

- Kevin Levey, Sandy Hustwick, Peter Cox, Cathy Oelofse, Garth Spencer-Smith, David Rogers, Greg Sneddon and Mary George for pibal tracking and surface data collection;

- Mr. D. Brider, security officer at Koeberg Nuclear Power station, who was the liason for flight clearance. Also the Head of Security Mr. Bob Howard and the Power Station Manager Mr. B. Oaten for initial clearance of the research flights;

- Dr. Tony Surridge of the CSIR Atmospheric Sciences Division, Dr. Anton Eberhardt of the UCT Energy Research Institute and George Davis of the UCT Botanical Research Unit, for their respective loans of the acoustic sounder, field data logger and the memory module reader;

- The Foundation for Research Development, CSIR, for funding the research project *NPWCAR-GBE 1* and providing a Masters degree bursary for the first year of this project;

- Finally, to my fiancée Lee, for her ever present support, advice and encouragement. I am deeply appreciative of all the many hours of discussion and help invested over the last two years.

Andrew Comrie

Cape Town, February 1988.

CHAPTER 1

# THESIS INTRODUCTION

## INTRODUCTION

Coastal regions possess an environment that is not only conducive to the evolution of complex atmospheric dispersion conditions, but that is also optimal for the location of urban and industrial centres. Shoreline environments such as open coastlines or lakeshore areas offer easy access to transportation facilities and supplies of cooling water, and major industrial complexes are therefore frequently situated within these areas. Industries of this nature typically include oil terminals, chemical and mineral processing plants, manufacturing industries, fossil fuel power stations and nuclear reactors.

The growth and development of these activities has led to an increase in the number of air pollution sources located in the coastal zone, and large quantities of airborne effluent may at times be emitted into the atmosphere. The deterioration of coastal air quality has thus become a cause for concern, especially under conditions of fair weather. In these circumstances unfavourable diffusion conditions may occur over the land, either during stable onshore gradient flows or in the presence of mesoscale effects such as the sea breeze. In both cases a reduction in air quality is associated with the formation of a complex meteorological phenomenon, the Thermal Internal Boundary Layer.



## BOUNDARY LAYER FORMATION

In studies of fluid dynamics, the boundary layer is defined as the region of a flow in which the effects of its boundaries are experienced. The atmospheric boundary layer is hence that region of the lower atmosphere which is influenced by the thermal and frictional effects of the earth's surface. The depth of the this layer typically varies from a few tens of metres on calm, clear nights to a few thousand metres on hot, sunny days just after noon.

An airflow that has travelled over a relatively homogeneous area will, after some time, display meteorological characteristics that have reached a dynamic equilibrium with the underlying surface. However, if the airflow passes over another surface with different properties, the change in the underlying conditions will result in an adjustment to the flow from the surface upwards, and a new set of equilibrium characteristics will eventually develop. This transition does not occur immediately at all heights, but instead takes place gradually in the form of a layer that grows upwards from the point of surface discontinuity. The upper limit of this new boundary layer may be regarded as a surface dividing the lower atmosphere into two zones of distinctly different meteorological characteristics, the lower one being termed the internal boundary layer (IBL).

IBLs are commonly formed wherever sharp changes in surface roughness or surface temperature occur (Figures 1a & 1b). Perhaps the most striking example of this is found during onshore flow in coastal regions, where the cool and aerodynamically smooth water surface interfaces the warmer, rougher land surface. The change in surface shear stress at the coast constitutes a frictional discontinuity, which induces a roughness IBL downwind. Similarly the temperature discontinuity causes a change in surface heat flux, and a free convective IBL develops over the land. Under stable onshore conditions, IBL formation tends to be dominated by the stronger thermal effects, giving rise to the development of a special type of IBL. This well mixed, turbulent region of the coastal atmosphere is thus termed the Thermal Internal Boundary Layer, frequently referred to by the acronym TIBL (Figure 1c).

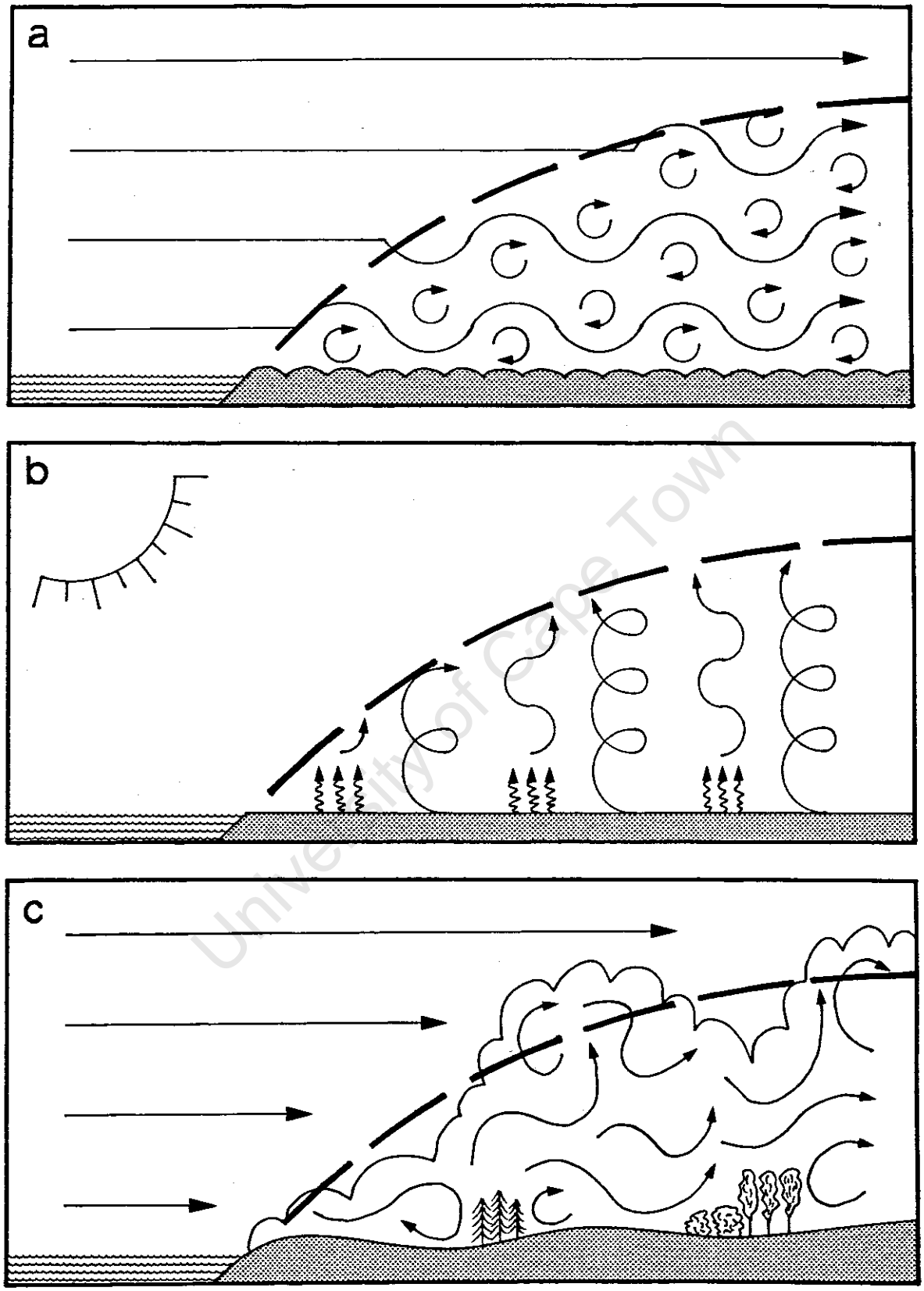




**Figure 1:** Schematic of the effects of (a) surface roughness and (b) surface temperature on the development of the TIBL (c).

## TIBL GROWTH AND FUMIGATION

The TIBL is an important and characteristic feature of the atmospheric environment in coastal regions. TIBL formation typically starts at the coastal interface, developing upwards in the direction of flow. The adjustment of the atmosphere to new surface conditions over the land takes place most rapidly near the shoreline, becoming more gradual further downwind. The TIBL is thus characterised by a convex upper boundary with a relatively steep initial slope nearer the coast, and a more shallow slope further inland.

The rate at which the height of the TIBL increases with distance from the coast is dependent on the properties of the downwind surface, and on the original characteristics of the onshore flow. Increased physical roughness together with thermal conduction and convection over the land generate mechanical and thermal turbulence that promote the growth of the TIBL. With passage inland, the relatively stable onshore flow is eroded from below and a mixed layer of modified air evolves near the surface. The unmodified air that remains above forms a stable inversion layer that caps the TIBL.

The location of two entirely different dispersion regimes adjacent to each other can place severe limitations on the vertical diffusion of pollutants near the coast, compared to neighbouring areas inland. Airborne effluent emitted near the surface within the TIBL is contained below the overlying stable layer, in a process known as plume trapping (Figure 2). Pollutant plumes may also be emitted at higher levels above the TIBL. In this case a relatively undispersed emission can be carried a considerable distance downwind in the stable air aloft, until it intersects the TIBL interface. At this point it is entrained and fumigates downwards, also becoming trapped in the TIBL (Figure 2). This process of continuous fumigation may occur at irregular intervals for extended periods of time, as the plume engages or becomes detached from the TIBL. As horizontal scales are

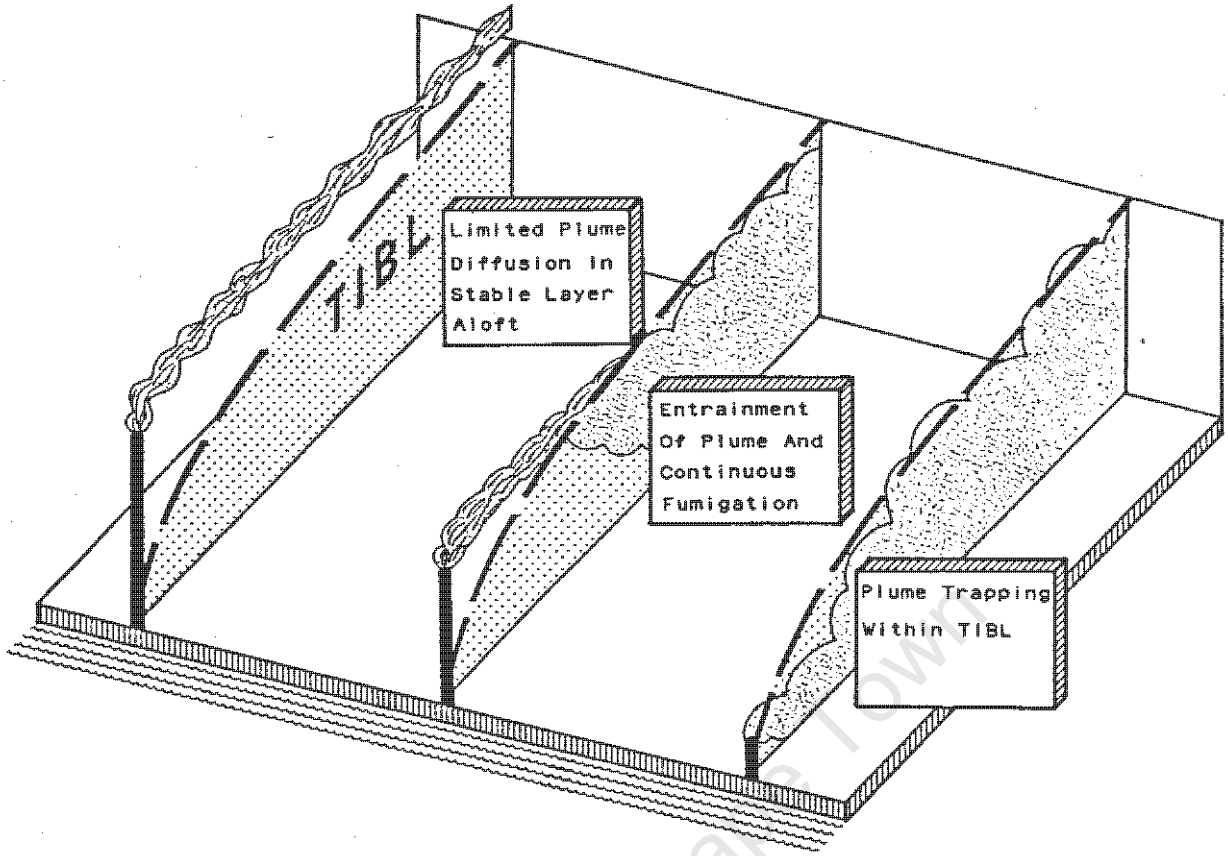


Figure 2: Coastal dispersion characteristics in the presence of the TIBL.



of the order of kilometres, and TIBL height only a few hundred metres, relatively small changes in the latter can have an appreciable effect on the location of the fumigation zone. Both elevated and ground level concentrations downwind may therefore be many times greater than in the absence of the TIBL.

## OVERVIEW OF TIBL RESEARCH

### EARLY STUDIES

The existence of the TIBL was first identified in the early literature on studies of the atmospheric internal boundary layer., Ogura (1950) and Elliot (1958) provided a theoretical

basis for the development of a convex internal boundary layer from a change in surface temperature, and presented a small number of measurements confirming this behaviour. The formation of internal boundary layers in shoreline environments was initially examined with regard to atmospheric transport and diffusion in coastal regimes by Prophet (1961), and Van der Hoven (1967) who provided an early empirically based model of TIBL height.

## COASTAL DIFFUSION

The importance of the TIBL was recognised in much of the ensuing measurement and modelling of coastal diffusion in the presence of the lake or sea breeze. The impact of stack height on fumigation conditions during these conditions was examined in a number of studies (Bierly and Hewson, 1962; Hewson and Olsson, 1967; Collins, 1971; Lyons and Olsson, 1972). Lyons and Cole (1973) investigated plume trapping and fumigation of sulphur dioxide and particulate emissions in stable onshore flows off Lake Michigan, and found serious degradation of air quality for both phenomena. Meroney *et al* (1975) modelled shoreline atmospheric transport in the laboratory, using a meteorological wind tunnel. It was found that, although emissions from short stacks caused the worst fumigation, an increase in stack height did not result in greatly reduced ground level concentrations. Later studies continued to concentrate on the effects of TIBL fumigation and dispersion (Knox and Lyons, 1975; Dooley, 1976), a number of which also included early theoretical equations of TIBL height (Weisman and Hirt, 1975; Peters, 1975; Van Dop *et al*, 1979). Lyons (1975) synthesised much of the knowledge at the time in a monograph on pollutant diffusion in shoreline environments. The TIBL was also parameterized in models of the sea breeze circulation (Pielke, 1974; Anthes, 1978).

## FIELD EXPERIMENTS

More recently a number of large scale field studies of the coastal atmosphere have been performed. These investigations employed substantial resources to perform comprehensive measurements of the TIBL. At Brookhaven, Long Island in the United States, Raynor *et al* (1979) collected airborne and surface data on the turbulence, temperature patterns and slope of the TIBL. Measured levels of turbulence and temperature were several times higher in the TIBL, with the initial steep growth of the TIBL modulated by atmospheric stability. An equilibrium height was found in many cases, which merged into the inland mixed layer during free convection, and which was absent during the sea breeze. At Nanticoke, Lake Erie in Canada, measurements of onshore flow structure and boundary layer formation were made using acoustic sounders, free and tethered sonde systems and surface instruments (Portelli, 1982; Kerman *et al*, 1982). Two types of internal boundary layer were detected, one adjusting to contrasts in bulk buoyancy and hence entrainment growth, and the other to upward heat flux into the onshore flow. The latter type was more significant in defining the location and magnitude of maximum ground level concentrations during continuous fumigation. Gamo *et al* (1982) also made airborne measurements of the TIBL. Data on turbulence, temperature, humidity and calculated parameters were collected 100Km to the east of Tokyo, Japan over Kashimaura beach. Different internal boundary layers were also detected in this study, with the TIBL determined by turbulence roughly 1.5 times higher than that by temperature. This difference was attributed to the entrainment of plumes into the overlying marine air, the stability of which strongly influenced TIBL height and the potential temperature increase within the TIBL.

## TURBULENCE

Examinations of the more detailed turbulent structure of the

TIBL took place concurrently with the studies of shoreline diffusion and TIBL structure outlined above. The vast bulk of knowledge relating to boundary layer turbulence parameters has been accumulated from theoretical and empirical studies of turbulence in the Planetary or Convective Boundary Layer (PBL or CBL). There have been many studies covering all aspects of the CBL, including inversion height, convection, similarity, and budgets of mixed layer properties (Ball, 1960; Lilly, 1968; Wyngaard *et al*, 1971; Betts, 1973; Carson, 1973). A general exposition of these processes was contained in a review paper by Tennekes (1974). Later studies made closer examinations of turbulence parameter structure and entrainment (Kaimal *et al*, 1976; Stull, 1976; Caughey and Palmer, 1979; Tennekes and Driedonks, 1981). Important findings have also been obtained via laboratory study and numerical modelling (Deardorff *et al*, 1969; Deardorff, 1972). Studies of the boundary layer over the sea have also been performed (Nicholls and Readings, 1979), and more recently have included the development of the 'reverse' TIBL with the formation of the surface stable layer over the sea during offshore flow (Hsu, 1983; Garratt, 1987).

Theoretical studies of detailed turbulence specifically for the TIBL have been largely numerical in nature, concentrating on the effects of a change in surface roughness on turbulent boundary layer formation (Peterson, 1969; Taylor, 1970; Shir, 1972; Rao *et al*, 1974). Although basic turbulence measurements were made by aircraft for the larger field studies at Brookhaven and Kashimaura (*ibid.*), the majority of detailed turbulence measurements for the TIBL have been made at a relatively low level fairly close to the shore, and not covering the whole TIBL at the mesoscale. The most common method of data collection has been by means of one or more instrumented towers located a few kilometres, or in some cases a few hundred metres, from the shore (Echols and Wagner, 1972; Smedman and Hogstrom,

1983; Ogawa and Ohara, 1985; Ohara and Ogawa, 1985). A slightly larger scale examination of turbulence during lake breeze penetration was performed by Ogawa *et al* (1985), who employed a kytoon-mounted instrument package up to a height of 600m at a site 3km from the shore.

### MODELLING

A further facet of TIBL research has involved the incorporation of a range of input parameters into specialised equations, in order to accurately predict the height of the TIBL. Certain of these formulae were developed in some of the diffusion studies outlined earlier, while others were derived from a more theoretical basis (Van der Hoven, 1967; Moroz, 1967; Plate, 1971; Raynor *et al*, 1975; Schuh, 1975; Peters, 1975; Weisman, 1976; Venkatram, 1977 & 1986; Misra, 1980; Steyn and Oke, 1982; Kerman, 1982; Misra and Onlock, 1982; Lyons *et al*, 1983; Gamo *et al*, 1983; Hsu, 1986). Although only a limited number of independent evaluations of these models have been performed, it would appear that the more advanced theoretical models show the most promise (Di Vecchio *et al*, 1976; Stunder and SethuRaman, 1985).

## EXPERIMENTAL APPROACH

### BACKGROUND

The growth of industrial activity in coastal regions, coupled with the complex diffusion meteorology of such areas, has created the need for an increased understanding of atmospheric processes in shoreline environments. Existing models of diffusion in the coastal zone are widely used for air pollution forecasting in both regulatory and emergency response planning, especially in the field of atomic energy. It is important that such models include refinements that

incorporate the TIBL as a dynamic feature of the coastal atmosphere.

A comprehensive treatment of the TIBL has however been hampered by the lack of information on various structural and temporal aspects of TIBL formation. A workshop on Coastal Atmospheric Transport Processes was convened during the 3rd Conference on Meteorology of the Coastal Zone (SethuRaman, 1984) to address this and other related problems. The workshop presented a tabulation of the current status and research goals for coastal atmospheric diffusion. Particular emphasis was laid on future TIBL research to improve predictions of diffusion and downwind concentrations from sources near the coast. It was recommended that, among other considerations, studies be performed to rectify the lack of experimental data on TIBL formation and characteristics, profiles of turbulent quantities and intercomparisons of available models.

## STUDY APPROACH

Coastal boundary layers occur within offshore and onshore flow in stable, neutral and unstable atmospheric conditions, with a variety of surface temperature and roughness characteristics. This study concentrates on the category of primary interest, namely the formation of the TIBL during onshore flow, with the land rougher and warmer than the adjacent body of water. Studies of the TIBL have taken place along many coastlines around the world, but to date no such work has been performed in Southern Africa. In recent years, however, a number of local authors have alluded to the importance of the TIBL with regard to air pollution and potential plumes from nuclear power stations (Keen, 1979; Jury and Mulholland, 1986).

The West Coast of the subcontinent to the north of Cape Town is an ideal location for the occurrence of westerly onshore flows under fair weather synoptic conditions. The Benguela

Current of the South Atlantic Ocean maintains cool sea temperatures in the region, and at this latitude (34°S) in summer, hot surface temperatures are experienced over the land. An initial pilot project (Comrie, 1986) aided in the siting of a suitable study area (Figure 3), and in the identification of an optimum methodology and operational design. It was decided to adopt a similar approach to the comprehensive field studies outlined earlier, acquiring both airborne and surface data for the provision of relatively complete data coverage of the TIBL. A light aircraft was used to fly transects up to 20Km long and 1500m in altitude, while a network of meteorological masts, surface instruments and an acoustic sounder were deployed at various sites on the ground.



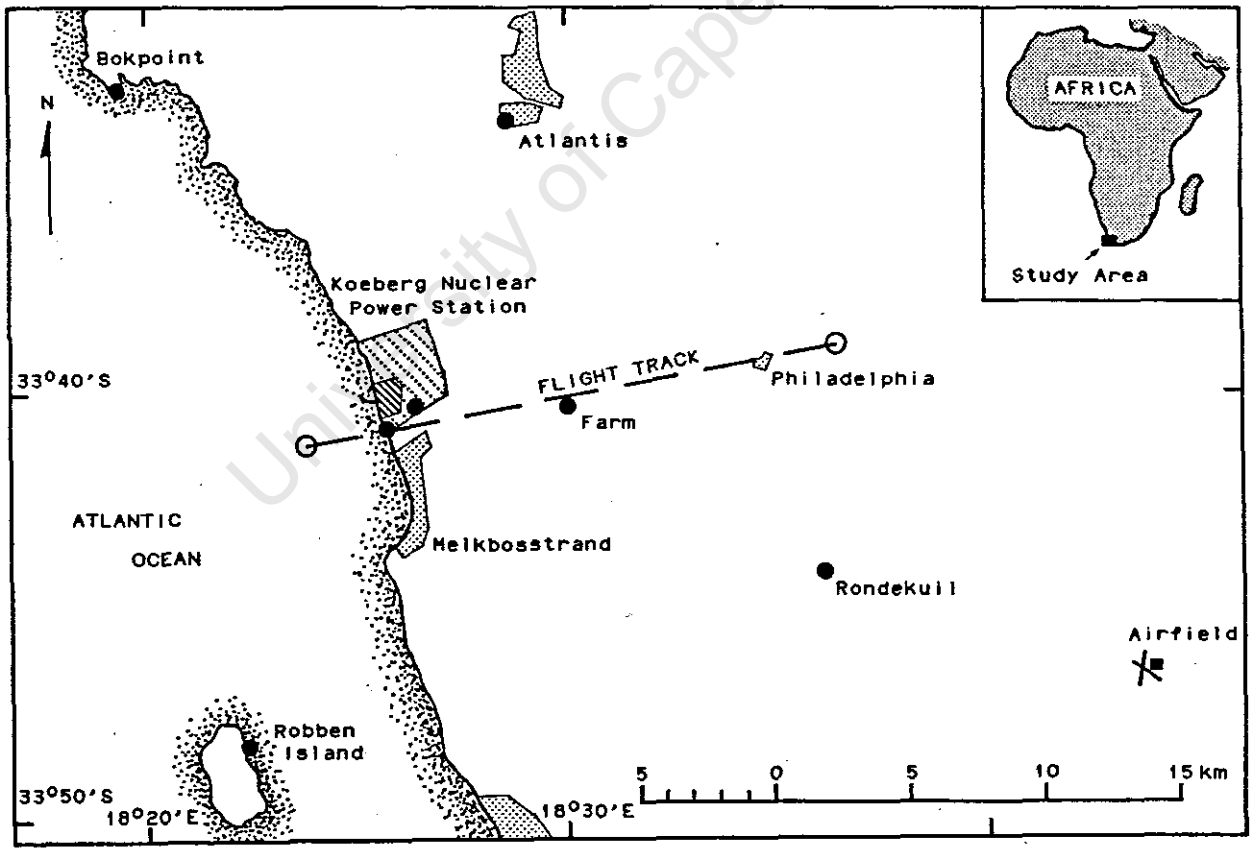


**Figure 3:** Location of the study area on the Southern African coastline showing the flight track (broken line) and instrument locations (dots).

The aircraft measurements included temperature, humidity and turbulence, and were collected by means of specially developed digital instrumentation. Turbulence (vertical velocity) measurements were based on a methodology outlined by SethuRaman *et al* (1979), following a method used by Lenschow (1976) to measure updrafts in storms. The vertical motions of the aircraft itself were used to measure turbulence by means of high frequency sampling of pressure-height changes. The aircraft was flown at constant pitch angle and thrust, allowing it to be sensitive to eddies in the vertical plane, whilst maintaining the general direction of flight. Calibrated values were obtained by flights past an instrumented tower.

## STUDY AIMS

The overall aim of this study was to undertake an empirical examination of the growth, structure and prediction of the TIBL, by means of comprehensive airborne and ground based measurements.

The approach adopted for the presentation of this thesis is one whereby the body of the text is comprised of four chapters written as scientific papers in journal format. These discrete papers are preceded by a general introduction chapter, and followed by a chapter which summarises the overall thesis conclusions. The empirical aspects of the TIBL were investigated in terms of general meteorological characteristics, turbulent structure, and an evaluation of the TIBL height equations, while a synthesis of these approaches was provided by a case study. The focus of each chapter can be outlined as follows:

### Chapter 2

### METEOROLOGICAL CHARACTERISTICS OF THERMAL INTERNAL BOUNDARY LAYERS

This chapter investigates the characteristic patterns of

meteorological parameters from eight test days. Surface and airborne data were used to quantitatively define the typical surface and upper level wind fields, diurnal TIBL growth patterns, and the two-dimensional structures of temperature, humidity and standard deviation of vertical wind speed;

## Chapter 3

### THE MESOSCALE TURBULENT STRUCTURE OF THE THERMAL INTERNAL BOUNDARY LAYER

This chapter examines the structure of various turbulent parameters for one selected case of TIBL formation. Aircraft data were used to detail the observed and non-dimensionalised (scaled) patterns of turbulent flow characteristics, sensible heat fluxes ($w'\theta'$), and standard deviations of potential temperature and vertical velocity ($\sigma_T$ and $\sigma_w$);

## Chapter 4

### AN EVALUATION OF THERMAL INTERNAL BOUNDARY LAYER EQUATIONS

This chapter evaluates the comparative performance of eight TIBL height prediction equations available in the literature. The equations were tested via the application of statistical summary and difference measures to 143 cases of observed TIBL height;

## Chapter 5

### FORMATION, STRUCTURE AND HEIGHT OF THE THERMAL INTERNAL BOUNDARY LAYER - A CASE STUDY

This chapter provides an overall perspective of TIBL growth and decay, meteorological and turbulent characteristics, and observation and prediction of TIBL height, illustrated by means of a case study.

Each aspect of the study thus receives attention in a

separate chapter (paper), while the overall continuity of the thesis format is preserved. The special symbols, supplementary information and data used in each chapter are presented in the appropriate Appendix (ie. Chapter 2's data can be found in Appendix 2), following which a full listing of references used in the thesis is provided.

CHAPTER 2

# METEOROLOGICAL CHARACTERISTICS OF THERMAL INTERNAL BOUNDARY LAYERS

The structure of the Thermal Internal Boundary Layer (TIBL) was investigated on eight test days, using an instrumented light aircraft and ground based measurements. Thermal and frictional effects in the TIBL caused the oblique onshore flow to become more normal to the coastline, with higher wind speeds and large increases in low level turbulence inland. The TIBL grew rapidly from convective conditions in the morning, peaking at midday and gently decreasing in the afternoon. The strength of the overwater lapse rate and the presence of an initial mixed layer controlled the build-up of the neutral layer near the surface, and the degree of entrainment into the TIBL aloft. The resulting warmer temperatures throughout the TIBL increased the specific humidity by allowing greater uptake of evaporative moisture, but caused relative humidity to decrease. Maxima of relative humidity were found in the entrainment region, and were associated with occasional scattered cloud. Temperature structure also strongly influenced the intensity of turbulence and the TIBL height, with strongly stable onshore flow resulting in the most limited vertical dispersion.

## INTRODUCTION

Many potential pollution sources such as industrial plants, petrochemical complexes, power stations, nuclear reactors and urban centres are located in shoreline environments. The understanding of air pollution and its dispersion in these areas has been hampered by the complex meteorology associated with the coastal zone, especially under conditions of fair weather when mesoscale effects such as the sea breeze are present. An important concern under such conditions is the development of a Thermal Internal Boundary Layer (TIBL).

The TIBL is formed over the land under conditions of onshore flow as a result of surface discontinuities in roughness and temperature that occur at the coastline. It is characterised by a convex upper boundary that separates the evolving mixed layer near the surface from the overlying unmodified stable air. The slope of the TIBL increases most rapidly nearest the shore becoming more gradual with distance inland. Vertical diffusion can thus be severely limited near the coast compared to adjacent inland areas. Plumes emitted within the TIBL will be contained near the surface, causing plume trapping, while plumes emitted at levels above the TIBL may travel inland in the stable layer aloft before intersecting the TIBL, where the plume will fumigate downwards. Under both circumstances the ground level concentrations will be far greater than those normally predicted.

Initial knowledge on TIBLs emerged largely from studies on coastal air quality and sea breezes, and was reviewed in Prophet (1961) and Van der Hoven (1967). Continued research in this field included Hewson and Olsson (1967), Lyons and Cole (1973), Knox and Lyons (1975) and Weisman and Hirt (1975), which was further summarised in a monograph by Lyons (1975). Evaluations of the characteristics of the TIBL included those made at low level in Echols and Wagner (1972)

and Ogawa and Ohara (1985). In recent years a number of studies have involved extensive resources and a comprehensive treatment of the TIBL using both aircraft and ground based measurements, including studies at Brookhaven National Laboratory (Raynor *et al*, 1979), Nanticoke (Portelli, 1982; Kerman *et al*, 1982) and at Kashimaura in Japan (Gamo *et al*, 1982). The need for comprehensive field observations such as those above was a major research recommendation of the Workshop on Coastal Atmospheric Transport Processes (SethuRaman, 1984).

The aim of this study was to undertake a comprehensive examination of the meteorological characteristics of the TIBL, by means of ground based and airborne measurements, and to quantitatively define its typical horizontal and vertical structure.



## EXPERIMENTAL PROGRAM

### Study site

Figure 1 shows the location of the study area on the Atlantic coastline of Southern Africa about 30km to the north of Cape Town. Surface temperature contrasts between land and sea are as high as 20°C to 30°C in summer, and a sea breeze component is common during fair weather when weak or favourable gradient winds prevail (Keen, 1984). The coastline is approximately linear with a NNW to SSE alignment. The terrain slopes gently upward from the coast, reaching a height of roughly 100m further inland (≈20km), displaying very little relief apart from a few small hills further to the south and north of the study area. Ground cover is mostly ploughed wheatfields with some grass and bush cover nearer the coast. The major human activity is the centrally located 2000MW Koeberg nuclear power station, with

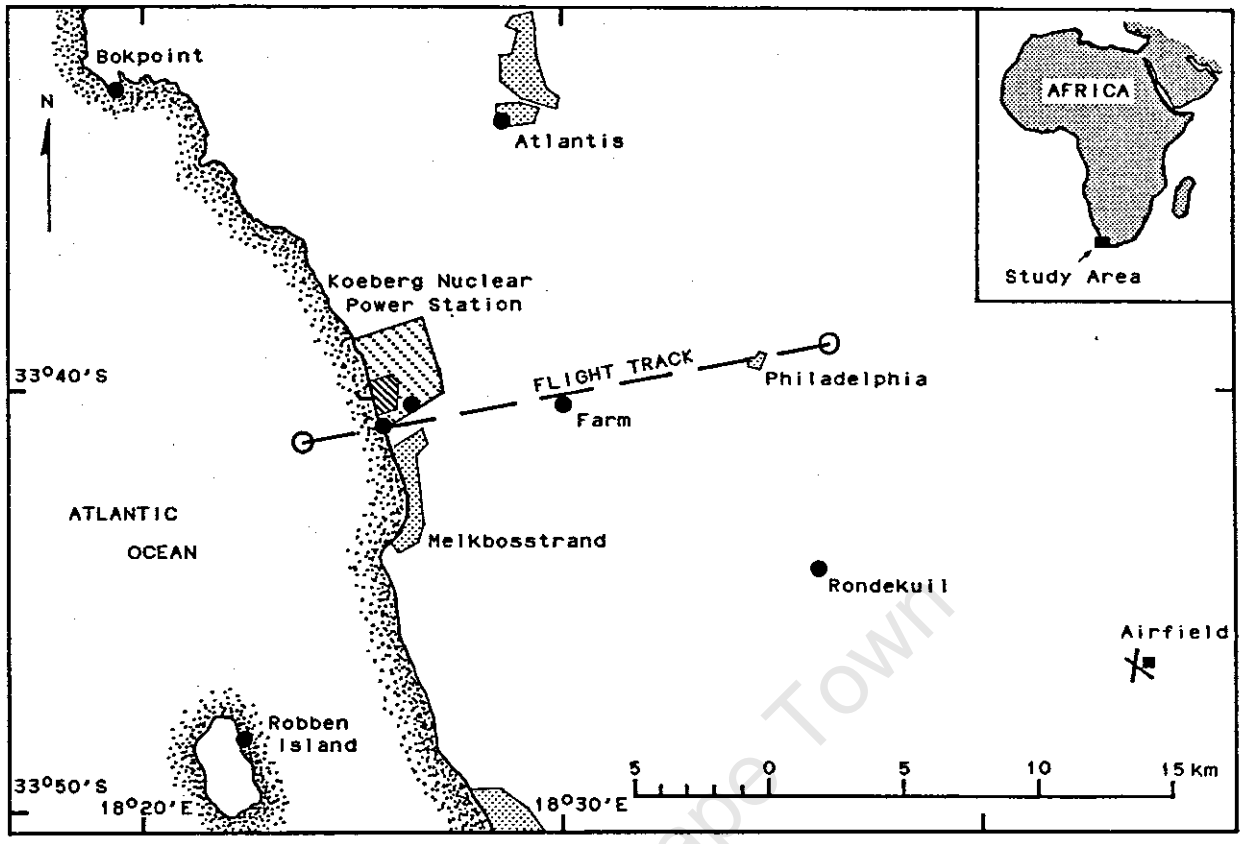


**Figure 1: Location of the study area showing instrument locations (dots) and the flight track (broken line).**

a number of small settlements located towards the edge of the study region.

It was decided after an initial pilot study (Comrie, 1986) to adopt the use of both ground based and airborne measurements. This approach has proved to be the most effective method of obtaining a full data set over distances of 20km and heights of 2000m within as short a time as possible. The field experiments took place during the late southern summer in March and April of 1987, where full data sets were obtained on eight test days (Table 1). It was found necessary to take data near the middle of the day when conditions were fully developed and more constant over time, and a number of check flights were made which confirmed that differences over the above period could be considered negligible.

**TABLE 1**
Data inventory for the eight test days

| Run | | 318 | 319 | 327 | 330 | 331 | 401 | 413 | 421 |
|---|---|---|---|---|---|---|---|---|---|
| Time | | 14h40-15h40 | 13h30-14h50 | 15h05-16h30 | 12h45-14h10 | 15h05-16h10 | 12h45-14h15 | 12h40-14h25 | 13h20-14h35 |
| Insolation | $W.m^{-2}$ | 910 | 945 | 860 | 930 | 830 | 850 | 880 | 860 |
| Overwater lapse rate | $^{o}C.100m^{-1}$ | 1.33 | 0.51 | 0.48 | 0.50 | 0.58 | 0.56 | 0.77 | 0.47 |
| Type | | A-b | A-b | A-a | A-a | B-a | B-b | A-a | B-a |
| Initial TIBL height | m | 860 | 160 | 140 | 200 | 0 | 0 | 240 | 0 |
| Land sfc. temperature | $^{o}C$ | 35.1 | 36.8 | 39.9 | 35.4 | 33.6 | 37.9 | 36.0 | 29.7 |
| Sea sfc. temperature | $^{o}C$ | 12.2 | 13.4 | 14.5 | 13.9 | 14.5 | 15.8 | 11.6 | 13.4 |
| DATA TAKEN | | | | | | | | | |
| Airborne temperature | | X | X | X | X | X | X | X | X |
| Airborne turbulence | | X | X | X | X | X | X | X | X |
| Pibals | | X | X | X | - | - | X | - | X |
| Surface turbulence | | X | X | X | - | - | X | - | - |
| Acoustic sounder | | X | X | X | X | X | X | X | - |



**TABLE 2**
Low level (10m) turbulence parameters averaged for the eight test days

| Site | | Coast 0km | Koeberg 1km | Farm 6km | Rondekuil 16km |
|---|---|---|---|---|---|
| $u$ | $m.s^{-1}$ | 4.4 | 4.5 | 6.0 | 5.9 |
| $\sigma_u$ | $m.s^{-1}$ | 0.5 | --- | 1.4 | --- |
| $\sigma_u/u$ | $m.s^{-1}$ | 0.1 | --- | 0.3 | --- |
| $\theta$-180° | ° | 86 | 79 | 102 | 114 |
| $\sigma_\theta$ | ° | 10.5 | 5.4 | 11.4 | 11.9 |
| $T$ | $^{o}C$ | 17.7 | 18.1 | 22.2 | 22.8 |
| $\sigma_T$ | $^{o}C$ | 0.6 | --- | 3.0 | --- |

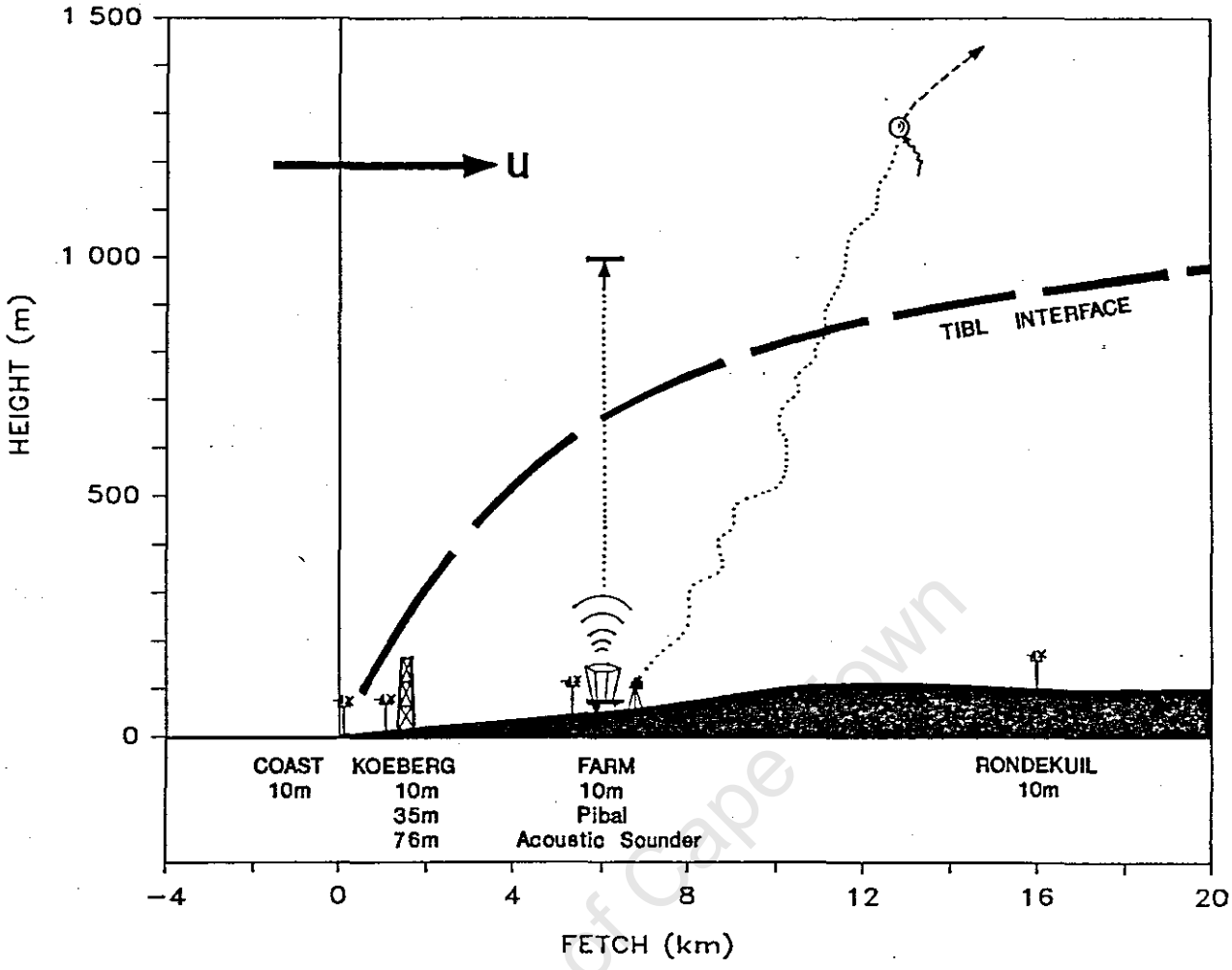


**Figure 2:** Deployment of surface instruments within the study area (instruments not to scale).



## Surface instrumentation

Seven instrumented 10m masts were located in the region, measuring hourly means of temperature, wind speed and direction. Of these, four were located in the TIBL study area (Figure 2). In addition the coast and farm towers recorded 15 minute means, and logged at one minute intervals for the duration of each test enabling comparisons of low level turbulence. At the Koeberg meteorological station there were two towers of 35m and 76m, each equipped with 3D vane anemometers and other instruments, which were used for reference and calibration. Surf temperatures were also recorded at this site.

A number of other measurements were made at the farm base site. Vertical profiles of wind speed and direction were obtained with double theodolite pibal soundings to over 2000m height at 10 to 15 minute intervals. Solar radiation measurements were taken on test days (LI-COR portable radiometer), as were land surface temperatures (YSI thermistor probes). A standard 1600Hz monostatic acoustic sounding system (AeroVironment Model 300) was operated continuously and provided vertical profiles of the atmosphere to a height of 1000m, from which the stability and turbulence structure could be inferred. In this way, although the TIBL height was only fixed once during the day, the sounder trace could be 'calibrated' and the growth and decay of the TIBL followed throughout the day.

**Airborne instrumentation**

Airborne measurements of atmospheric turbulence are conventionally achieved using the relative motion of an aircraft with respect to the wind, combined with an inertial navigation system or doppler radar. An alternate method is to make use of the aircraft response itself, measuring the actual motions of the aircraft which are proportional to the vertical velocity fluctuations experienced. The latter methodology was adopted for this study, having the benefits of ruggedness, simplicity, economics and ease of application. The method is fully outlined in SethuRaman *et al* (1979), where it was used successfully for boundary layer work at Brookhaven National Laboratory, and was based originally on work by Lenschow (1976) on the estimation of updrafts in storms.

Briefly, the method consists of flying a light aircraft at constant thrust and pitch angle, allowing it to be sensitive to eddies in the vertical plane, whilst still maintaining the general flight path. SethuRaman *et al* (1979) made use of a variometer, a common aviation instrument for determining rate of climb or descent, which was specially calibrated to

read vertical velocities. For this study a more sensitive system was developed using a miniaturised quartz diaphragm pressure transducer which was sensitive to motions of 0.5m (0.05mB) or more. The transducer was linked to a static pressure line located outside the cabin and, together with a thermistor psychrometer mounted under the wing, was read at 10Hz.

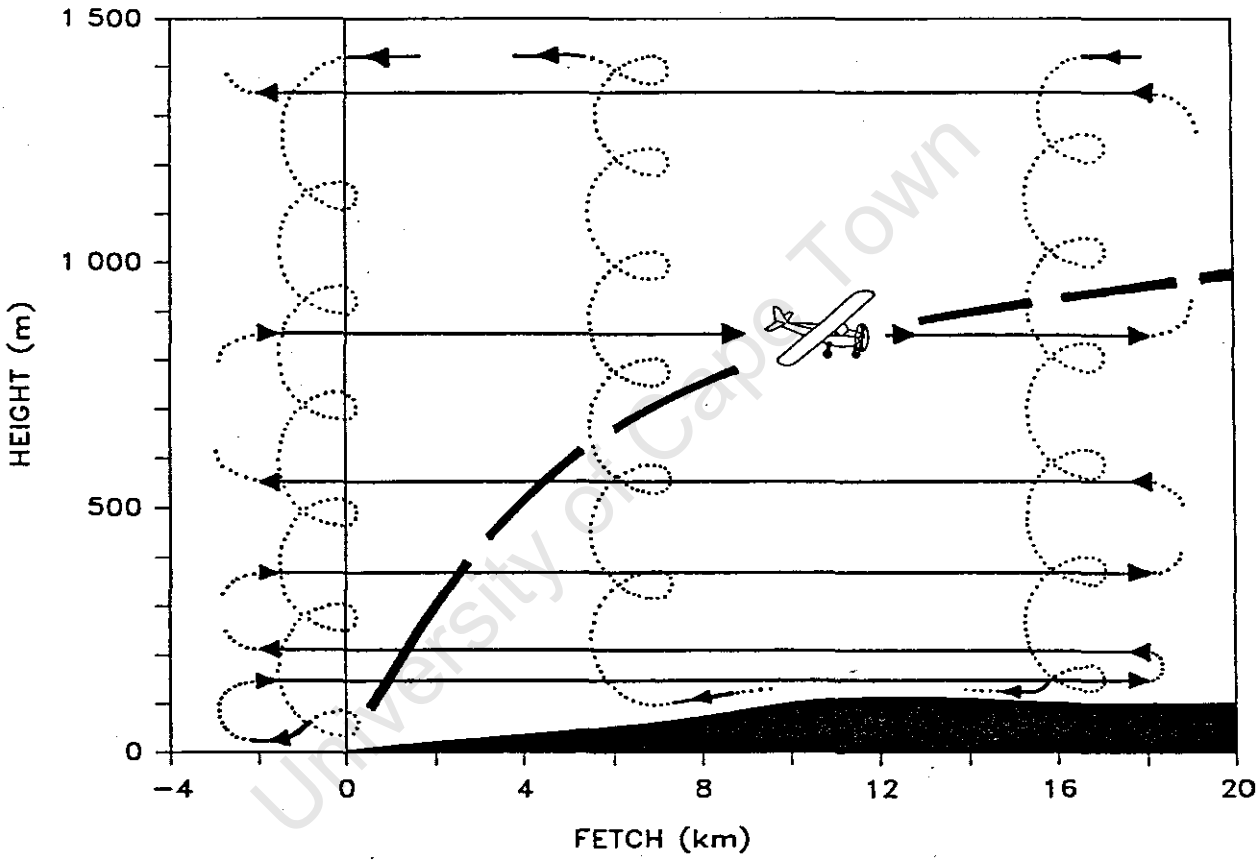


**Figure 3: Aircraft flight plan for vertical profiles of temperature (dotted line) and horizontal transects of turbulence and temperature (solid line).**

Measurements of temperature, humidity and turbulence throughout the length and height of the TIBL were taken using a single-engined Cessna 172. Figure 3 illustrates the flight plan, which consisted of three vertical temperature profiles followed by six horizontal traverses. These traverses were exponentially spaced from 150m to 1400m

altitude to enable proper delineation of the curved TIBL boundary. An entire run took under 90 minutes, and achieved a complete horizontal and vertical mapping of the TIBL.

## ANALYTICAL PROCEDURE

All data collected, other than that from the acoustic sounder, was computer compatible and was processed to provide graphic output of various raw and calculated values. Analysis of the airborne turbulence data revealed an optimum response time of roughly 0.5 seconds, which was the same figure arrived at by SethuRaman *et al* (1979). The data were then processed to provide integral values of five samples at 2Hz. Consecutive differences between these values provided pressure-height changes which were calibrated to individual *w*-values of vertical velocity in 16 flights past the instrumented tower. Conversion factors between the aircraft milliBar pressure-height change and the vane anemometer were derived for each run to provide a mean calibration ratio of 2.36 between the two systems.

Raynor *et al* (1979) derived only two values of turbulence, $\sigma_w$ within and outside the TIBL. Instead, the 'moving' $\sigma_w$ approach used by Gamo *et al* (1982) was adopted. A sampling time of 50 seconds was found to be the optimum required to calculate $\sigma_w$, and yet provide a sufficiently detailed horizontal profile of turbulence. Distances in the TIBL were calculated along the mean wind direction, after which all aircraft data was then graphed and compiled into isopleth diagrams for various parameters (definitions in Appendix 2.1). Potential temperatures were calculated using conventional temperature and pressure-height corrections. TIBL height was fixed from inflections in the vertical and horizontal parameter profiles.

## RESULTS AND DISCUSSION

### Ground based measurements

#### SURFACE CONDITIONS

The eight days of experiments were characterised by fair weather conditions, with clear skies or scattered cloud. Sunrise and sunset were at 07h00 and 19h00, with solar radiation peaking at 13h00 between 850W.m$^{-2}$ and 945W.m$^{-2}$. Land surface temperatures during the tests averaged 37°C with a range from 26°C to 42°C. Sea temperatures had a mean of 13.7°C, ranging between 11.6°C and 15.8°C. The mean land-sea temperature difference was thus 23°C, providing ample energy to drive a sea breeze component, and for convective and conductive heating in the TIBL.

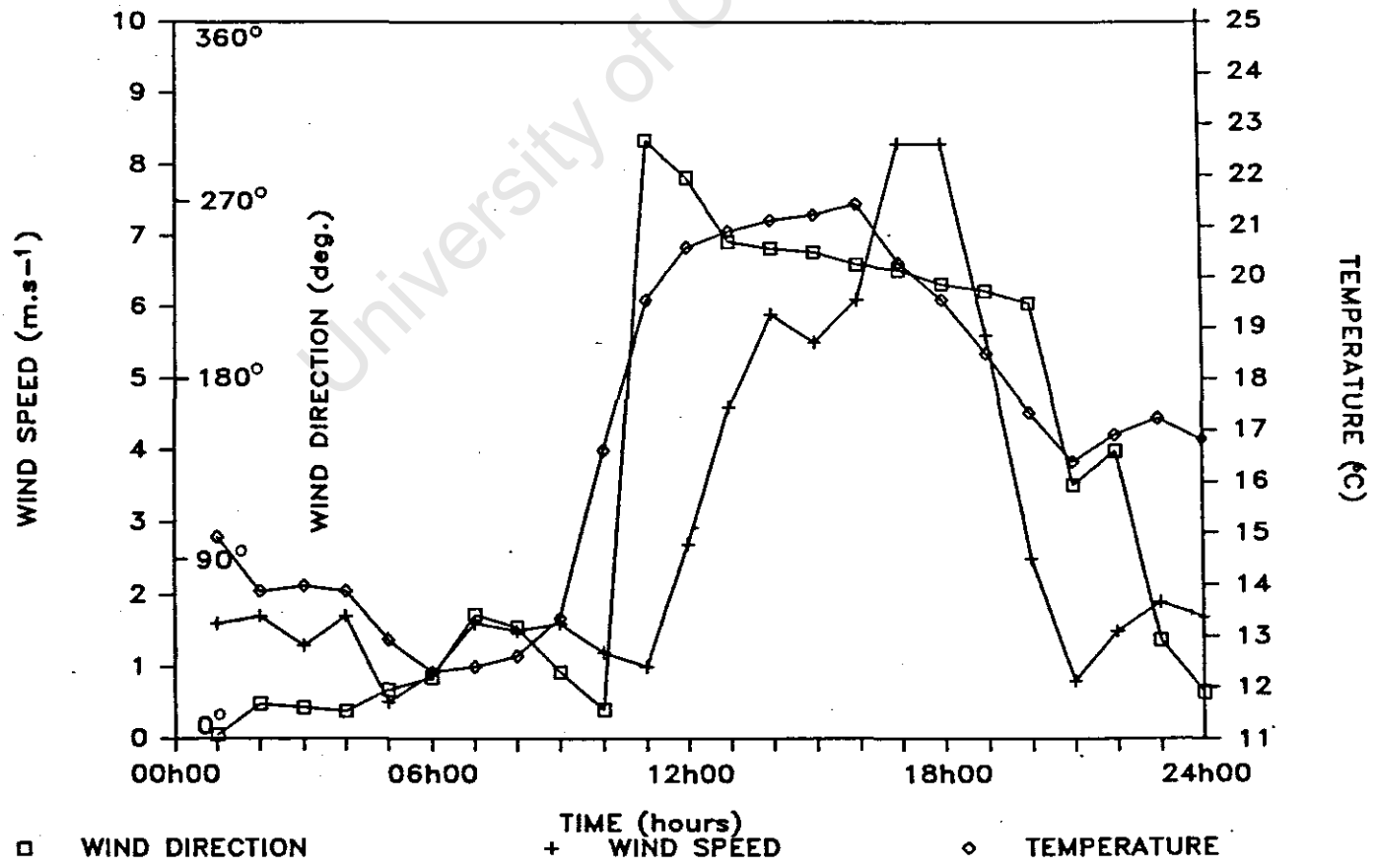


**Figure 4: Hourly averages of 10m data at Rondekuil on 31-3-87 showing typical diurnal trends.**

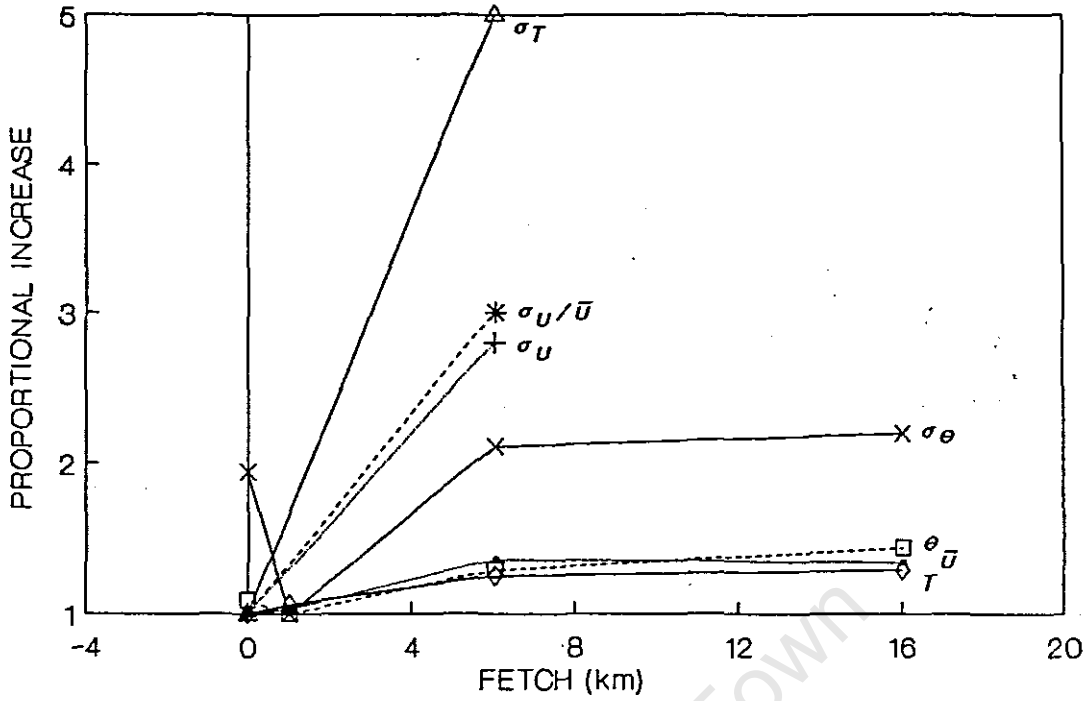


**Figure 5: Proportional increases of 10m data and turbulence differentials between nearshore and inland sites.**



AIR TEMPERATURE

Cool morning air warmed soon after sunrise, and temperatures increased rapidly until about 10h00. A gentle peak was reached over the middle of the day, decreasing gradually in the afternoon, and dropping more sharply from about 18h00 (Figure 4). While temperatures inland always increased after sunrise, temperatures at the coast either increased or decreased depending on the persistence of a low level marine inversion, and on changes in wind direction. Daytime 10m air temperatures had a mean of 17.9°C near the coast and 22.5°C in the TIBL, with corresponding extremes of 15°C to 35°C. During the experiments, inland temperatures were 5°C to 10°C higher than at the coast, with the greatest horizontal temperature gradient occurring in the first 6km (Figure 5).

## SURFACE WINDS

Wind data from the 10m network indicated sea breeze formation to some extent on all experiment days. In the morning the existing land breeze or light gradient wind of $1m.s^{-1}$ to $3m.s^{-1}$ usually swung through north, the westerly sea breeze component building up from about 10h00. Wind speeds showed the expected increase and decrease during the day, following the pattern of surface temperature differences (Figure 4). Wind direction was frequently different at the various sites in the morning but, with the progressive influence of the sea breeze, all sites had become similar by about 13h00.

Although Raynor *et al* (1979) found a decrease in surface wind speed inland, it was generally observed to increase, in contrast to the expected decrease (Figure 5). This effect has been found previously in the area (Comrie, 1986) and is a surface phenomenon related to the persistence of the low level marine inversion close to the coastline. Wind speed parameters at the coast and inland are given in Table 2.

Wind direction displayed a strong tendency of becoming more normal to the coastline with passage inland, although the gradient wind was almost always oblique to the coastline over the sea. This effect was also noted in Raynor *et al* (1979). It is thought that increased frictional drag in the TIBL, and thermal differences resulting in a sea breeze component, caused the flow to become more perpendicular to the coast. This change in wind direction can be seen in Figure 4.

## LOW LEVEL TURBULENCE

Marked increases in 10m turbulent quantities (standard deviations) were found inland within the TIBL (Figure 5). A threefold increase in $\sigma_u$ occurred between 0km and 6km, with a similar increase for $\sigma_u/u$. A doubling of $\sigma_\theta$ took place

Wind speeds were also linked to the presence of an initial mixed layer (see Airborne temperature structure below). Days with a mixed layer exhibited wind speeds around $9m.s^{-1}$ in the lower 1000m, while on days with stable lapse rates near the surface, this figure was about $5m.s^{-1}$. Measured TIBL heights were found to be just above the region of peak wind speed and well below the region of minimum wind speed, the latter usually being associated with the swing between the sea breeze component and the overlying gradient wind direction.

Figure 6b shows the mean vertical pattern of wind direction. The normal flow nearer the surface was typically 1000m or more deep, with varying amounts of change towards the synoptic flow above. Although the latter was observed from the SW, W and NW, flow near the surface was always close to WSW ($250^{o}$), which was exactly normal to the coast. As the sea breeze and TIBL developed during the day the depth of this layer increased, and likewise as the layer shrunk in the late afternoon the gradient flow descended again, as seen below in the lapse rate and acoustic sounder data. Increased variability in wind direction is generally associated with lower wind speeds, and thus the greatest variations in direction were found near the ground and at the top of the sea breeze layer.



### ACOUSTIC SOUNDER

Acoustic echo sounders are well known to display a strong link to the turbulence and temperature structure of the atmosphere (Beran *et al*, 1973), and are thus ideally suited to TIBL analysis. Acoustic signatures were strongest in the most well defined TIBLs, which as expected possessed the strongest lapse rates and greatest contrasts in turbulence. Figure 7 shows a facsimile of the acoustic sounder trace from Run 401, together with the observed TIBL height above the farm (6km). Figure 8 shows a time-height representation of TIBL heights for the study days, as read off acoustic

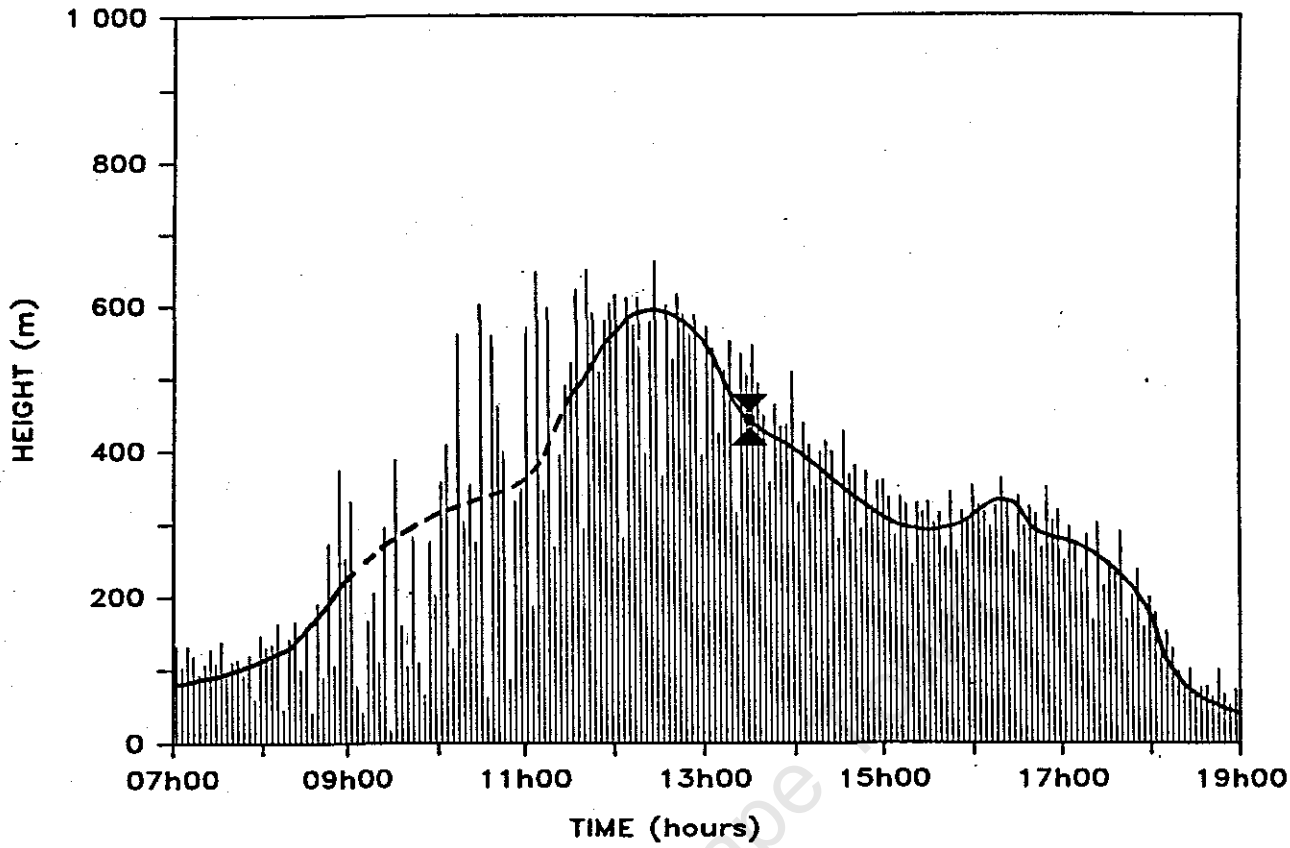


**Figure 7:** Facsimile of acoustic sounder trace from Rin 401 showing measured TIBL height at 13h20 and derived height for other times of the day (see text). Broken line indicates unclear TIBL height due to convective activity.

sounder charts using the above technique. Both the above diagrams illustrate the characteristic growth and decay of the TIBL, which followed the diurnal cycles of insolation, wind and temperature. Considerable variation occurred from day to day as well as during each day, depending on meteorological conditions.

The first part of the morning was generally characterised by increased convective and thermal activity, after which mixing height tended to stabilize as the TIBL became established. Growth of the TIBL seemed most rapid in the late morning, reaching a maximum height around midday, and then dropping off more gradually during the afternoon until about 18h00 when it disappeared with a change in wind and temperature conditions. This pattern is in close agreement with that outlined in Kerman *et al* (1982).

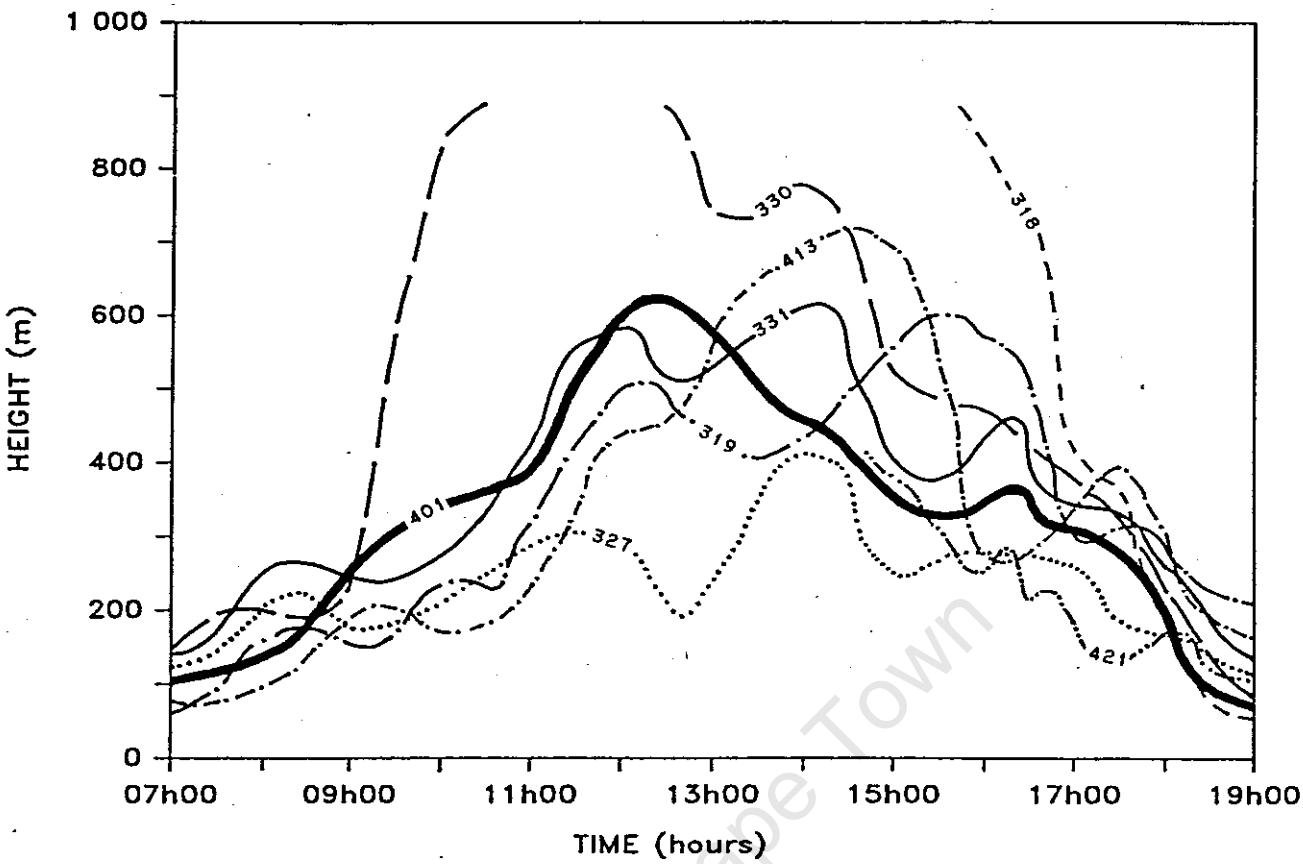


**Figure 8:** Derived TIBL heights for the eight study days taken at the farm site (≈6km inland).



## Airborne measurements

### TEMPERATURE STRUCTURE

An important feature of the temperature structure of the TIBL is lapse rate of the onshore flow over the sea. The patterns of turbulence and temperature which result over the land are to a large extent determined by this factor, although many other complex relationships are also involved.

In these experiments, atmospheric stabilities ranged from stable ($0.47^{o}C.100m^{-1}$) to unstable ($1.33^{o}C.100m^{-1}$). Two broad types of onshore flow were recognisable from the data: those where the TIBL had an initial height due to the existence of a mixed layer near the surface, and those where the stable layer extended throughout the entire flow. The importance of

these two types has been recognised in the literature (Lyons, 1975), where they have been labelled Category I and II TIBLs (Stunder and SethuRaman, 1985). They have also been recognised in field studies, where a classification of this nature was made in Gamo *et al* (1982), using horizontal and vertical variations in potential temperature. The former were denoted Type A and the latter Type B. Variations within these categories have been further classified (Figure 9): Type A-a where a single neutral layer was present, and Type A-b where more than one level of stratification existed. Type B-a displayed strong stability with a simple temperature increase in the TIBL, while in Type B-b weaker lapse rates allowed greater variation in temperature structure, showing a characteristic decrease in temperature near the TIBL boundary prior to an increase within the TIBL.

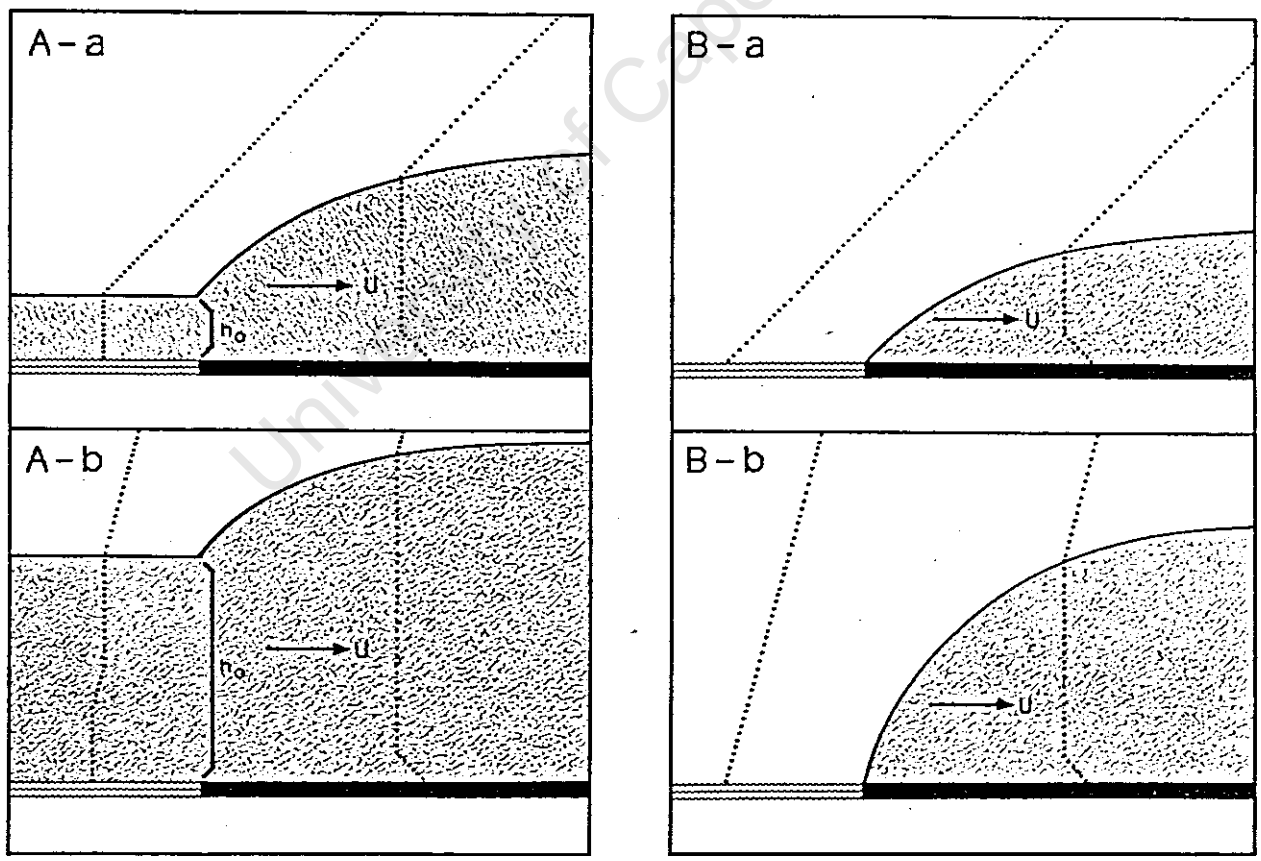


**Figure 9:** Categorization of TIBL types according to vertical and horizontal variations in potential temperature ($h_O$ = initial TIBL height; dotted lines denote potential temperature).

Over the sea a very shallow inversion (less than 100m) was always present due to surface cooling, although this was soon dissipated over the land and resulted in only localised effects on surface TIBL characteristics.

Figure 10a illustrates the patterns of potential temperature found during Run 413, Type A-a. An initial TIBL height of 240m existed over the sea. This mixed layer became fully warmed a few kilometres inland, at which point the height of the isothermic surface began to increase, up to a height of about 900m. A characteristic pattern developed, whereby 'unbending' of the isotherms occurred near the surface as the unstable layer became evenly mixed. There was also a net increase in temperature of about 4°C to 5°C associated with the TIBL. Vertical temperature profiles (Figure 11a) display the growth from the initial mixed layer of 240m over the sea to 550m at the farm (7km), and to 900m inland (18km). The large temperature variations above 1000m inland coincided with scattered cloud at this level.

Figure 10b shows Run 319, typical of Type A-b. Although displaying essentially the same general structure of a mixed layer overlain by a stable layer aloft, the mixed layer itself was more complex, with an intervening stable layer at about 200m. Although slight stratification existed over the ocean, it was intensified by surface heating before the entire layer became more mixed further inland. The TIBL thus increased from about 160m to 1000m over the whole distance. Vertical profiles from Run 318 (Type A-b) similarly indicated the establishment of a neutral mixed layer, especially near the surface, which became warmer with increased surface heating inland (Figure 11a).

Type B-a is illustrated by Run 421 in Figure 12a. The onshore flow was stable throughout and became eroded from the surface upwards with passage inland. This is the simple or idealised type of TIBL formation with the mixed layer developing from the surface at the coast. Temperatures in

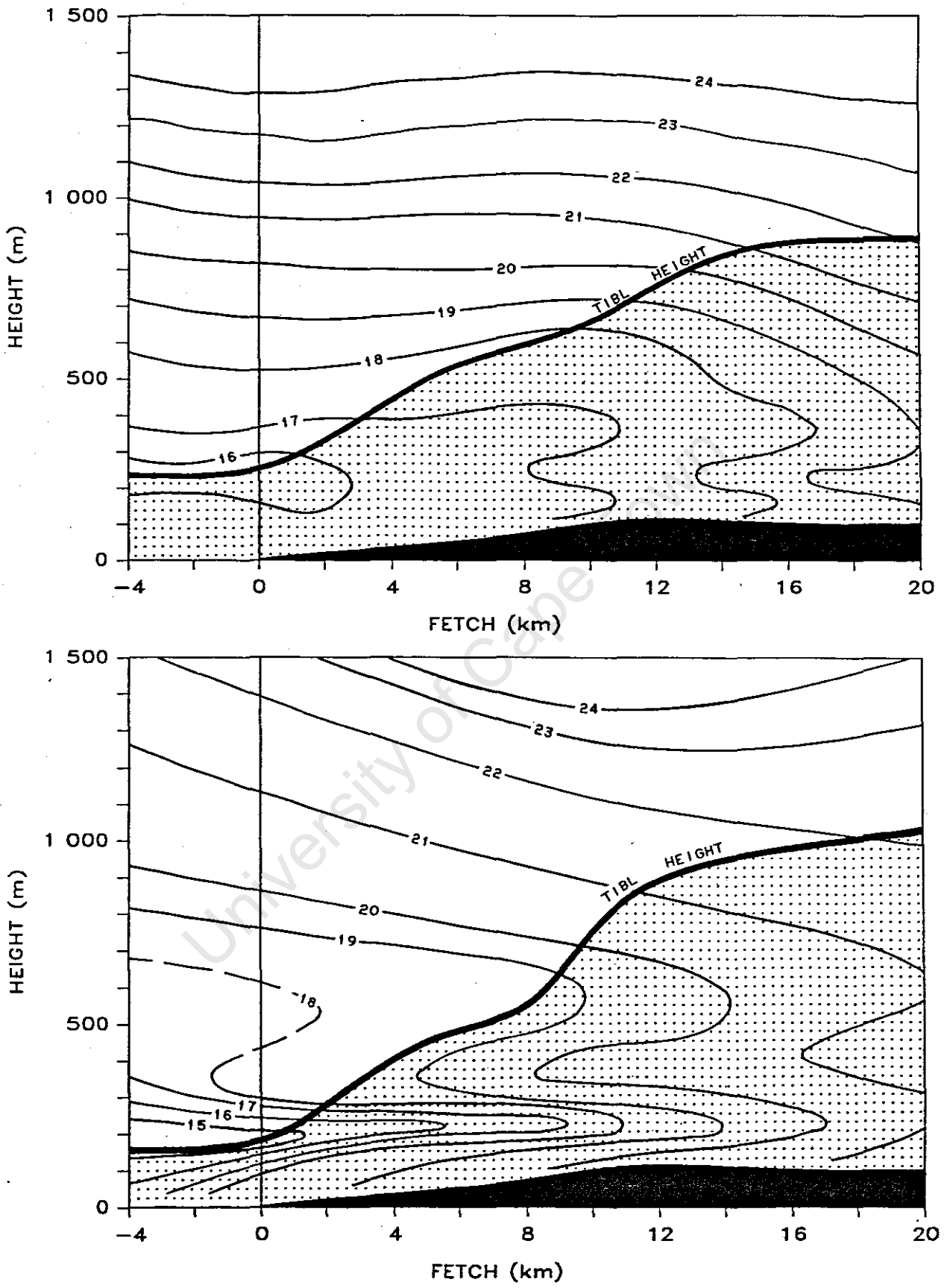


**Figure 10:** Patterns of potential temperature ($^{o}C$) for (a) Run 413, Type A-a and (b) Run 319, Type A-b.

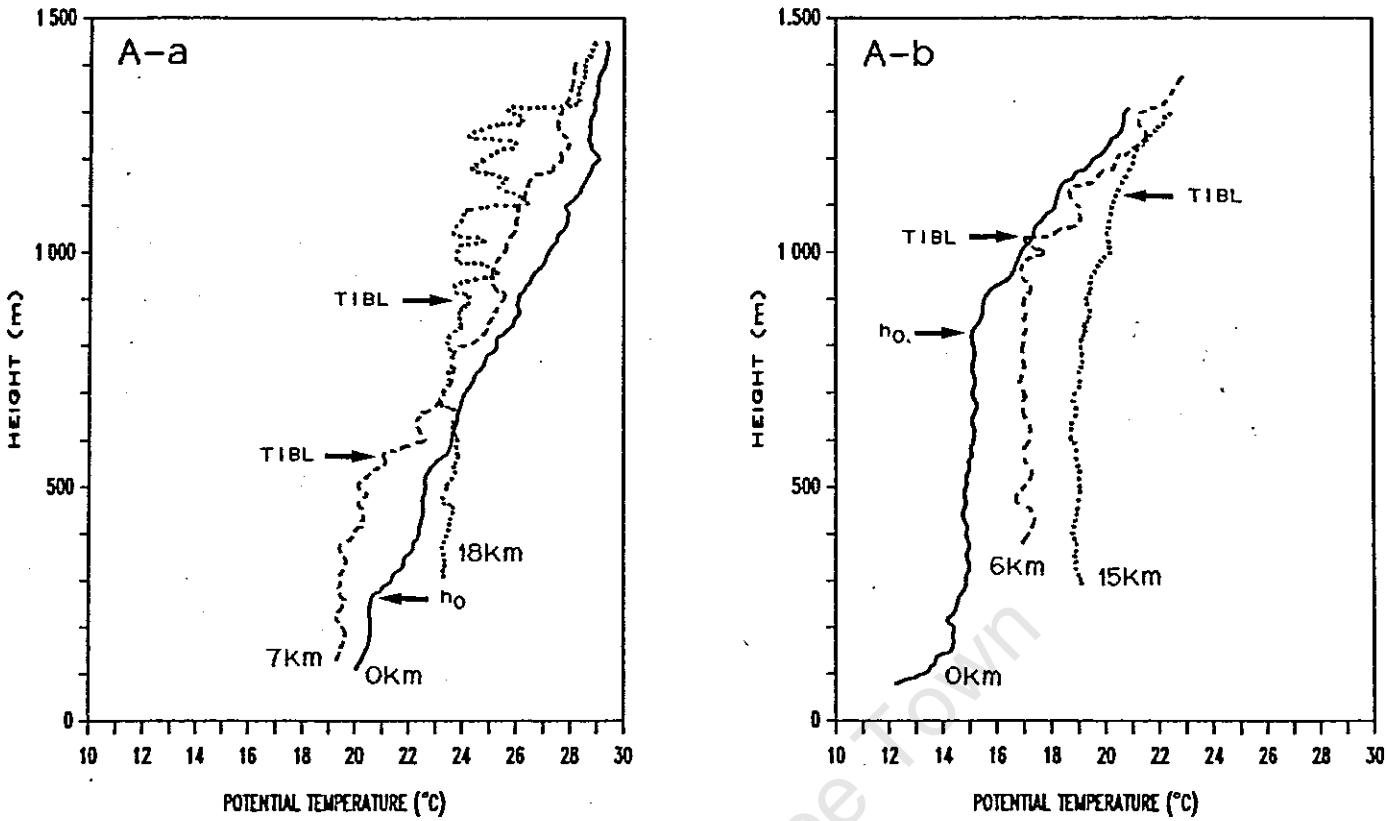


**Figure 11a:** Vertical temperature profiles ($^{o}$C) for Run 413, Type A-a and Run 318, Type A-b.

the stable layer remained constant until the TIBL was intersected, at which point there were increases of 1$^{o}$C aloft and 3$^{o}$C nearer the surface. Vertical temperature profiles illustrate the stable flow over the sea (Figure 11b), which became mixed to a height of about 300m at the farm (6km), and to about 800m further inland (15km).

Figure 12b shows Type B-b as Run 401. In this example, the mixed layer grew from the surface at the coast to about 400m at the farm, with a more gradual increase further inland. This pattern was very similar to Type B-a, in that the initial stable layer was eroded by the development of the TIBL with passage inland. Perhaps due to a weaker lapse rate, entrainment was more enhanced in this case, causing a characteristic slight decrease in potential temperature before the TIBL was encountered. Gamo *et al* (1982) drew attention to the similarity of the above pattern to the 'temperature crossover' effect found in urban heat island

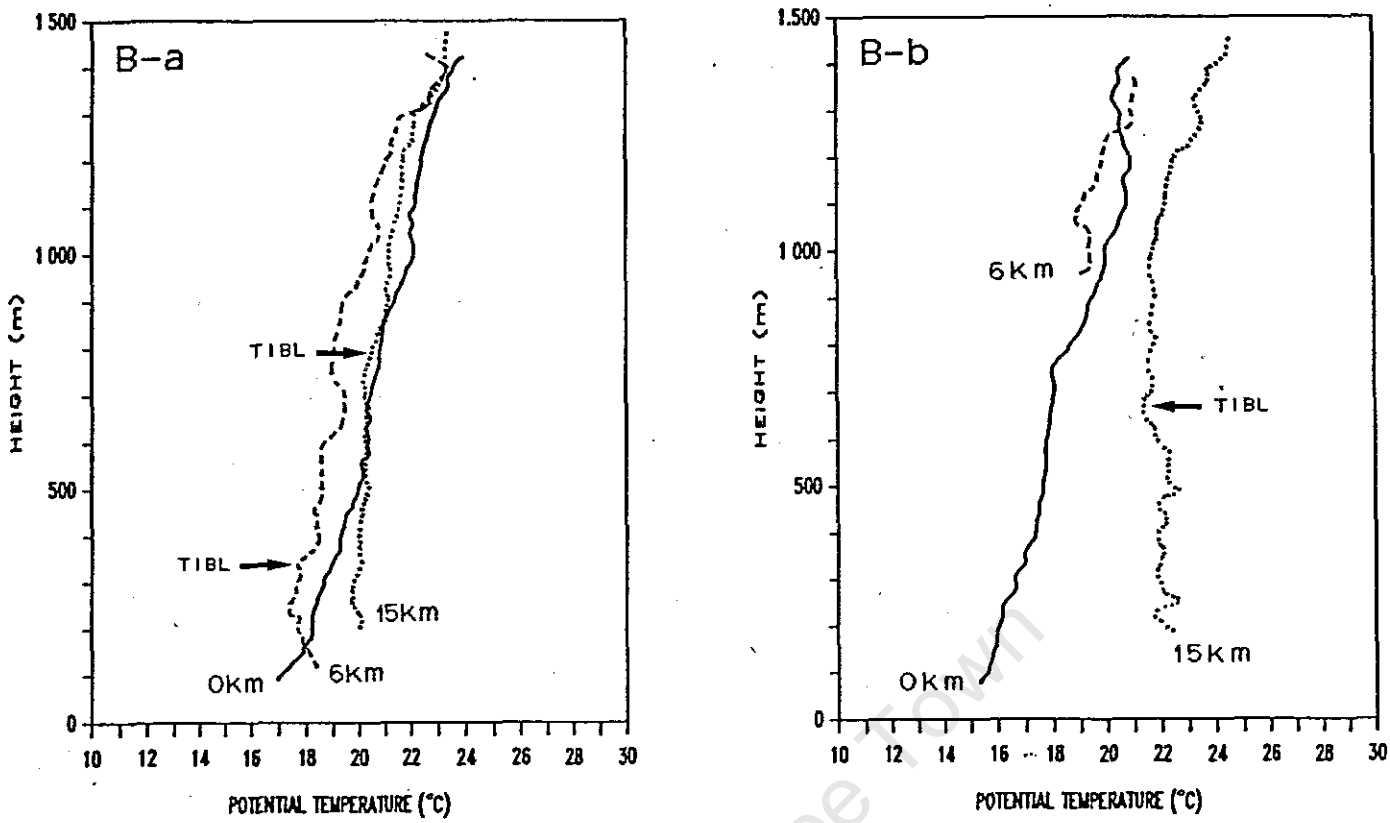


**Figure 11b:** Vertical temperature profiles ($^{o}C$) for Run 421, Type B-a and Run 401, Type B-b.



studies (Bornstein, 1968). This pattern is also evident from the vertical temperature profiles, which indicated a weaker lapse rate and higher TIBL height than in Type B-a (Figure 11b). The height of the TIBL was greatest in Type A-a under conditions of weak lapse rates and enhanced vertical mixing. Conversely, the lowest TIBLs were Type B-a with strongly stable onshore flow and severely limited vertical mixing. The height of the TIBL defined by temperature is known to be roughly 70% of the height defined by turbulence (Stunder and SethuRaman, 1985), and similar tendencies, although of lesser magnitude, were found in this study. This difference in height was accounted for by the existence of the entrainment region at the base of the stable layer, where although penetrative convection occurred, temperatures were cooler than within the TIBL. This is in general agreement with Gamo *et al* (1982).

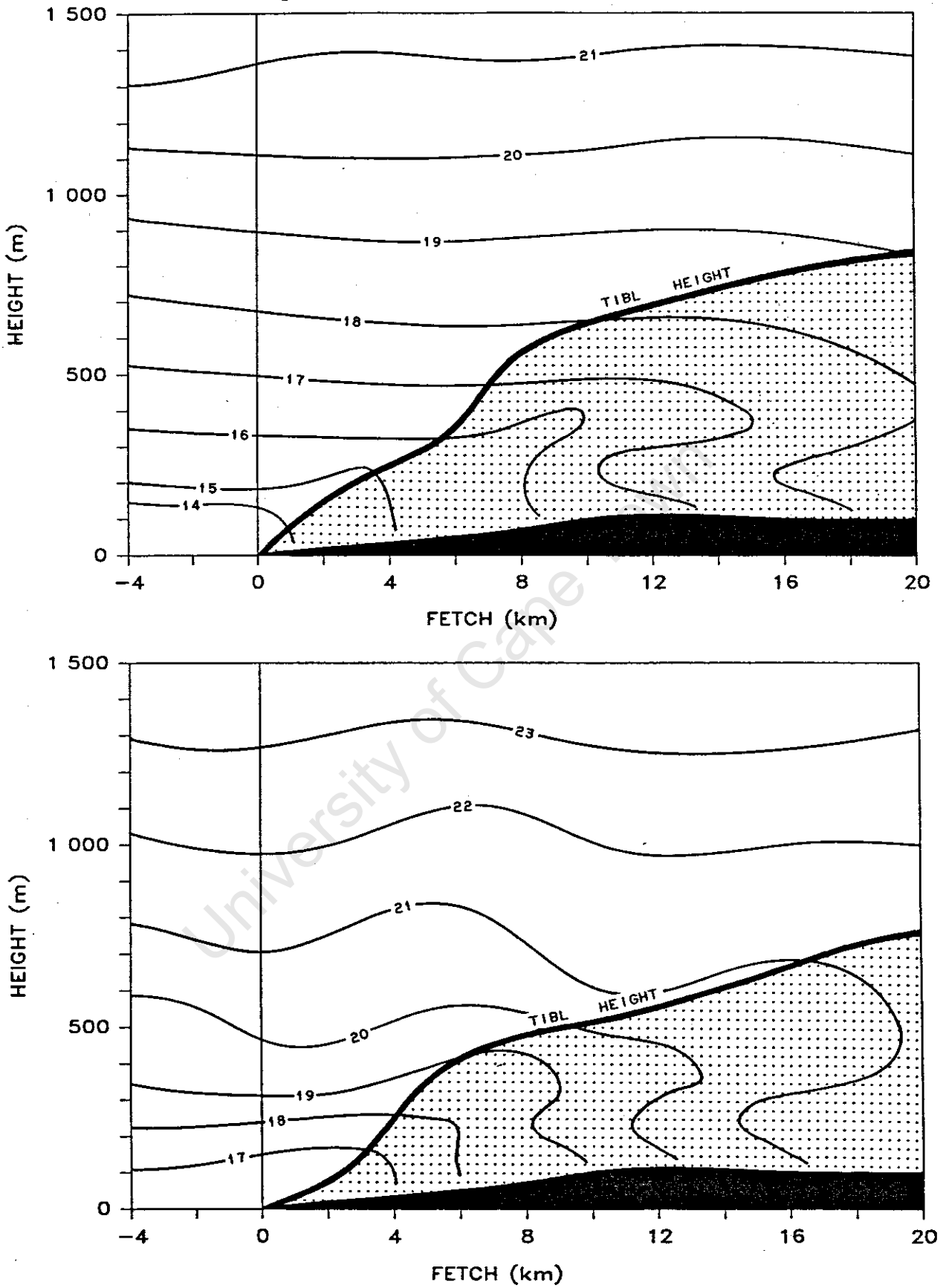


**Figure 12: Patterns of potential temperature (°C) for (a) Run 421, Type B-a and (b) Run 401, Type B-b.**

HUMIDITY

Although not used in many studies, humidity can be an important indicator of the TIBL. Patterns of specific humidity were relatively similar for all cases of the TIBL, with additional moisture accumulated off the land surface resulting in a mean increase in the TIBL of 1.8g.kg$^{-1}$, and a range of 1.3g.kg$^{-1}$ to 2.6g.kg$^{-1}$. Gamo *et al* (1982) found similar increases in moisture content of 1g.kg$^{-1}$ to 2g.kg$^{-1}$. These were typical values found between 100m and 400m height in the TIBL. Much larger increases occurred nearer the surface due to localised temperature increases, the opposite occurring aloft. Specific humidity had a mean of 9.9g.kg$^{-1}$ outside the TIBL and 11.7g.kg$^{-1}$ within, indicating that on average the moisture content in the TIBL increased by 18%. Largest increases took place in Type A-b TIBLs, under weak lapse rate conditions with the greatest mixing, while the smallest differences occurred under the opposite conditions in Type B-a.

Relative humidity displayed a decrease within the TIBL due to warmer temperatures. In addition, higher humidities were found at the TIBL boundary in the entrainment region between warm and cool air. Figure 13a shows Run 413 (Type A-a) typical of all Type A's, where the high humidities at the top of the initial TIBL height were lifted up as the TIBL depth increased inland. This pattern was simplified in Type B's (Figure 13b, Run 331) where a simple drying out occurred in the region of TIBL formation, with greater humidity further above.

In general, both dry bulb ($T$) and wet bulb ($T_w$) temperatures increased in the TIBL, the rate of increase of $T$ being greater than that of $T_w$. The resulting dryer conditions within the TIBL thus enabled the taking up of extra evaporative moisture over the land. Clouds were observed at the boundary of the TIBL in cases where relative humidities were slightly above 100%, characterising the differences in

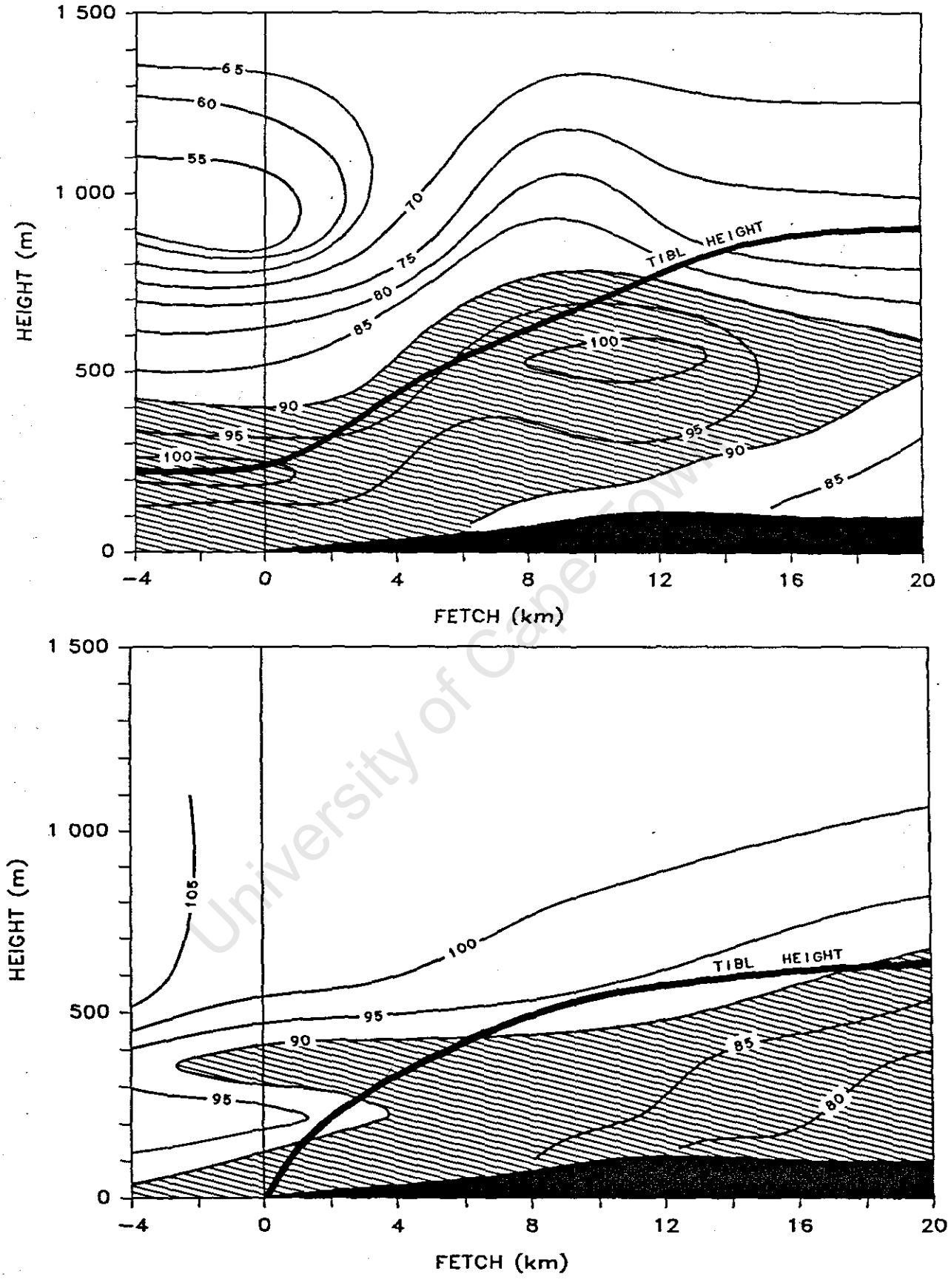


**Figure 13: Patterns of relative humidity (%) for (a) Run 413, Type A and (b) Run 331, Type B.**

moisture content within the entrainment region. Occasionally additional clouds associated with the sea breeze were also observed. The same structure of an evolving dry layer near the ground with more moist conditions aloft was evident from the vertical profiles of relative humidity (see Figures 14a and b, Run 413 and Run 331).

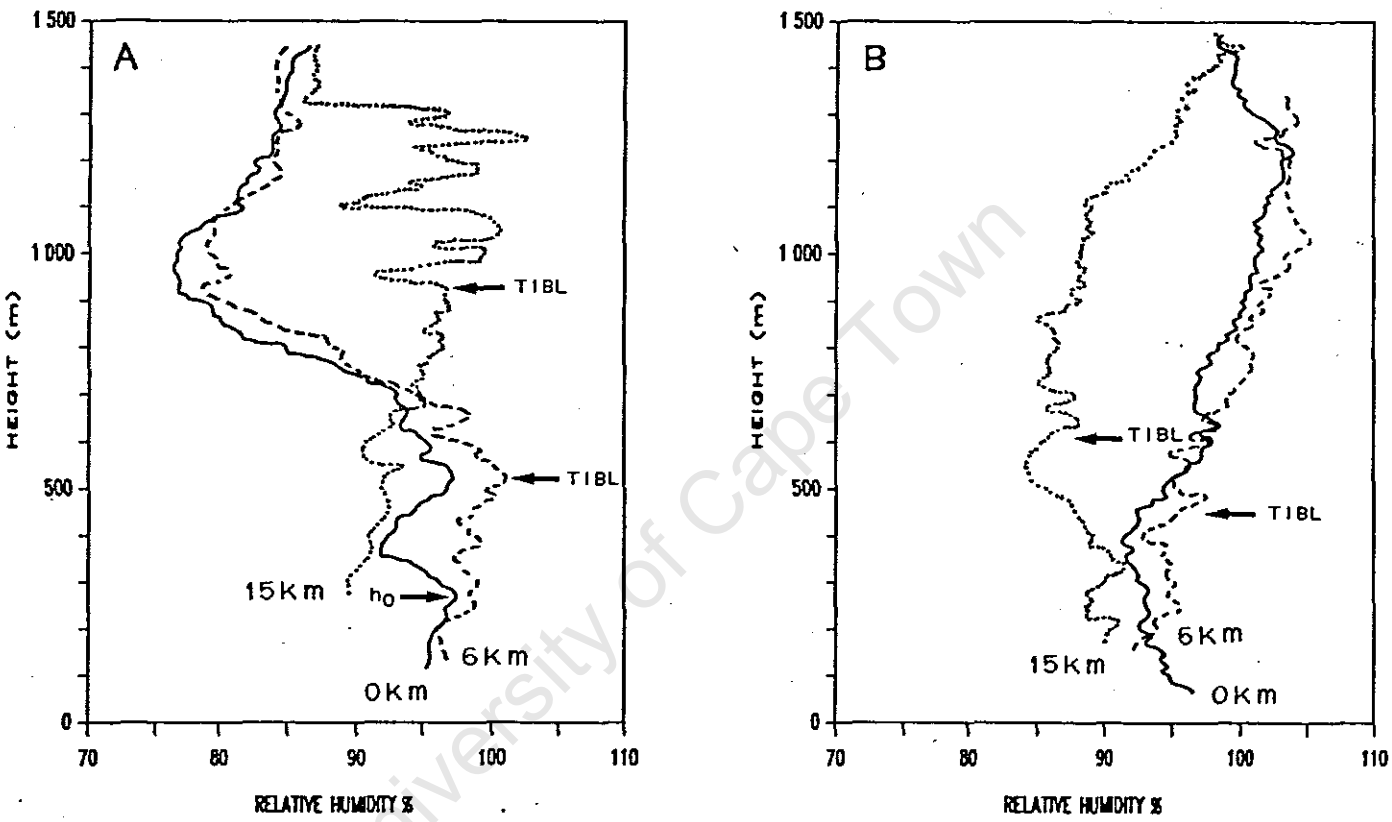


**Figure 14:** Vertical relative humidity (%) profiles for (a) Run 413, Type A and (b) Run 331, Type B.



TURBULENCE STRUCTURE

The pattern of turbulence in Type A-a is illustrated by Run 330 in Figure 15a. Values of $\sigma_w$ in the initial mixed layer and in the TIBL were 0.2m.s$^{-1}$ to 0.35m.s$^{-1}$, while out of the TIBL $\sigma_w$ was about 0.15m.s$^{-1}$. The growth of the TIBL took place from the top of the initial mixed layer at about 200m height near the coast. Free convection at 6km to 7km

moisture content within the entrainment region. Occasionally additional clouds associated with the sea breeze were also observed. The same structure of an evolving dry layer near the ground with more moist conditions aloft was evident from the vertical profiles of relative humidity (see Figures 14a and b, Run 413 and Run 331).

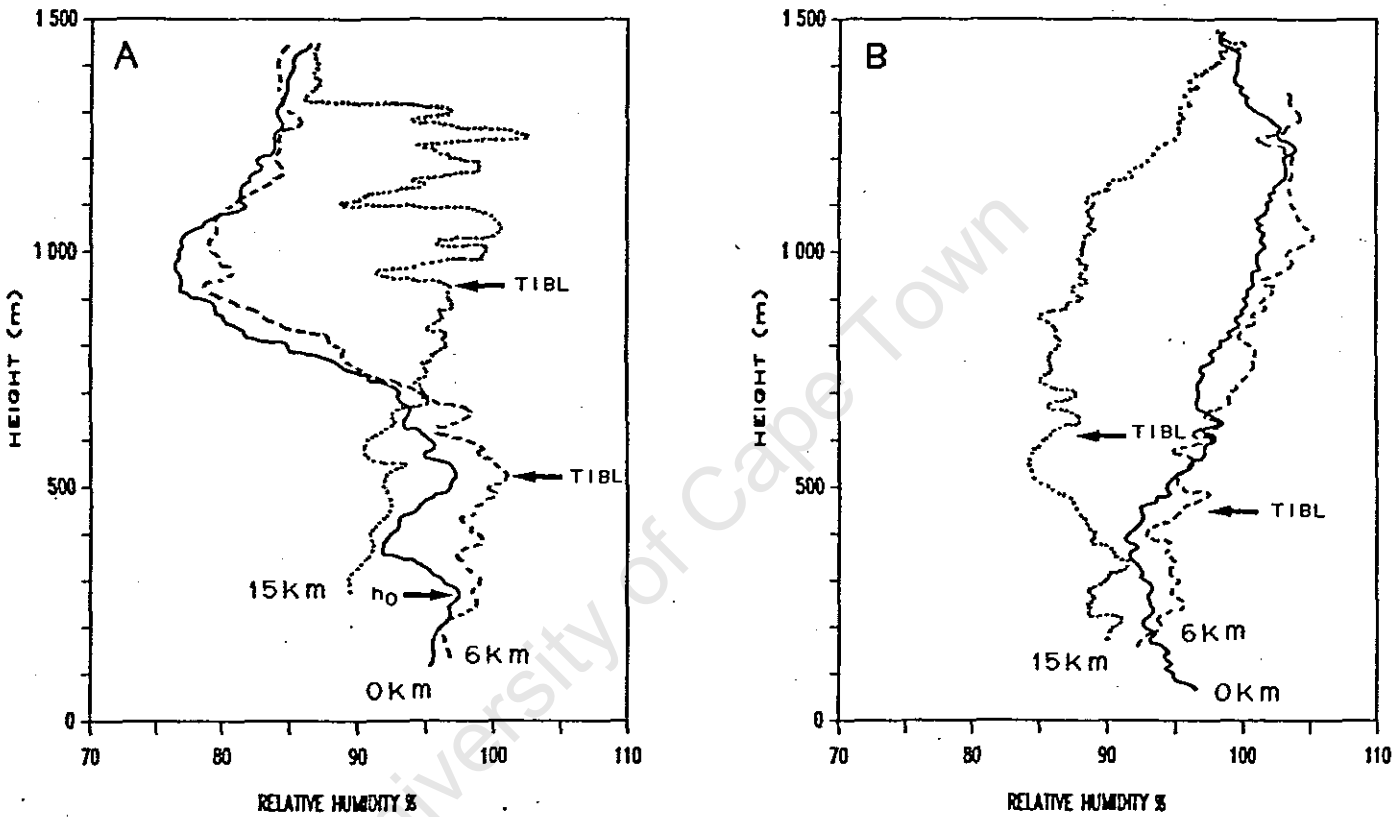


**Figure 14:** Vertical relative humidity (%) profiles for (a) Run 413, Type A and (b) Run 331, Type B.



TURBULENCE STRUCTURE

The pattern of turbulence in Type A-a is illustrated by Run 330 in Figure 15a. Values of $\sigma_w$ in the initial mixed layer and in the TIBL were 0.2m.s$^{-1}$ to 0.35m.s$^{-1}$, while out of the TIBL $\sigma_w$ was about 0.15m.s$^{-1}$. The growth of the TIBL took place from the top of the initial mixed layer at about 200m height near the coast. Free convection at 6km to 7km

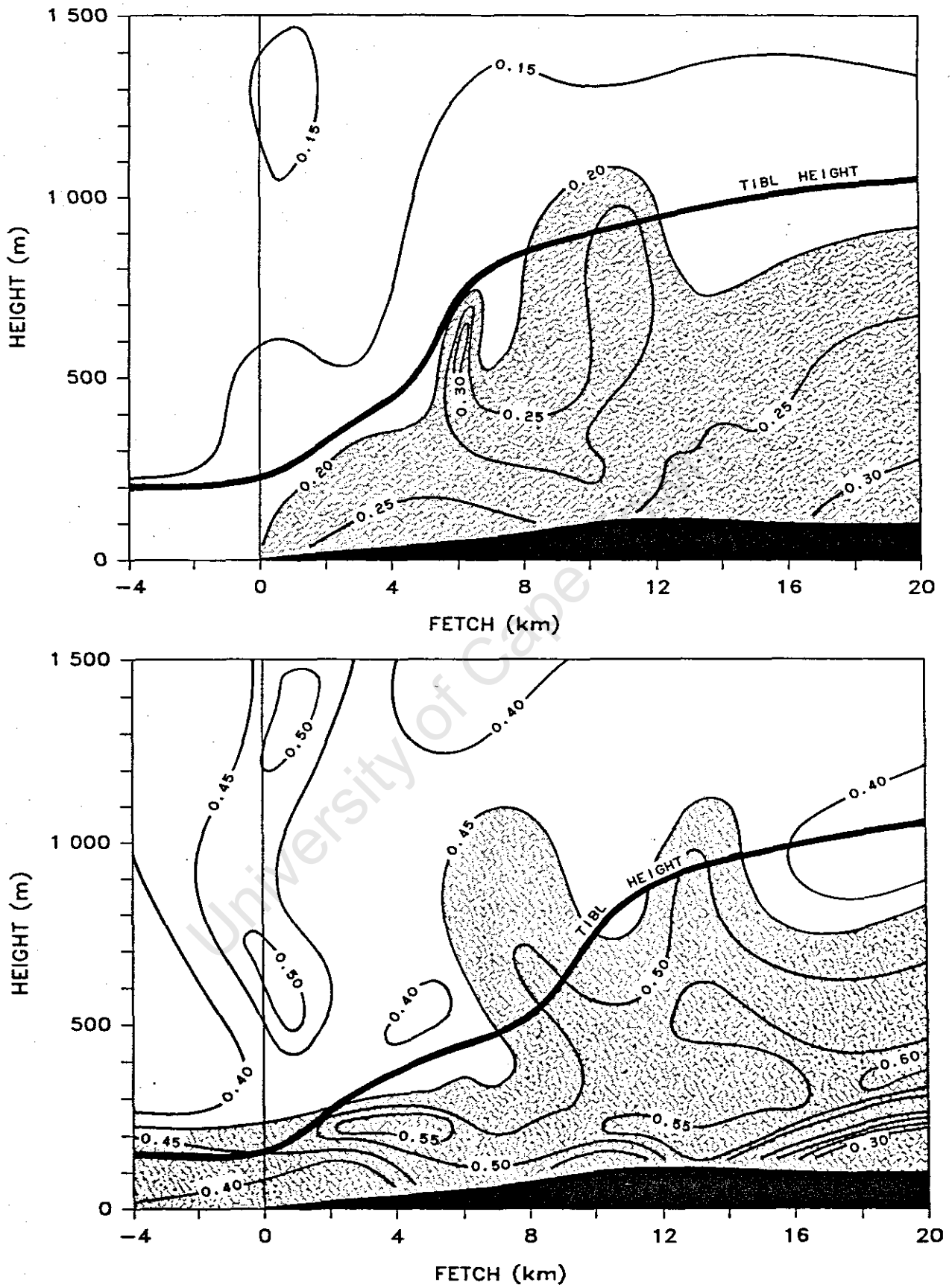




**Figure 15:** Turbulence ($\sigma_w$ in $m.s^{-1}$) cross-sections for (a) Run 330, Type A-a and (b) Run 319, Type A-b.

resulted in a strong turbulent upcurrent, probably a thermal, the effects of which were felt up to 800m. Further inland (≈11km) increased turbulence associated with patches of cloud was found near the TIBL boundary.

The most striking feature of Type A-b (Figure 15b, Run 319) was the generally higher level of turbulence. This was attributable to the weak lapse rates found in this type, especially in the mixed layer which was unstable in places. Background turbulence was about $0.4m.s^{-1}$, increasing to $0.65m.s^{-1}$ in strong bands of turbulence nearer the ground. These bands were associated with regions of instability and the breakdown of vertical temperature gradients, especially in the lower layers of the TIBL. The convex TIBL boundary was badly defined and contorted, due to the persistence of complex patterns of turbulence aloft. As in all types, $\sigma_w$ was observed to decrease somewhat with height.

Type B-a (Figure 16a, Run 331) had the strongest lapse rates, and hence the lowest TIBLs were found in this case. Background levels of $\sigma_w$ were generally $0.1m.s^{-1}$, increasing to $0.25m.s^{-1}$ within the TIBL, with even greater values near the surface. The height of the TIBL never exceeded 600m, and was observed to cause serious plume trapping. The highly stable conditions evident in Type B-a resulted in a flattened convex TIBL boundary. Strong differences from Type A were evident in the lack of a turbulent mixed layer over the ocean, which in Type B-a only began at the coastline. The sharpest $\sigma_w$ gradient occurred at this point, with changes in turbulence elsewhere in the TIBL being less marked. Due to its confined nature this is the most vertically abrupt of the TIBL types.

Type B-b (Figure 16b, Run 401) behaved in a similar way to Type B-a, except that turbulence in the TIBL was somewhat higher and more widespread. This was caused by slightly weaker lapse rates, which allowed a larger degree of vertical mixing and entrainment. Very evenly spread

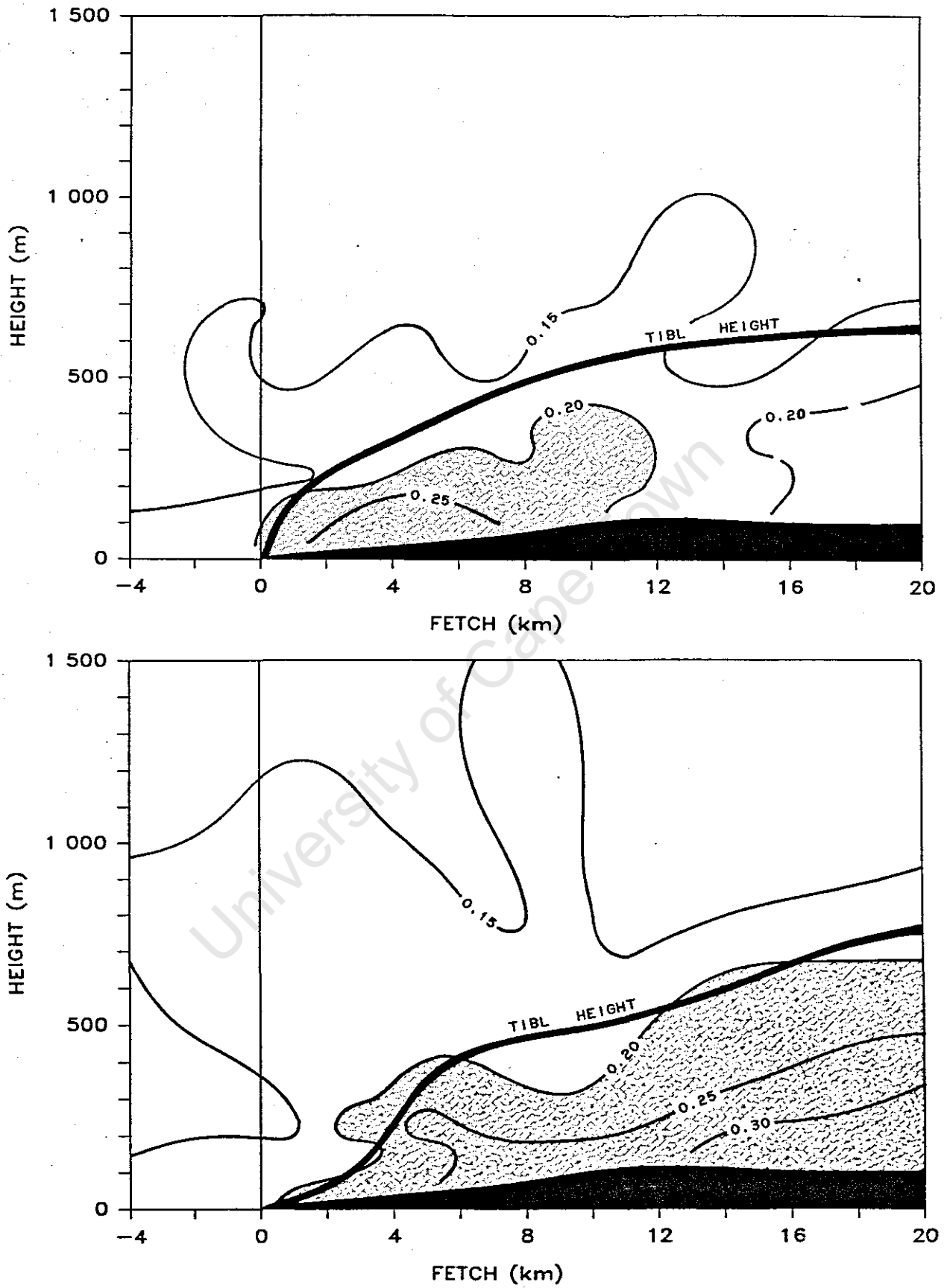


**Figure 16:** Turbulence ($\sigma_w$ in $m.s^{-1}$) cross-sections for (a) Run 331, Type B-a and (b) Run 401, Type B-b.

background turbulence was revealed by $\sigma_w$ values of about 0.15m.s$^{-1}$, with values in the TIBL of 0.2m.s$^{-1}$ to 0.3m.s$^{-1}$. The convex boundary of the TIBL exhibited a good spatial definition, and reached a height of over 700m inland. A common occurrence throughout all the data was the nature of the increase in turbulence at the TIBL boundary. Near the surface, $\sigma_w$ underwent a step change, with a more gradual transition at greater heights. This was due firstly to the steep slope of the TIBL near the coast, and secondly to the decreased intensity of turbulence away from the ground.

## SUMMARY AND CONCLUSIONS

This study has examined the meteorological characteristics of the TIBL in order to quantitatively define its typical mesoscale structure. This was achieved in a comprehensive coverage using ground based and airborne measurements over the length and height of the TIBL. This study has found that :

1) TIBLs were promoted under conditions of moderate to strong insolation with clear skies or scattered cloud. Large surface temperature differences occurred between sea and land, supplying convective and conductive energy for TIBL formation, and resulting in strong air temperature gradients;

2) Wind speeds in the TIBL were generally lower during more stable conditions, and higher during well mixed conditions. Speeds were significantly higher inland than at the coast due to the persistence of low level stability near the shore. The TIBL was located just above the height of the wind speed maximum, and was well below the wind speed minimum at the top of the sea breeze layer;

3) Wind direction of the onshore flow was usually oblique to the coastline, becoming normal over the land owing to the

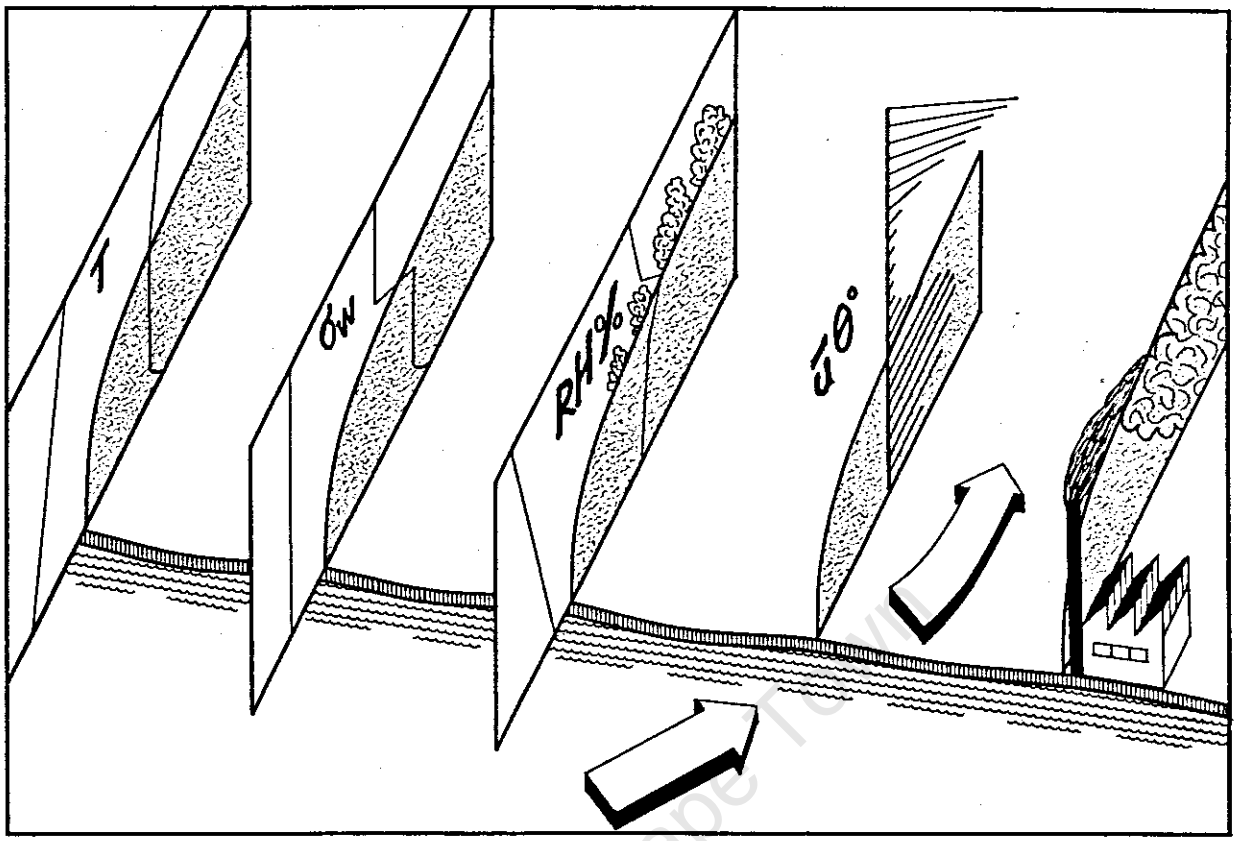


**Figure 17: Composite summary schematic of selected meteorological characteristics of the TIBL.**



effects of frictional drag in the TIBL, and thermal differences that cause the sea breeze. These effects were most pronounced near the surface, with wind direction showing a greater tendency towards the gradient flow with increased height;

4) Low level turbulence parameters showed a strong gradient near the coastline, with a two to fivefold increase occurring within the TIBL;

5) The shape of the TIBL was subject to flattening or expansion under different conditions, but the general convex form was maintained at all times. The sharpest change in TIBL characteristics took place in the first six kilometres, with the bulk of TIBL growth completed in the first fifteen to twenty kilometres;

6) The growth and decay of the TIBL closely followed the diurnal patterns of insolation, temperature and wind speed. The TIBL grew rapidly in the late morning after developing from earlier convective conditions. The TIBL height evened out during the day, decreasing slowly in the afternoon and more rapidly towards sunset;

7) Relative humidity decreased in the TIBL due to warmer temperatures in the mixed layer, which allowed greater uptake of evaporative moisture, and a consequent increase in specific humidity. The area of maximum relative humidity delineated the TIBL boundary in the entrainment region, and was associated with occasional scattered cloud;

8) The structure of the TIBL was strongly influenced both by the stability of the onshore flow and the presence or absence of an initial mixed layer. The height of the TIBL and the intensity of turbulence showed an inverse relationship with lapse rate. Least well defined TIBLs of the greatest vertical extent showed the highest degree of mixing, possessing an initial neutral layer and weak lapse rates. TIBLs occurring with stable onshore flow and strong lapse rates experienced severely limited vertical dispersion, with serious implications for air quality.

A composite summary schematic of the TIBL is given in Figure 17, illustrating the relative behaviour of the various parameters with respect to the structure of the TIBL. The eight cases of the TIBL examined in this study have outlined both the range and the typical patterns of meteorological variables that may be found, many of which complement the findings of other similar studies. Insight has also been gained of the complex overlay of component features that together comprise the TIBL.

## REFERENCES

Beran, D.W., Hooke, W.H. and Clifford, S.F., 1973: Acoustic echo sounding techniques and their application to gravity wave, turbulence and stability studies. *Boundary-Layer Meteorol.*, 4, 133-167.

Bornstein, R.D., 1968: Observations of the urban heat island effect in New York City. *J. Appl. Meteorol.*, 7, 575-582.

Comrie, A.C., 1986: Thermal internal boundary layers in the South Western Cape - a report on the first field investigation. Unpublished Internal Report, Dept. of Environ. and Geog. Sci., Univ. of Cape Town, 15pp.

Echols, W.T. and Wagner, N.K., 1972: Surface roughness and internal boundary layer near a coastline. *J. Appl. Meteorol.*, 11, 658-662.

Gamo, M., Yamamoto, S. and Yokoyama, O., 1982: Airborne measurements of the free convective internal boundary layer during the sea breeze. *J. Meteorol. Soc. Japan*, 60, 1284-1298.

Hewson, E.W. and Olsson, L.E., 1967: Lake effects on air pollution dispersion. *J. Air Poll. Control Assoc.*, 17, 757-761.

Keen, C.S., 1984: Sea breezes in the complex terrain of the Cape Peninsula. Postprints from the Third Conf. on Meteorology of the Coastal Zone, Miami, Florida, *Amer. Meteorol. Soc.*, Boston, 129-134.

Kerman, B.R., Mickle, R.E., Portelli, R.V., Trivett, N.B. and Misra, P.K., 1982: The Nanticoke shoreline diffusion experiment, June 1978-II: Internal boundary layer structure. *Atmos. Environ.*, 16, 423-437.

Knox, N.E. and Lyons, W.A., 1975: The thermal internal boundary layer in a shoreline environment during summer fumigation episodes. Presented at the First Conf. on Regional and Mesoscale Analysis and Predictions, Las Vegas, Nevada, *Amer. Meteorol. Soc.*, Boston.

Lenschow, D.H., 1976: Estimating updraft velocity from airplane response. *Mon. Wea. Rev.*, 104, 618-627.

Lyons, W.A., 1975: Turbulent diffusion and pollutant transport in shoreline environments. Lectures on air pollution and environmental impact analysis, Workshop on Meteorology and Environmental Assessment, *Amer. Meteorol. Soc.*, Boston, 136-208.

Lyons, W.A. and Cole, H.S., 1973: Fumigation and plume trapping on the shores of Lake Michigan during stable onshore flow. *J. Appl. Meteorol.*, 12, 494-510.

Ogawa, Y. and Ohara, T., 1985: The turbulent structure of the internal boundary layer near the shore. *Boundary-Layer Meteorol.*, 31, 369-384.

Ogawa, Y., Ohara, T., Wakamatsu, S., Diosey, P.G. and Uno, I., 1985: Observation of lake breeze penetration and subsequent development of the thermal internal boundary layer for the Nanticoke II shoreline diffusion experiment. *Boundary-Layer Meteorol.*, 32, 207-230.

Portelli, R.V., 1982: The Nanticoke shoreline diffusion experiment, June 1978-I: Experimental design and program overview. *Atmos. Environ.*, 16, 413-421.

Prophet, D.T., 1961: Survey of available information pertaining to the transport and diffusion of airborne material over ocean and shoreline complexes. Tech. Report 89, Aerosol Lab., Stanford Univ., 53pp.

Raynor, G.S., SethuRaman, S. and Brown, R.M., 1979: Formation and characteristics of coastal internal boundary layers during onshore flows. *Boundary-Layer Meteorol.*, 16, 487-514.

SethuRaman, S., (ed.), 1984: A Summary of the Brookhaven Workshop on Coastal Atmospheric Transport Processes. Postprints from the Third Conference on Meteorology of the Coastal Zone, Miami, Florida, *Amer. Meteorol. Soc.*, Boston, 121-128.

SethuRaman, S., Brown, R.M., Raynor, G.S. and Tuthill, W.A., 1979: Calibration and use of a sailplane variometer to measure vertical velocity fluctuations. *Boundary-Layer Meteorol.*, 16, 99-105.

Stunder, M. and SethuRaman, S., 1985: A comparative evaluation of the coastal internal boundary-layer height equations. *Boundary-Layer Meteorol.*, 32, 177-204.

Van der Hoven, I., 1967: Atmospheric transport and diffusion at coastal sites. *Nuclear Safety*, 8, 490-499.

Weisman, B. and Hirt, M.S., 1975: Dispersion governed by the thermal internal boundary layer. Presented at 68th Meeting, Air Poll. Control Assoc., Boston.

CHAPTER 3

# THE MESOSCALE TURBULENT STRUCTURE OF THE THERMAL INTERNAL BOUNDARY LAYER

The mesoscale structure of turbulence in a Thermal Internal Boundary Layer (TIBL) was investigated by making use of an instrumented light aircraft for measurements spanning the length and height of the TIBL. The TIBL developed from the initially stable onshore flow as a neutral and slightly unstable layer within the sea breeze, possessing regular strong fluctuations of temperature and vertical wind speed. The value of sensible heat flux within the TIBL varied greatly, but was strongly positive in the surface layer, moderate to slightly negative within the mixed layer, and negligible outside the TIBL. Analysis of standard deviations revealed a similar magnitude of data in comparison between the TIBL and the Convective Boundary Layer, but the increase in turbulence associated with the top of the latter was not generally present, and instead a smooth decrease of turbulence with non-dimensional height was found in the TIBL.

## INTRODUCTION

Coastal areas encompass not only the interface between marine and terrestrial surfaces, but also a zone in which a complex meteorological environment is evolved. Emissions from industries, petrochemical complexes, power stations and nuclear facilities into the coastal atmosphere have raised concern about the dispersion of air pollutants in these areas. Of particular influence are effects such as the sea breeze circulation, and the development of the Thermal Internal Boundary Layer (TIBL), which result in strong horizontal and vertical contrasts in turbulent diffusion parameters.

The TIBL is formed under conditions of onshore flow due to surface discontinuities of roughness and temperature, which generate mechanical and thermal turbulence. The adjustment of the atmosphere to the new conditions takes place most rapidly near the shoreline and is more gradual further inland, producing a characteristically convex shaped boundary that separates the modified turbulent air from the unmodified stable air aloft. The strong differences in stability and turbulence between the two regions can severely limit vertical dispersion in the TIBL, especially near the coast, causing fumigation and plume trapping and a consequent increase in ground level concentrations.

Initial TIBL studies evolved from both boundary layer work and from research into coastal air quality and land and sea breezes, with early contributions by Elliot (1958), Prophet (1961) and Van der Hoven (1967). Numerous papers have appeared on the complex fumigation phenomenon, including Collins (1971), Lyons and Cole (1973) and Peters (1975). More recently, large scale field studies of the TIBL have taken place at Brookhaven (Raynor *et al*, 1979), Nanticoke (Portelli, 1982; Kerman *et al*, 1982) and at Kashimaura in Japan (Gamo *et al*, 1982). Very few specific examinations of the structure and dynamics of turbulence within the TIBL

occur in the literature, especially at a scale covering the entire TIBL. Much theoretical and practical work on the Convective Boundary Layer (CBL) has been applied to turbulence in the TIBL, especially studies such as Wyngaard *et al* (1971), Deardorff (1972), Kaimal *et al* (1976), Caughey and Palmer (1979) and Nicholls and Readings (1979). Such analyses of the TIBL have been performed at low level near the shore, and further inland using meteorological towers and instrumented kytoons, for example Echols and Wagner (1972), Smedman and Högström (1983), Ogawa and Ohara (1985), Ohara and Ogawa (1985) and Ogawa *et al* (1985).

The purpose of this study is to undertake a mesoscale examination of the turbulent characteristics of the TIBL. It is intended to detail the structure of various turbulence parameters as observed in the field, by means of airborne measurements spanning the length and height of the TIBL.



## DATA ACQUISITION AND PROCESSING

### Methodology

Figure 1 illustrates the location of the study area on the Atlantic coast, about 30km to the north of Cape Town. The shoreline is approximately linear with a NNW to SSE alignment. The terrain slopes gently upward from the coast to about 100m at 20km inland, displaying little relief except for a number of hills further to the south and north of the study area. The land surface is mostly ploughed wheatfields, with some grass and bush cover nearer the shore. A number of small settlements and farms are found in the region, and centrally located on the coastline is the 2000MW Koeberg nuclear power station.

Airborne measurements of temperature, humidity and turbulence were taken using a light aircraft mounted with a thermistor psychrometer and a miniaturised quartz diaphragm

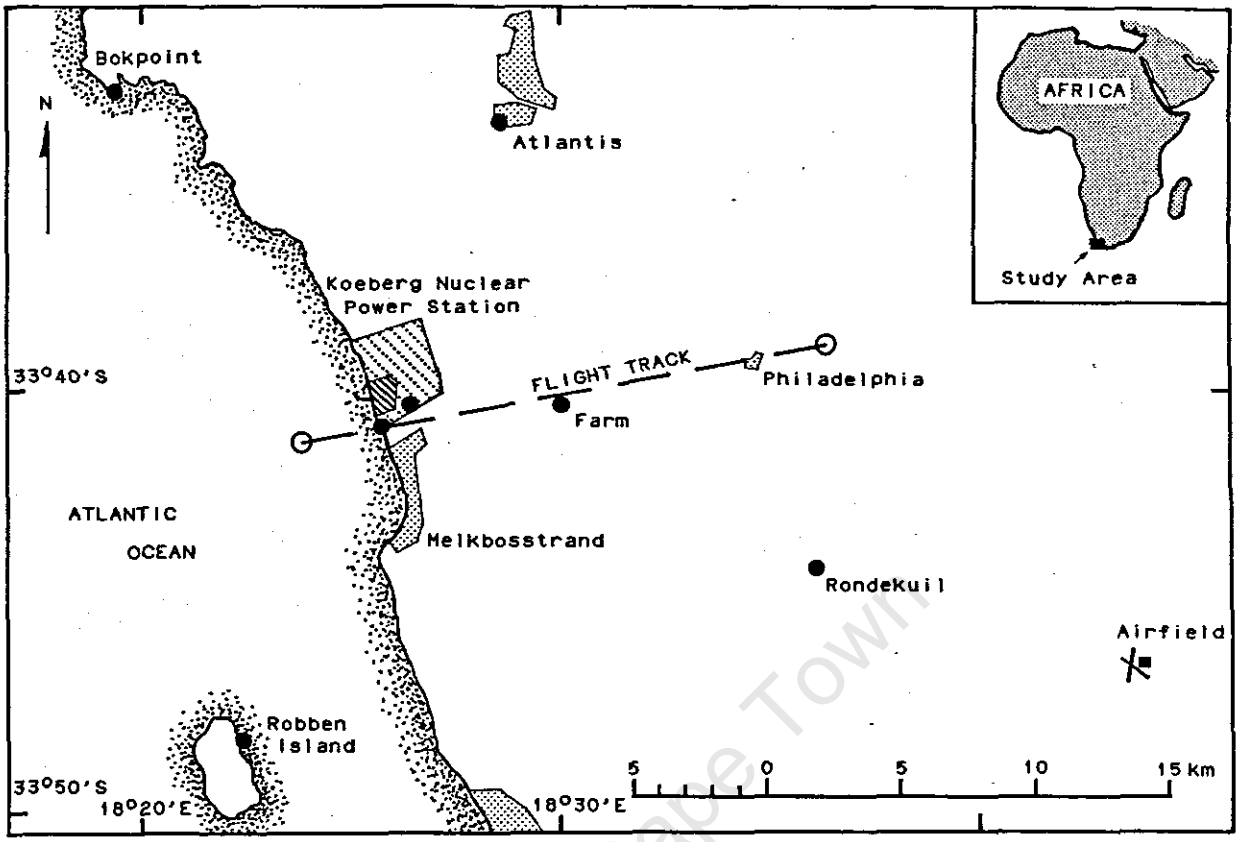


**Figure 1:** Location of the study area on the Southern African coastline showing aircraft flight track (broken line).



pressure transducer specially adapted for turbulence measurements (Comrie, 1988). This approach is similar to those of Raynor *et al* (1979) and Gamo *et al* (1982), and is based on the method outlined by SethuRaman *et al* (1979). The aircraft (Cessna 172) was flown at a constant thrust and pitch angle, allowing it to be sensitive to vertical eddies while still maintaining the general flight path, thus taking advantage of the motion and response of the aircraft itself to measure turbulence. Traverses across the study area were flown at six preselected levels, exponentially spaced from 152m to 1341m altitude, covering a horizontal distance of about 20km from offshore to well inland (Figure 2). Three vertical temperature profiles were made prior to turbulence measurements, one in the stable atmosphere over the sea and two at distances further inland. An entire run took a little over one hour, and was performed near midday when conditions were changing least.

Raw data were read at 10Hz and recorded directly by computer in the aircraft. Later analysis of the data revealed an optimum response time of 0.5 seconds using this method, the same figure arrived at in SethuRaman *et al* (1979). Data were then processed to provide integral values of 5 samples at 2Hz, after which the individual readings of temperature and vertical velocity were used to compute turbulence parameters such as fluxes and standard deviations. Wind speed and direction profiles were obtained using double theodolite pibal tracking from a site 6km inland.

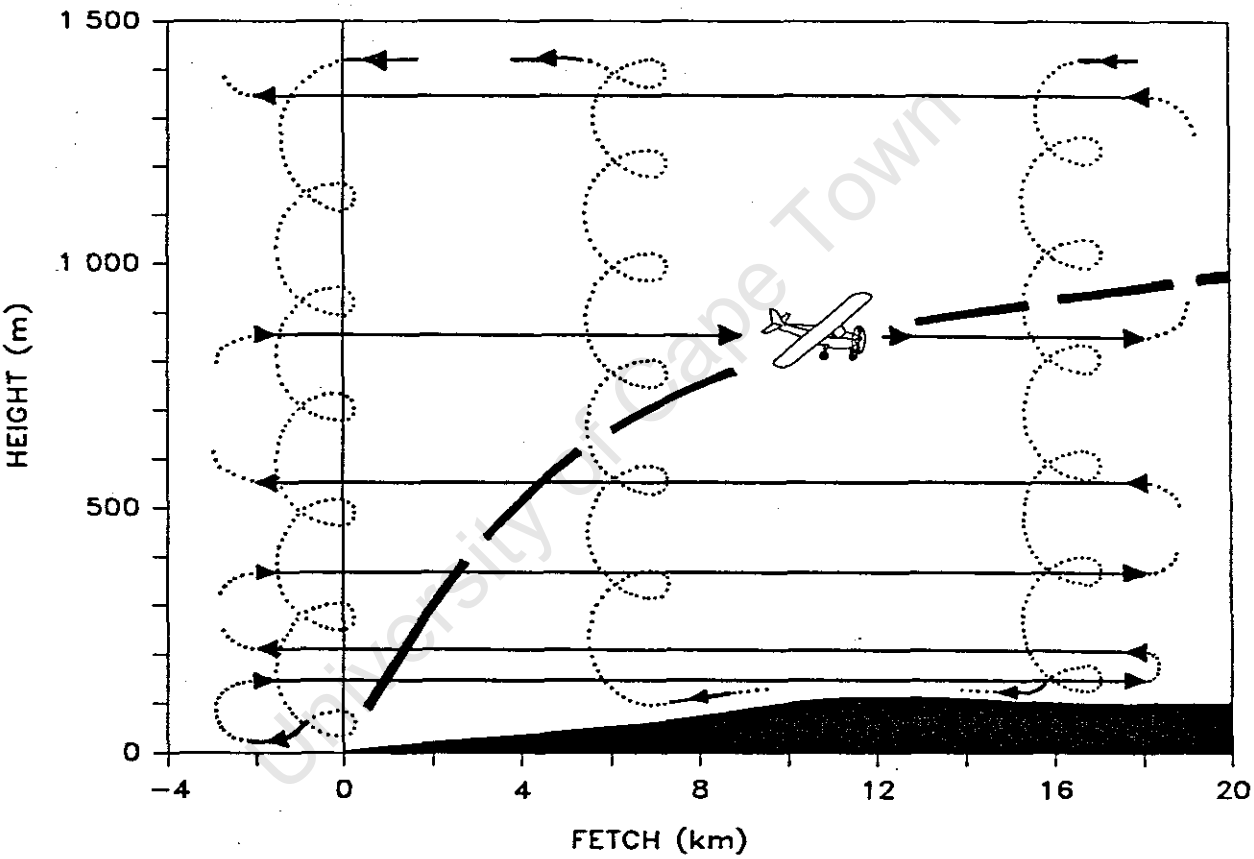


**Figure 2:** Aircraft flight plan for vertical profiles of temperature (dotted line) and horizontal transects of turbulence and temperature (solid line).



**Scaling**

Nicholls and Readings (1979) presented idealised limits of validity for various types of scaling based on values of the non-dimensional lengths $z/z_i$ and $z/L$. The data presented here fell chiefly in the mixed layer, but because some of the data fell in the free convection zone near the surface it was decided to apply both mixed layer and surface layer scaling to the data. The same approach was used to perform

the similarity analysis in Ohara and Ogawa (1985). The value of the friction velocity $u_*$ was approximated from the relationship

$$\sigma_w = a.u_*$$

where $a$ has been shown to be very close to 1.3 for the first few hundred metres of the boundary layer (Fiedler and Panofsky, 1972). A representative surface layer value for $\sigma_w$ of about $0.5 m.s^{-1}$ was obtained by three methods: from downward extrapolation of the data; from the Koeberg meteorological mast; and from other studies over similar terrain. This resulted in a $u_*$ value of approximately $0.4 m.s^{-1}$, a typical value for the terrain and wind speeds concerned (Kaimal *et al*, 1976; Wyngaard, 1983). A fairly close approximation of the surface heat flux $Q_0$ ($\overline{w'\theta'}_0$) was made from measurements of solar radiation ($S$) in the relationship

$$Q_0(t) = A.S(t)$$

with $A$ = 0.39 (Misra and Onlock, 1982; Venkatram, 1986). The resulting values for $Q_0$ of around $300 W.m^{-2}$ to $350 W.m^{-2}$ were very characteristic of a hot summers day near noon (Betts, 1973; Carson, 1973; Caughey and Palmer, 1979; André, 1983). Calculation of other surface and mixed layer parameters was then performed.

**TIBL height determination**

The determination of TIBL height $z_i$ was made largely from horizontal profiles of potential temperature in a similar fashion to Gamo *et al* (1982). The TIBL boundary was taken as the point where the temperature trace began to increase, which usually coincided with the onset of large fluctuations. Clarity was occasionally provided by reference to the $w'\theta'$ trace or the individual component traces, as well as the available vertical temperature profiles. This

enabled a fairly precise measurement of $z_i$, with discrepancies between temperature and turbulence definitions of TIBL height no more than 10% (50m), far less than the 40% quoted in Gamo (1982).

## RESULTS AND DISCUSSION

### Flow characteristics

#### SURFACE CONDITIONS

The field experiments were conducted during the late southern summer in March and April of 1987. For this study the results from one particular test period were used, 1 April 1987. On this day the weather was fair with a light scattering of cumulus cloud inland. The synoptic surface pressure gradient was weak, resulting in generally light WNW winds which became moderate WSW with the development of the onshore sea breeze flow. Observations were made between 12h45 and 14h15, during which time solar radiation ranged between 750W.m$^{-2}$ and 950W.m$^{-2}$, the mean sea and land surface temperatures were 15.8$^{o}$C and 37.9$^{o}$C respectively, and the mean 10m air temperature was 22$^{o}$C. Table 1 gives a number of measured and calculated boundary layer parameters, showing surface and mixed layer characteristics and the observed TIBL height at selected distances inland.

#### WIND PROFILES

Figure 3 illustrates the wind data, showing mean and individual vertical profiles of wind speed and direction, taken at roughly 10 minute intervals between 13h16 and 13h55. The bowed shape of the wind speed profile revealed the characteristic influence of a sea breeze component, with a maximum occurring at roughly 350m and a minimum at about 1500m. Wind speeds ranged from 5m.s$^{-1}$ to 10m.s$^{-1}$ in the lower regions and were 0.5m.s$^{-1}$ to 3m.s$^{-1}$ aloft, while above

TABLE 1
(a) Boundary layer parameters at x=5900m
and (b) TIBL height (12h45 - 14h15)

(a)*

| $Q_0$ | $u_*$ | $T_*$ | $-L$ | $w_*$ | $\theta_*$ | $\theta_0$ | $u_{152}$ | $u_{10}$ |
|---|---|---|---|---|---|---|---|---|
| 0.25 | 0.4 | 0.625 | 19.13 | 1.51 | 0.166 | 293 | 8 | 5.5 |

(b)

| $x$ | 0 | 3 | 6 | 9 | 12 | 15 | (Km) |
|---|---|---|---|---|---|---|---|
| $z_i$ | ≈0 | 130 | 410 | 490 | 580 | 680 | (m) |

* Units in appendix 3.1.

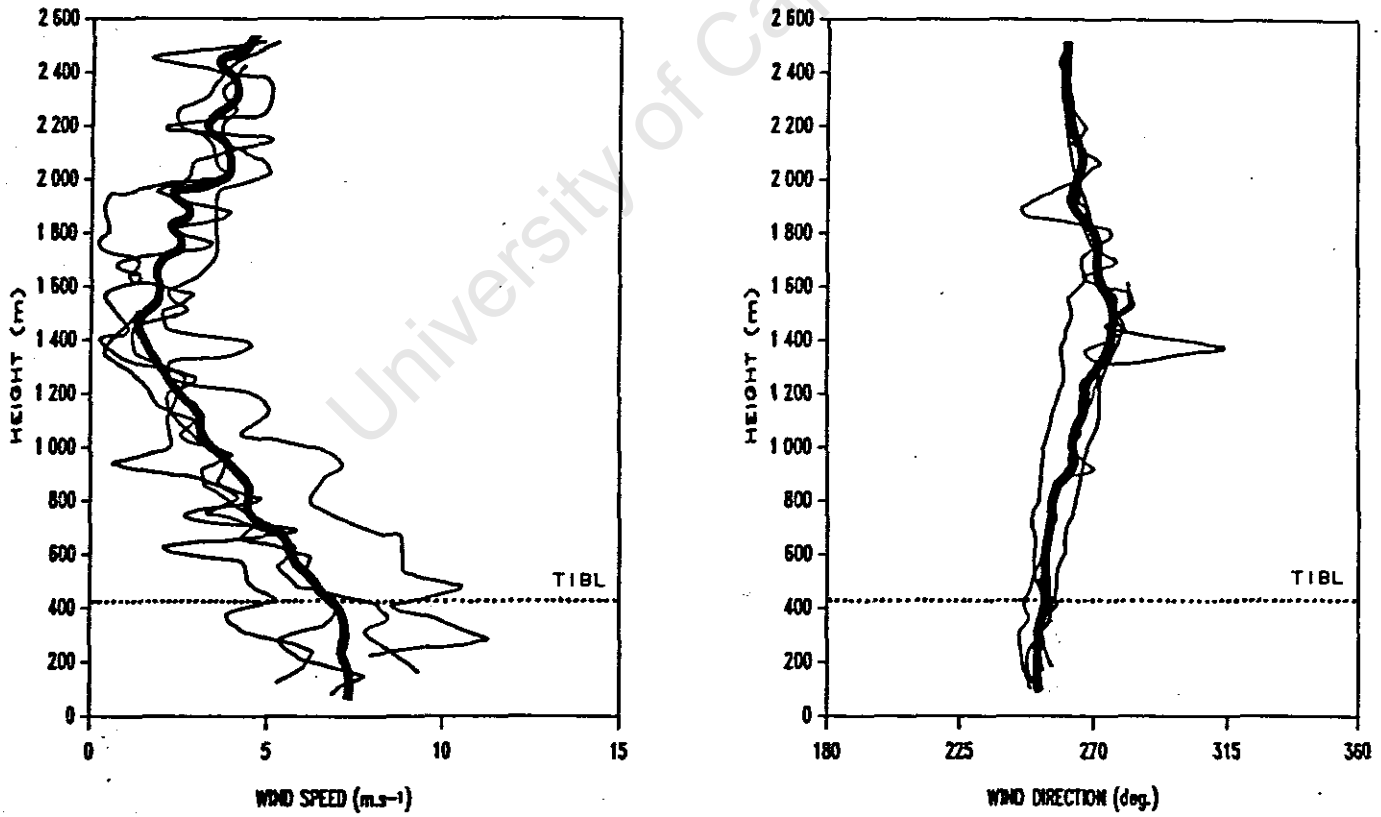


Figure 3: Vertical wind profiles showing mean wind speed and direction (bold lines) and individual profiles (feint lines), with the height of the TIBL boundary (dotted line).

1500m there was a layer of increasing wind speed unrelated to the TIBL or the sea breeze component, resulting from the prevailing gradient flow. The greatest variability in wind speed was found, as expected, nearer the ground, while the TIBL height was observed just above the wind speed maximum ($z_i$ = 410m). Ogawa *et al* (1985) noted much the same effect in relation to the TIBL in a lake breeze.

The wind direction profile reflected a similar situation to that above, with the influence of the sea breeze component being displayed nearer the surface. Close to the surface, wind direction was almost exactly perpendicular to the shoreline (250$^{o}$), matching the region of higher wind speeds, while higher up above the TIBL, wind direction swung gradually to a westerly gradient flow. This profile illustrated the lack of return flow aloft, while highlighting the flow normal to the coast near the ground, where wind direction remained roughly constant throughout the TIBL.

POTENTIAL TEMPERATURE

Figure 4 illustrates vertical profiles of potential temperature, taken over the sea and at 6km and 15km inland respectively. Onshore flow displayed a relatively constant stable potential temperature profile of about 0.005K.m$^{-1}$ throughout the atmosphere, with no initial mixed layer occurring near the surface. At 15km inland the mixed layer of the TIBL had reached a height of about 650m, displaying slight instability of about -0.005K.m$^{-1}$ in the lower regions and more neutral stability further up. Above the TIBL the stable layer persisted, although not as smooth in profile as over the sea.

Figure 5 shows a cross-sectional profile of potential temperatures in the TIBL constructed from horizontal traverses, from which a characteristic pattern was identified. The initial stable onshore flow was present,

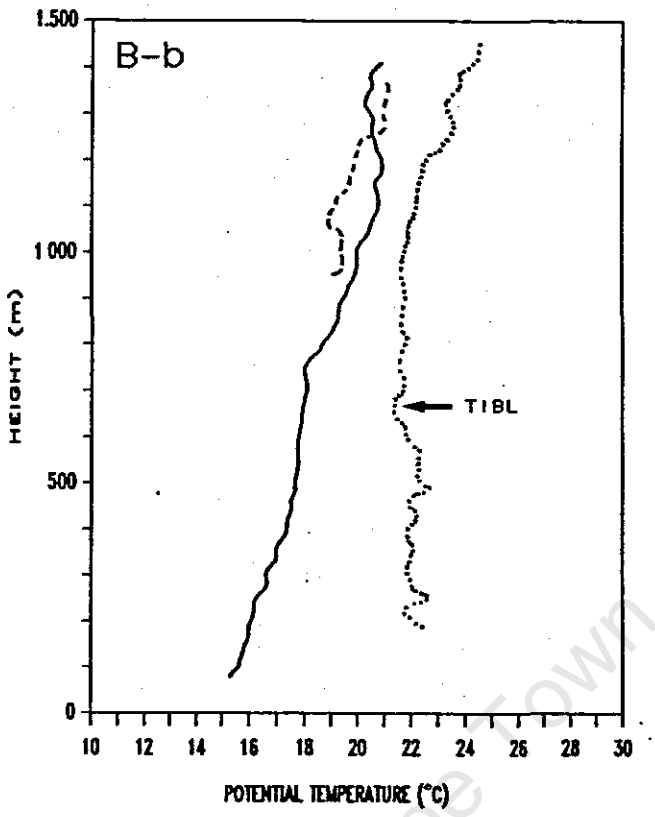


**Figure 4:** Vertical profiles of potential temperature (°C) taken over the sea (solid line), and at 6km (broken line) and 15km inland (dotted line).



with slightly stronger stability near the surface. Further inland, the height of the TIBL increased from the ground upwards forming a region of well mixed air. Above this was found the entrainment region, characterised by the first undulations of the isotherms, where changes in potential temperature originated. This transition zone between the TIBL and unmodified air was denoted by a decrease in stability, although not yet neutral, compared to aloft where potential temperatures were horizontally consistent and unaffected by boundary layer formation. The TIBL boundary was thus found to lie between the stable layer and the mixed layer in the entrainment region, and was somewhat irregular in nature due to the intermittent nature of the temperature changes. Also, the mean data used in this analysis indicated at least fairly coarse scale entrainment wave formation of the order of 10km in wavelength (see following section).

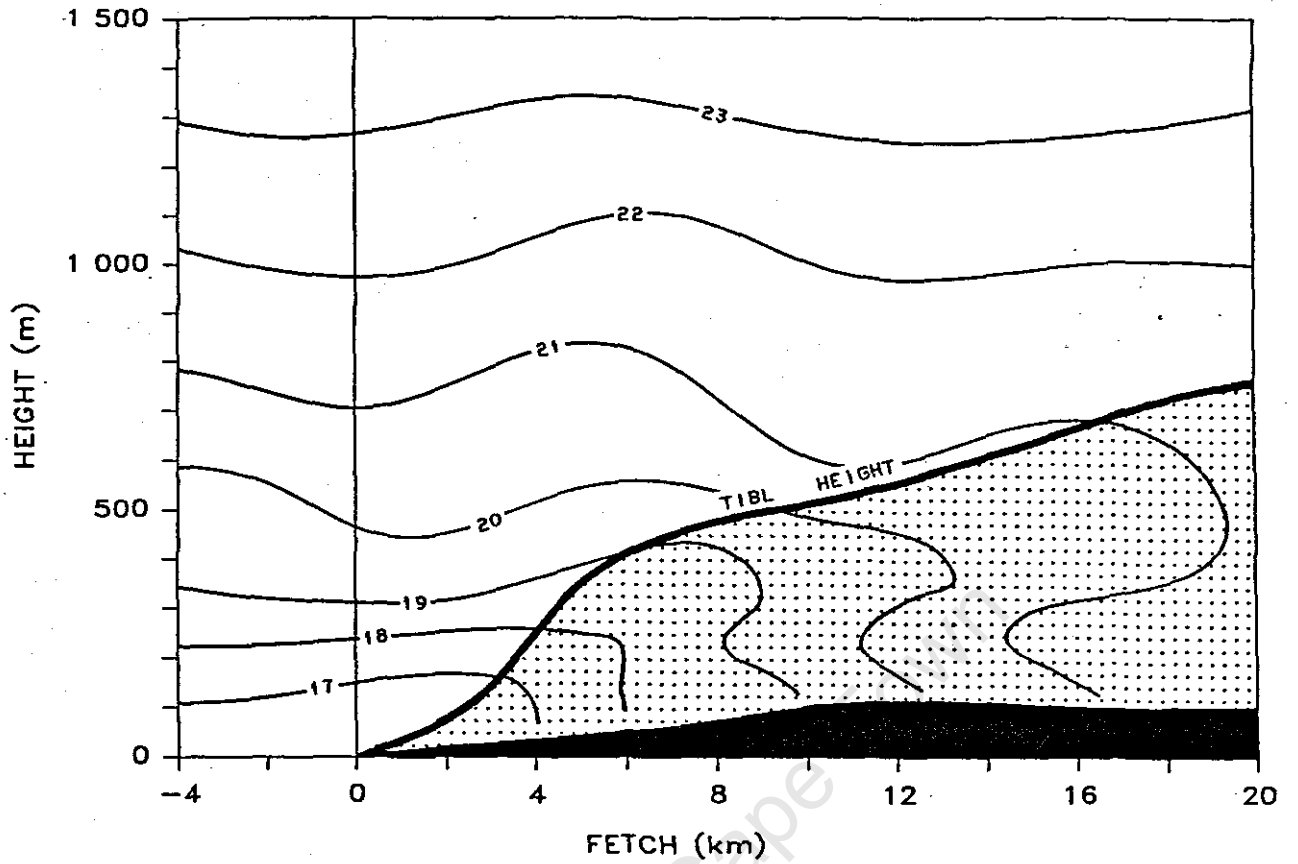


Figure 5: Cross-section of potential temperature pattern ($^{o}$C) for Run 401.



## INSTANTANEOUS FLUCTUATIONS

Figure 6 depicts the instantaneous potential temperature and vertical velocity fluctuations at different heights and distances downwind. The fluctuations in the temperature trace were of the least magnitude and frequency over areas nearer the coast and also with increased altitude, and were greatest further inland and nearer the surface. Temperature fluctuations outside the TIBL ranged from -0.1$^{o}$C to 0.1$^{o}$C, whereas values within the TIBL were -0.4$^{o}$C to 0.4$^{o}$C, with actual temperatures showing a corresponding increase. Closer to the ground the fluctuations were relatively frequent and evenly spaced, while higher up, especially near the top of the TIBL, they were more irregular and intermittent. Wavelengths of the variations in potential temperature were of the order of 500m.

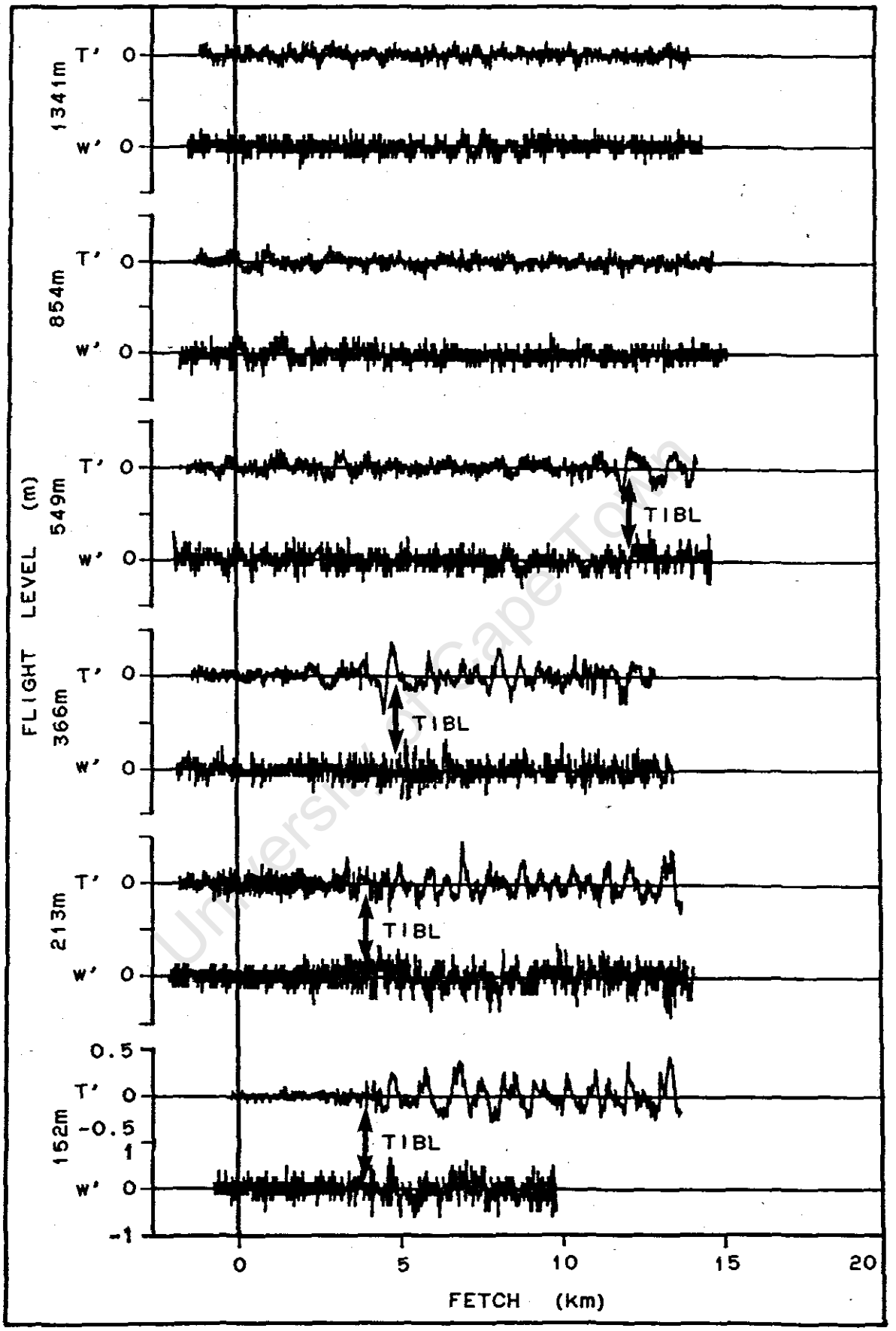


**Figure 6:** Instantaneous potential temperature (±0.5°C) and vertical velocity (±1m.s$^{-1}$) fluctuations for the six flight levels showing turbulence outside and within the TIBL.

Similar patterns can be seen in the vertical velocity traces where turbulence-induced variations in the vertical wind speed were also greatest both inland and nearer the surface, with decreased values at greater heights as well as over the sea. Within the TIBL, values of *w* varied between $-0.4m.s^{-1}$ and $0.4m.s^{-1}$, while outside the TIBL this range decreased to $-0.2m.s^{-1}$ and $0.2m.s^{-1}$. The patterns of intermittent turbulence noted above were more noticeable in the *w* trace than in the temperature trace. Downward variations in temperature were more damped than the corresponding motions for *w*, a phenomenon noted also in Lumley and Panofsky (1964). Fairly strong cycles or changes in vertical wind speed occurred inside the TIBL, and were most regular nearer the surface, with intermittent patches of turbulence near the upper boundary of the TIBL. In the unmodified air outside the TIBL relatively uniform patterns of background turbulence were present. Observations of the relative behaviour of the *T* and *w* traces seem to indicate that positive updrafts were largely associated with temperature increases, and vice versa for downdrafts, which resulted in a generally positive heat flux relationship.

## Fluxes

### HEAT FLUX

Figure 7 shows an example of raw sensible heat flux data, taken at 152m. This trace is illustrative of the variations experienced, and shows the minimal sensible heat flux that occurred outside the TIBL as well as the far greater increases and decreases encountered upon entering the TIBL. Background levels of heat flux were below $0.01m.s^{-1}.K^{-1}$ and increased as much as tenfold in the TIBL. Similar behaviour in vertical profiles of heat flux were found in Smedman and Högström (1983) and in Ogawa *et al* (1985). Observation of the mean heat flux (Figure 8) for the same data clearly illustrates the above increases (calculated values are 25

second averages). There was a definite tendency to a positive heat flux within the TIBL, although smaller scale variations and some degree of stable stratification in the atmosphere gave rise to regions of negative heat flux. Mean

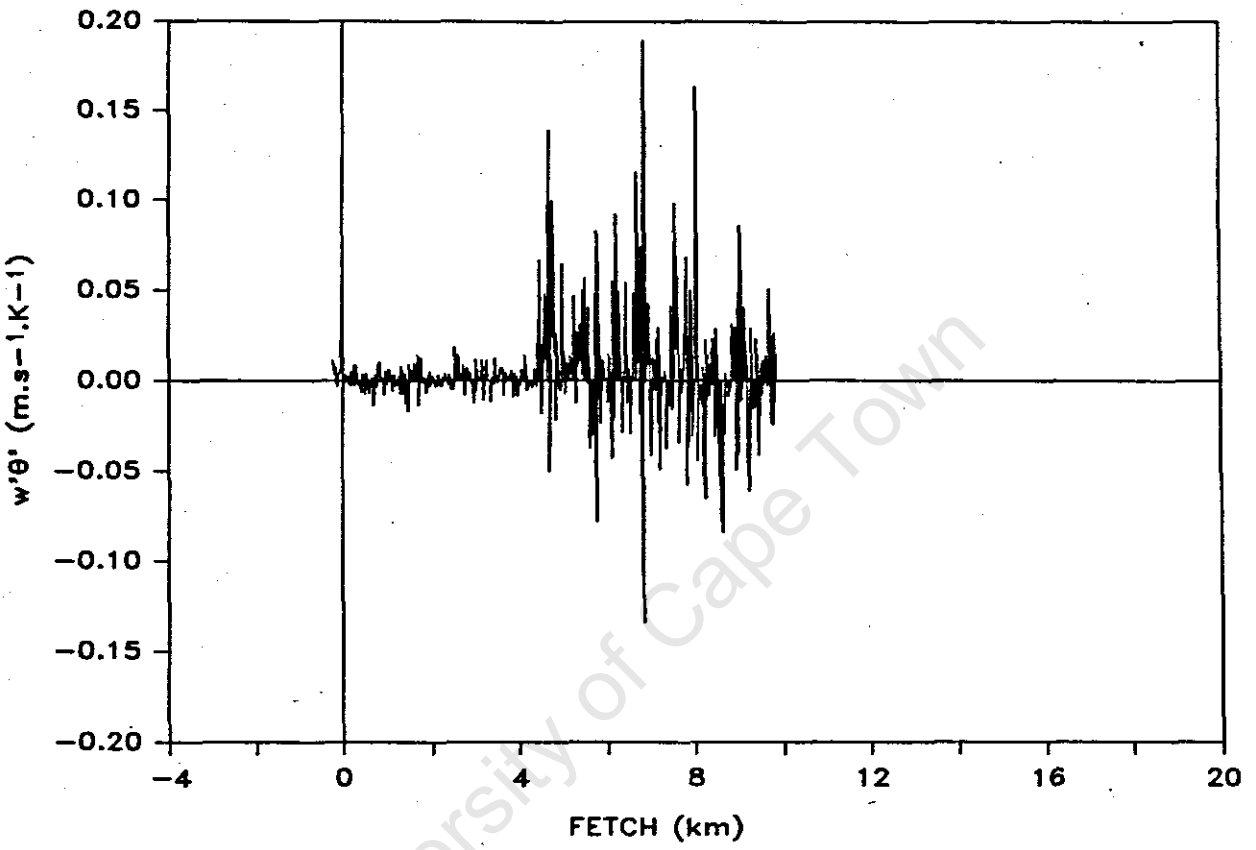


**Figure 7:** Horizontal profile of raw sensible heat flux data from 152m, illustrating increased heat flux at the TIBL boundary.



heat flux values showed increases of the same order as above, from $0.001 m.s^{-1}.K^{-1}$ up to $0.02 m.s^{-1}.K^{-1}$.

Figure 9 is a cross-section of the sampling area showing isopleths of mean heat flux compiled from the horizontal profiles. The data exhibited a large degree of horizontal and vertical variation over the times and distances measured. Apparent from the diagram was a region of stronger heat flux in the lower 150m (surface layer), above which was a region of alternate positive and negative heat fluxes of

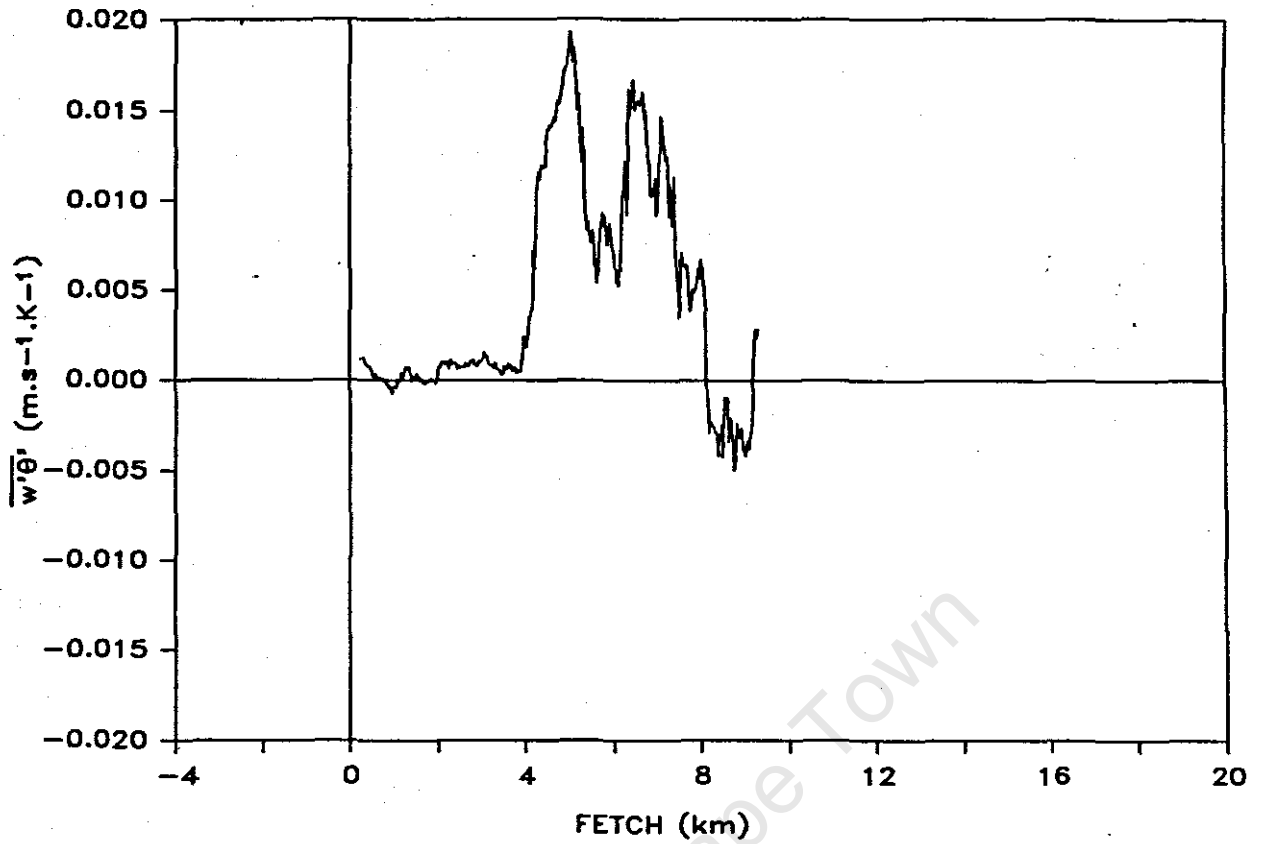


**Figure 8:** Horizontal profile of mean sensible heat flux at 152m, showing variation of heat flux within the TIBL.



varying strengths (mixed layer). Within this region were large areas of gentle upward or downward flux, which were interspersed with smaller pockets of more intense activity such as the convective elements at 4km and 12km where both $T'$ and $w'$ were both strongly positive. At greater heights, background levels close to zero were present. The mean heat flux analysis did not lead to great clarity in the definition of the TIBL, although an extended measurement and averaging time would have improved this to some extent. However, a clearer picture of the TIBL boundary was obtained by considering only the magnitudes or absolute values of mean heat flux (Figure 10). A feature noted in both diagrams was the dampening effect of the stronger marine stability at low level in the onshore flow near the coast, which persisted a little way inland until eroded by surface heating and turbulence. The height of the TIBL as reflected in the latter analysis seemed to be higher than that of the

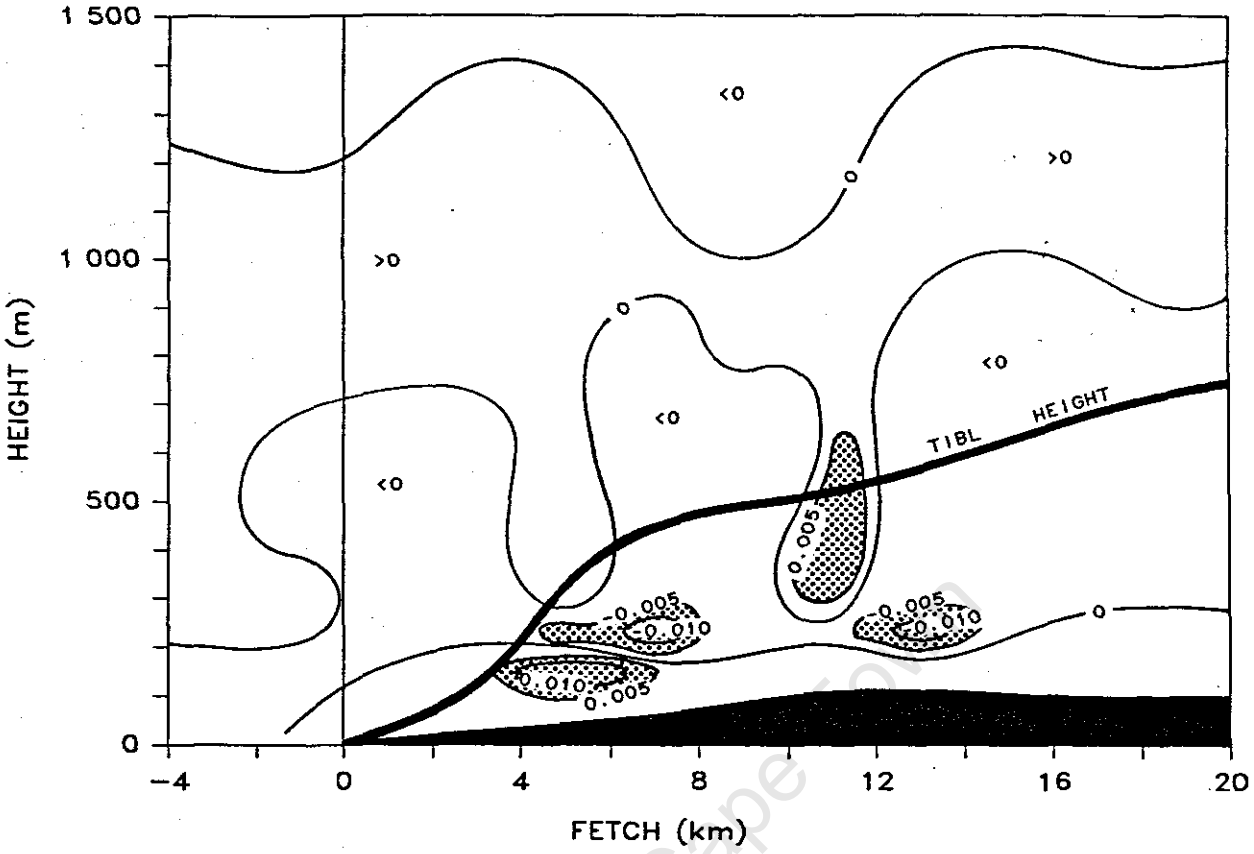


**Figure 9:** Patterns of mean sensible heat flux ($m.s^{-1}.K^{-1}$) for Run 401.

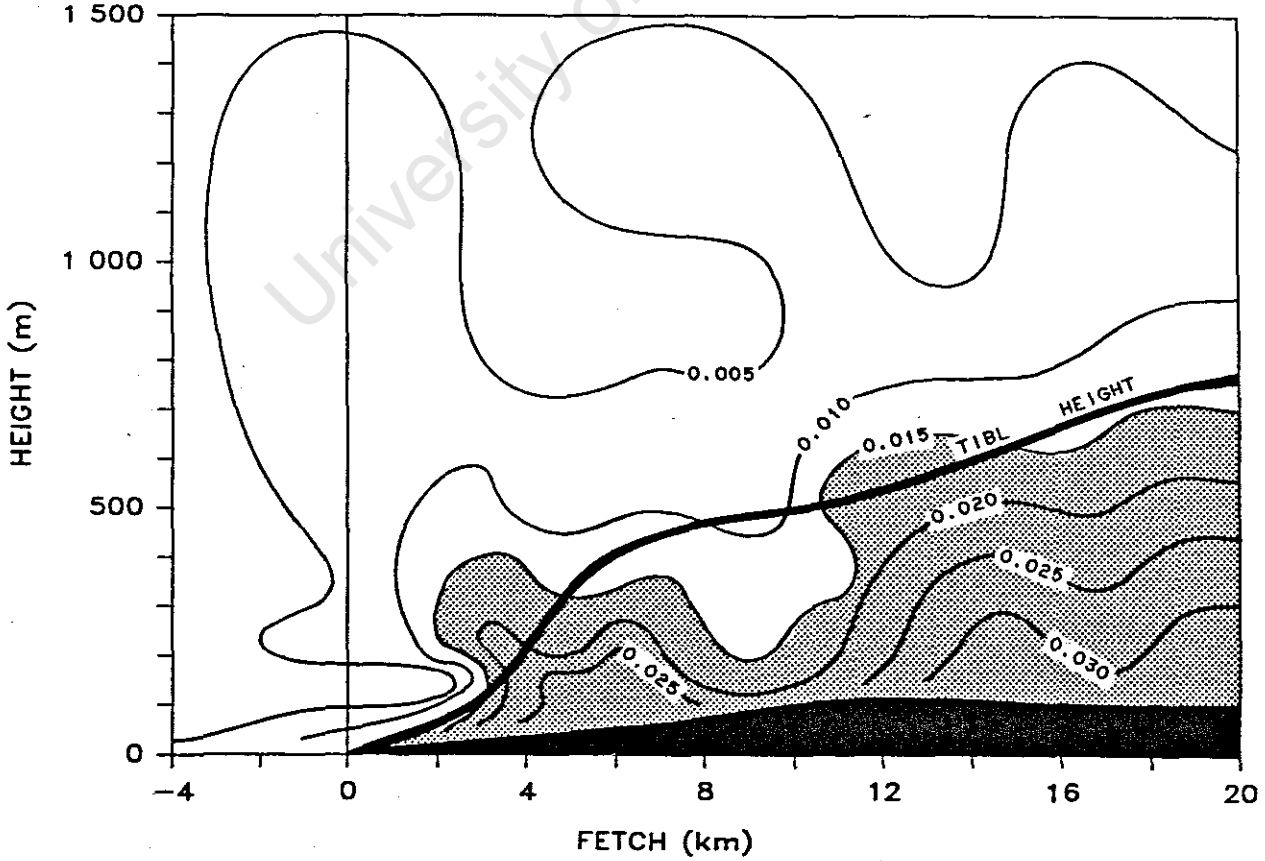


**Figure 10:** Patterns of the absolute mean sensible heat flux ($m.s^{-1}.K^{-1}$) for Run 401.

more conventional definitions, perhaps due to a more gradual decrease of heat flux when averaged across the entrainment region such as the effect of the thermal convection near 4km.

It was evident from the above that, even over periods of 10 minutes up to an hour or more, the patterns of heat flux in the TIBL were not as simple and constant as might have been expected. Although greater variations in temperature and vertical velocity occurred within the TIBL, it did not necessarily follow that a net positive heat flux was found

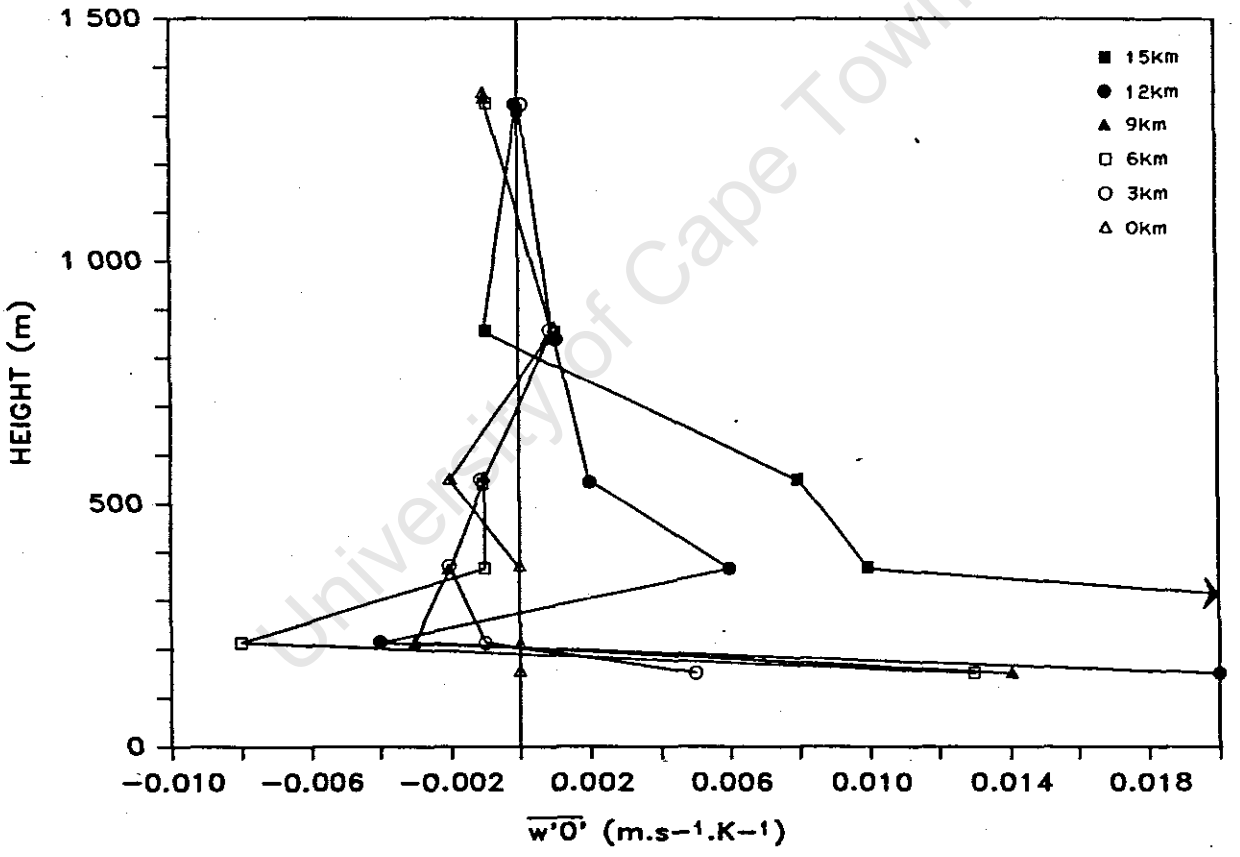


**Figure 11:** Vertical profiles of mean sensible heatflux ($m.s^{-1}.K^{-1}$) for a range of downwind distances.

throughout the TIBL. This applied particularly to the mixed region above the superadiabatic surface layer, where relative increases in stability caused small negative heat fluxes. Figure 11 illustrates a number of vertical profiles

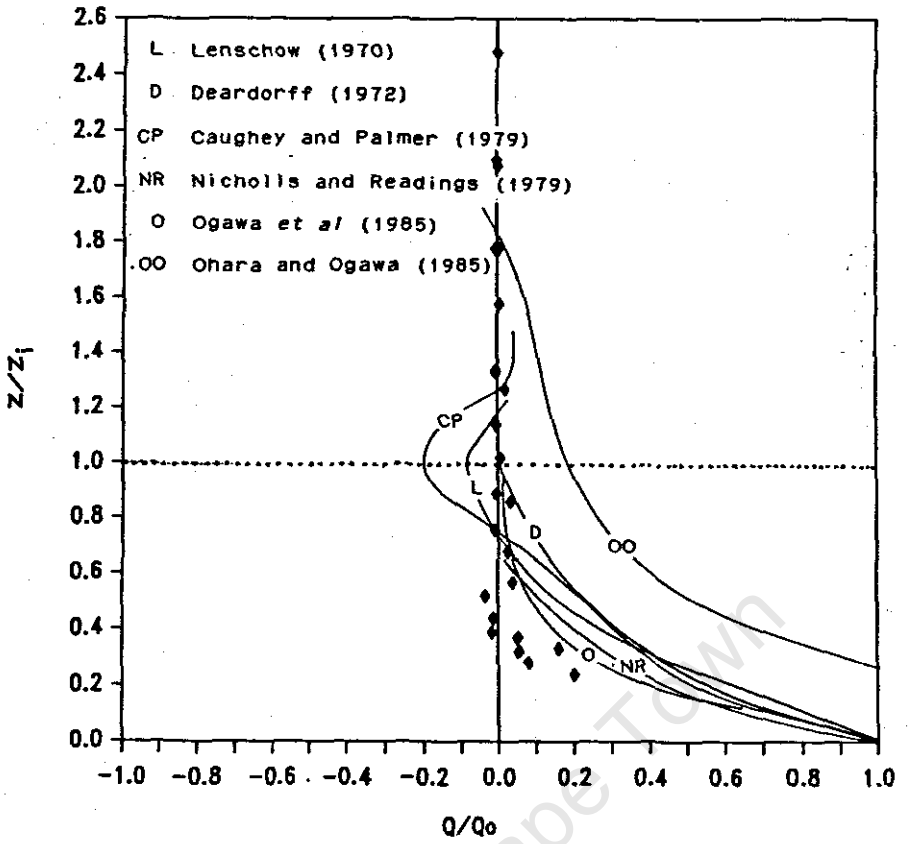


**Figure 12:** Normalised heat flux as a function of non-dimensionalised boundary layer height.



of heat flux for a range of downwind distances. Values were largely positive close to the surface, diminishing rapidly with height due to the stability structure of the atmosphere, which possessed a superadiabatic layer near the ground with neutral and slightly stable layers above. Small negative values of heat flux were associated with a relative increase in stability, and were not necessarily associated with the entrainment region (Caughey and Palmer, 1979). This was not as apparent at heights somewhat higher than the TIBL, where heat flux evened out around zero. Figure 12 shows these same data normalised by surface heat flux ($Q_0$) and TIBL height ($z_i$), with curves and data ranges from other studies (Lenschow, 1970; Deardorff 1972; Caughey and Palmer, 1979; Nicholls and Readings, 1979; Ohara and Ogawa, 1985; Ogawa *et al*, 1985). As was evident from the above discussion, a smooth heat flux profile with only small

negative values of heat flux were found at $z/z_i$ = 1, which became positive below $z/z_i$ = 0.5. The data were in fair agreement with those of Kaimal *et al* (1976) and Nicholls and Readings (1979), and close to but a little less than those of Ogawa *et al* (1985). The above studies took place under generally unstable conditions, while the present data were collected in a generally neutral TIBL. This gave a dampened effect to the heat flux profile, with values only increasing in the region of greater instability nearer the ground. Also, the strong superadiabatic layer at the surface possessed a large surface heat flux, which contributed to the generally smaller values of $Q/Q_0$ in the TIBL.

#### MOMENTUM FLUX

Although no concurrent measurements of horizontal wind velocity ($u'$) were available, conclusions drawn from the variations in $w$ data, and the available $\bar{u}$ data from pibals, suggest that the momentum flux or shear stress $\overline{u'w'}$ displays similar patterns to those identified in other studies. The greatest interaction between these variables took place near the surface in the TIBL, and decreased with height. Momentum flux is thus expected to be consistent with results from other authors as well as displaying patterns of a similar nature to the present heat flux data.

## Standard deviations

#### POTENTIAL TEMPERATURE

Figure 13 is an example of a horizontal cross-section of $\sigma_T$ at 152m (calculation period of 50 seconds). It illustrates the typical increase in temperature variations within the TIBL, with background values of less than 0.1$^{o}$C and values within the TIBL of up to 0.4$^{o}$C. Considerable horizontal variation in $\sigma_T$ was found to exist, with some areas showing far greater thermal activity than others in close proximity.

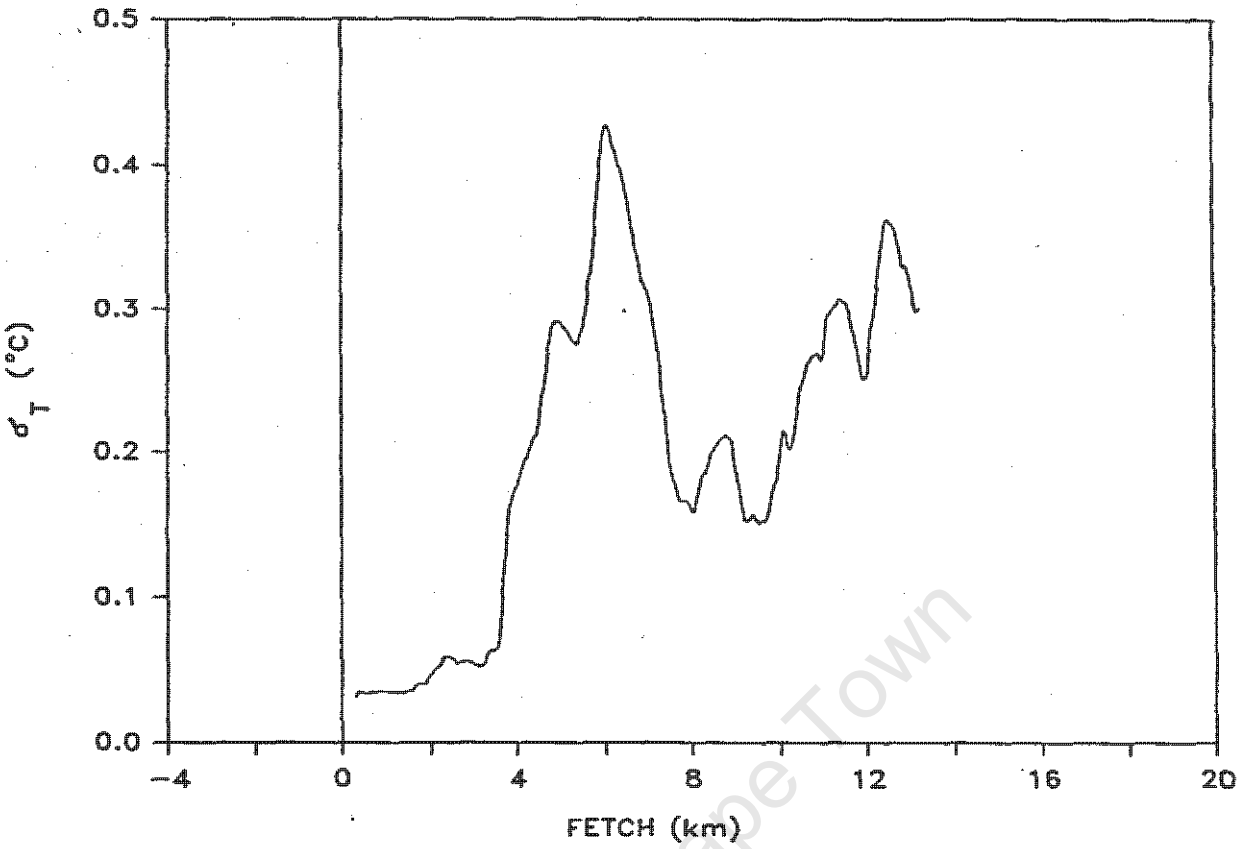


Figure 13: Horizontal profile of the standard deviation of temperature at 152m.



Figure 14 is a cross-section showing the patterns of $\sigma_T$ in the study region. The conventional TIBL pattern was at once evident, although perturbations introduced by persistent low level stability near the coast interacting with strong thermal activity near 4km caused the doubling back of the $\sigma_T$ profile a few kilometres inland. This type of pattern was typical of all regions of the TIBL boundary, due to the continual adjustments to changes in the flow characteristics which caused it to have a pulsating and undulating nature. In general, the standard deviations of potential temperature were, as for other parameters, greatest inland and nearer the surface, and least at higher altitudes and towards the sea. Atmospheric stability and its effect on the potential for turbulent and thermal differences within the TIBL particularly influenced $\sigma_T$. The entrainment region was not clearly seen in the above analysis, although the relatively contorted patterns of $\sigma_T$ occurred as a result of convective overshooting in the entrainment region. TIBL heights evident

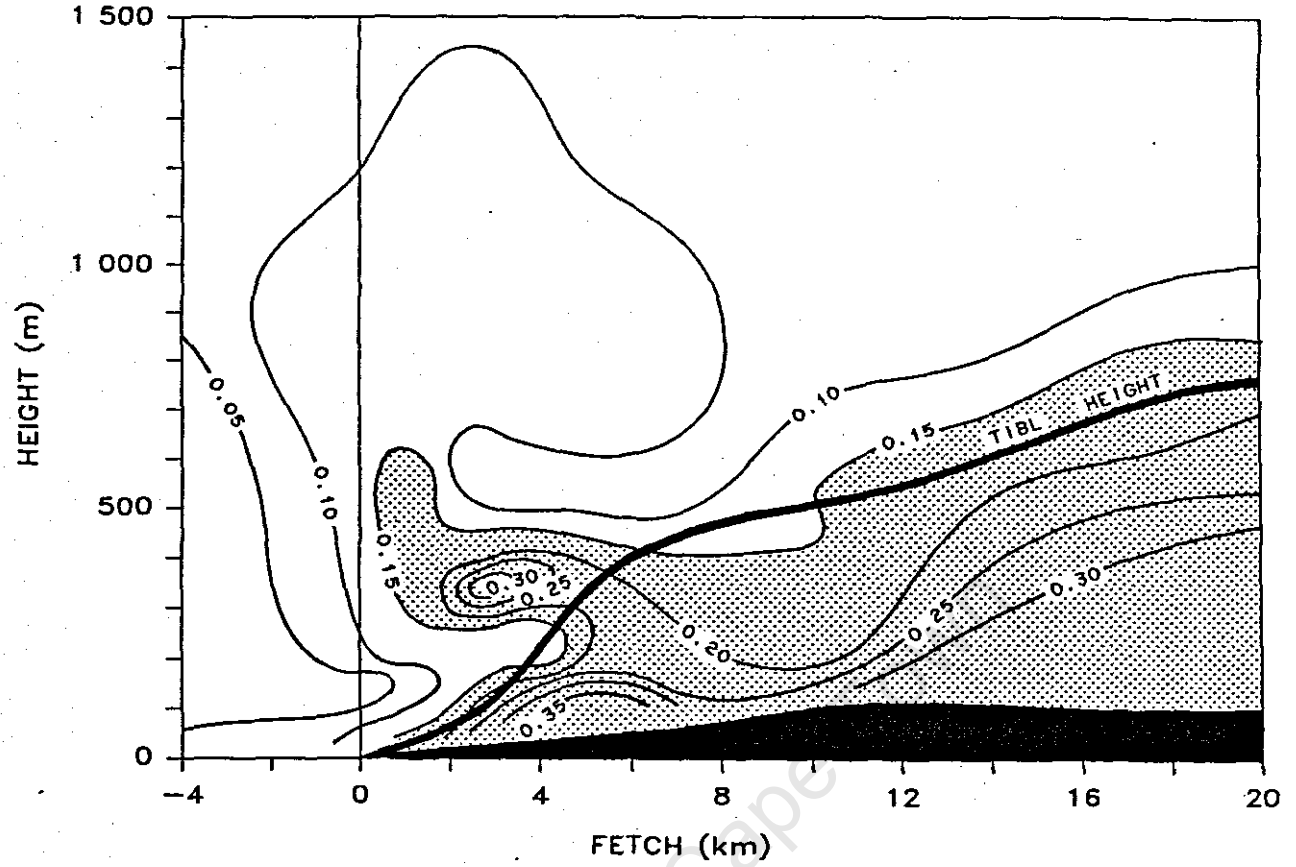


**Figure 14:** Cross-sectional patterns of $\sigma_T$ ($^0$C) for Run 401.

from the analysis compare favourably with those derived from turbulence data and temperature profiles.

Figures 15 and 16 show the non-dimensional plots of $\sigma_T/\theta_*$ and $\sigma_T/T_*$. Data were taken from the same range of heights and distances downwind as in the foregoing heat flux discussion. Mixed layer scaling by $\theta_*$ provided a good fit to the data, while $T_*$ scaling for the surface layer was predictably not as effective. A number of studies have indicated increased deviations and variability near $z/z_i$ = 1 in the $\theta_*$ case (Caughey and Palmer, 1979; Sun and Ogura, 1980) while others have indicated a more gradual decrease with height. A slight increase in $\sigma_T/\theta_*$ near $z/z_i$ = 1 was apparent from the data, although it was quite possibly due to scatter, and in any case not nearly as strong as for the CBL. The data followed a very similar pattern to that found

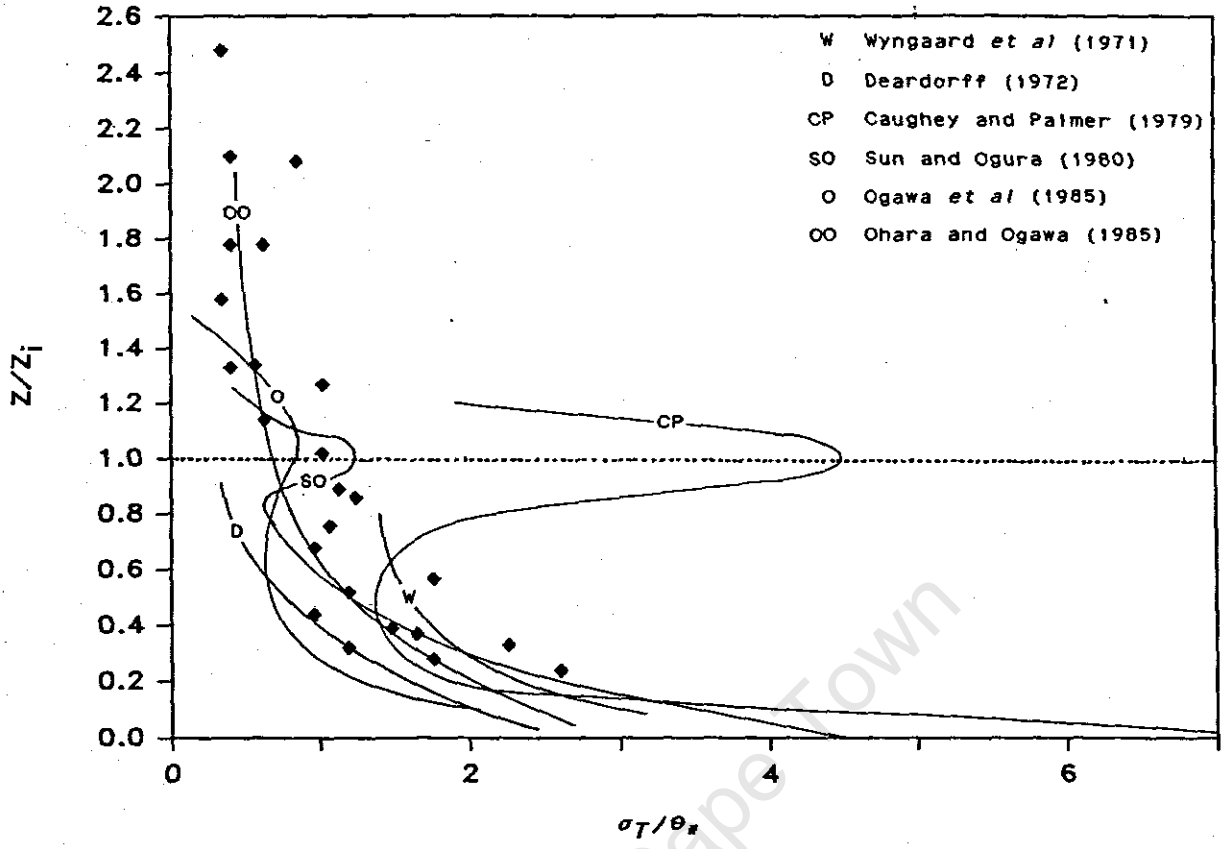


**Figure 15:** Vertical profiles of $\sigma_T$ normalised by mixed layer scaling ($\theta_*$) as a function of non-dimensionalised height. Curves indicate data from other authors (see text).

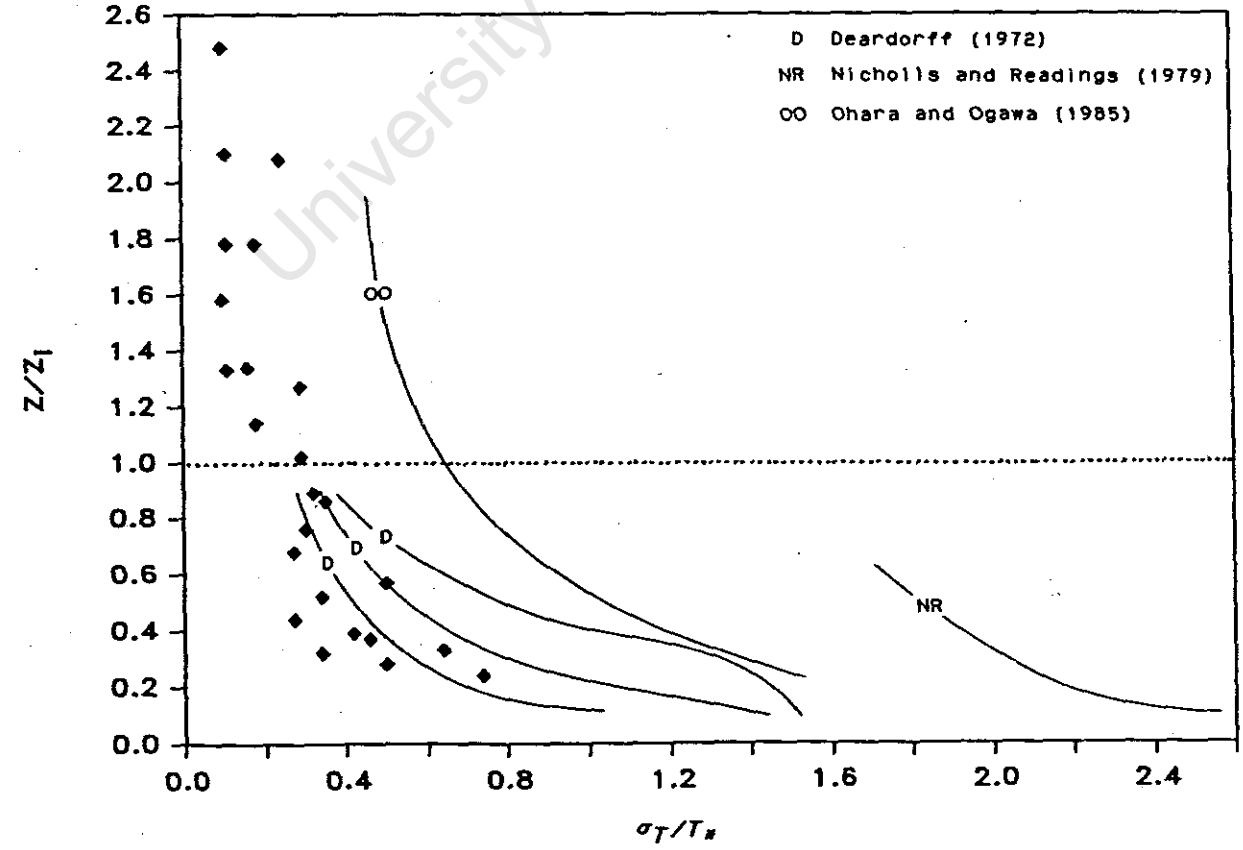


**Figure 16:** Vertical profiles of $\sigma_T$ normalised by surface layer scaling ($T_*$) as a function of non-dimensionalised height. Curves indicate data from other authors (see text).

by a number of other authors (Wyngaard *et al*, 1971; Deardorff, 1972; Ohara and Ogawa, 1985; Ogawa *et al*, 1985) which indicated a more simple curve that decreased with non-dimensional height. It would thus seem as though the strong increase in turbulence near $z/z_i = 1$ is limited to the top of the CBL only, while turbulence within the TIBL showed less variability at this height and decreased more regularly with altitude. Data values compared well with those presented in the above studies, and were of the same magnitude as both TIBL and CBL data. Similar comparisons for the $T_*$ case revealed reasonable similarities between the present data and the results of Deardorff (1972), but were well below the data collected over the sea by Nicholls and Readings (1979) and the low level data of Ohara and Ogawa (1985). While the lack of near surface data below $z/z_i = 0.2$ prohibited a complete comparison, the shape of the curve showed the same smooth decrease with height, which further suggested a difference between the non-dimensional profiles of temperature-related turbulence in the CBL and the TIBL.

### VERTICAL WIND VELOCITY

Figure 17 is an example of a horizontal $\sigma_w$ profile, taken at 213m. The trace shows the strong increase in turbulence associated with the TIBL, which rose from $0.13 m.s^{-1}$ to about $0.25 m.s^{-1}$ across the TIBL boundary (calculation period of 50 seconds). Variations of vertical turbulence within the TIBL were more horizontally consistent than those of temperature, while the magnitude of the increase across the interface became diminished and more gradual at greater altitudes. Figure 18 shows the $\sigma_w$ cross-section of the study area, from which the characteristic shape of the TIBL can be identified. The boundary of the TIBL was curved and slightly irregular, and displayed the same small region of diminished turbulence associated with the persistence of low level stability. The entrainment region was identified with a band of intermediate level turbulence which was subject to

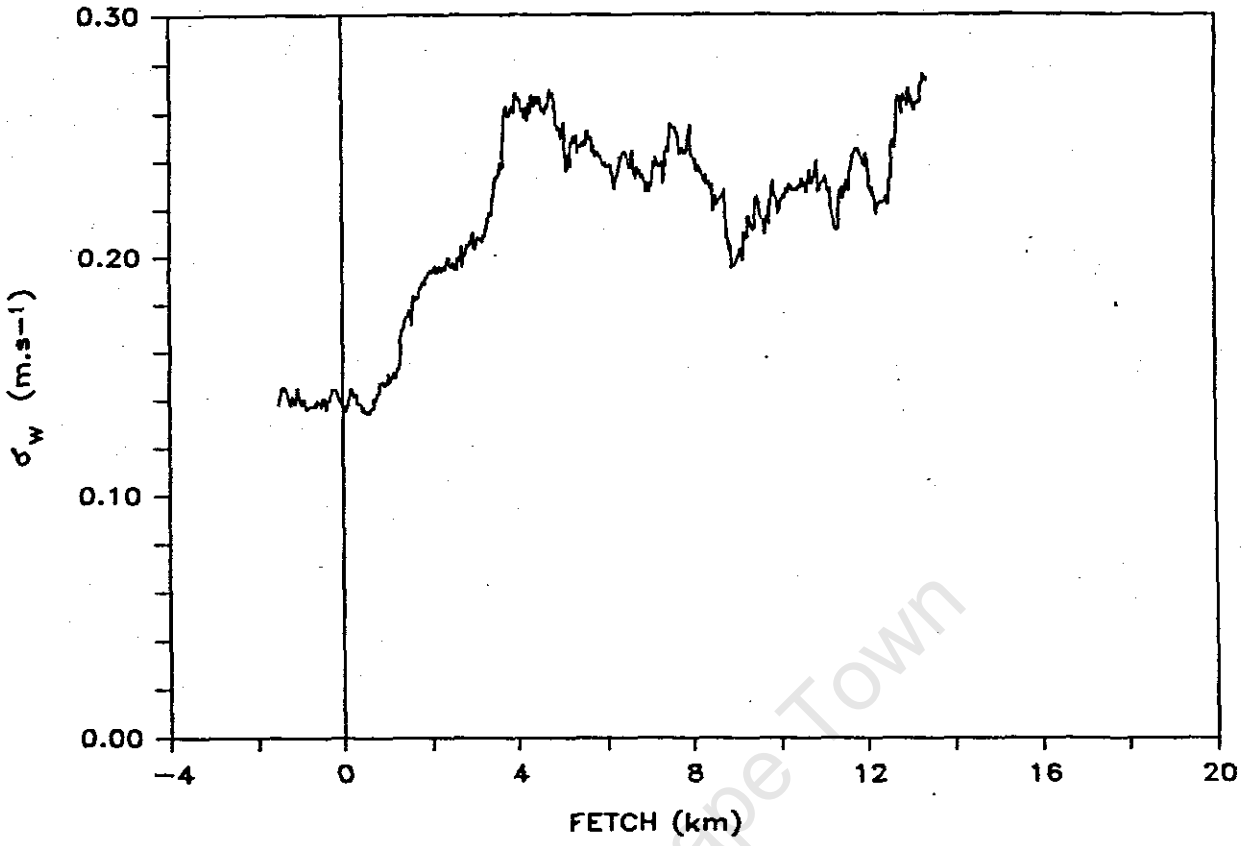


**Figure 17:** Horizontal profile of the standard deviation of vertical velocity (m.s$^{-1}$) at 213m.



occasional patches of strong or mild turbulence. Due to the intense nature of thermal upcurrents, sharp changes in vertical velocities were found within tens of metres of each other towards the edge of the TIBL, while in the fully mixed layer below many of these contrasts were evened out by the mechanical turbulence present at those levels. In Figure 18 the bulk of these small scale variations are no longer visible due to smoothing although larger variations can be seen, for example the turbulence associated with the thermal upcurrent at $x$ = 4km. Caughey and Palmer (1979) mentioned the observed finite value of the standard deviation above $z_i$, and its association with entrainment and with internal waves of 5 to 10 minute periods at higher altitudes. Examination of the $\sigma_w$ cross-section revealed the likely presence of this type of activity, which was also noted earlier in the discussions on instantaneous fluctuations and potential temperature. This $\sigma_w$ analysis also provided a good

indication of the TIBL height defined by potential temperature parameters, and is an important factor when considering the actual behaviour and vertical dispersion of air pollutants in the coastal zone.

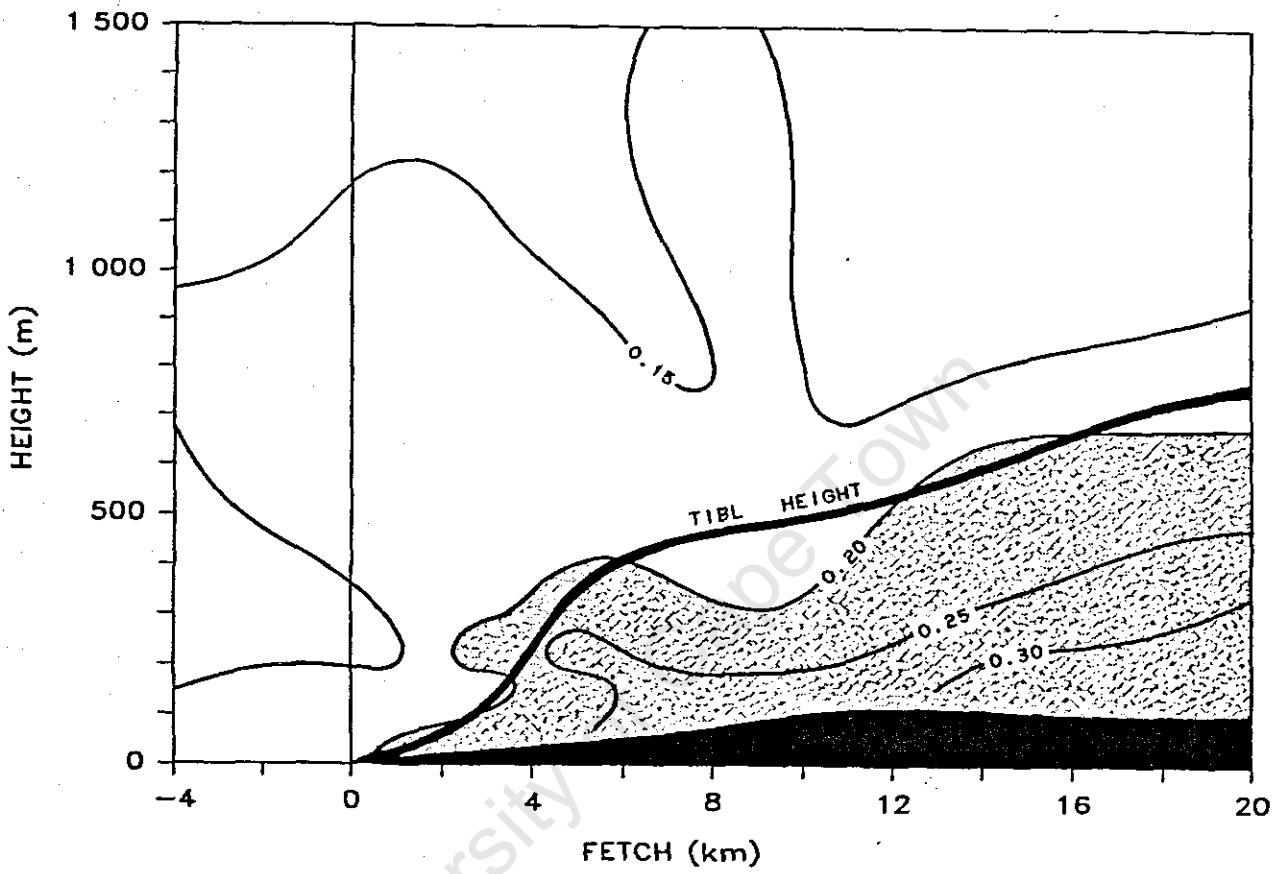


**Figure 18:** Cross-sectional patterns of $\sigma_w$ ($m.s^{-1}$) for Run 401.



The profile of $\sigma_w/\bar{u}$ (turbulent intensity) has not been considered here due to the overexaggerated effects of the uneven wind speed profile caused by sea breeze penetration, which effectively diminished turbulent intensity in the TIBL. There is thus little merit in comparing these data with those from the CBL, which is characterised by an almost constant logarithmic wind profile and a consequent increase in turbulent intensity near the surface. This explanation concurs with that in Ogawa *et al* (1985), where comparable behaviour was found in a lake breeze. The relationships of $\sigma_w/u_*$ and $\sigma_w/w_*$ to non-dimensional height $z/z_i$ are shown in

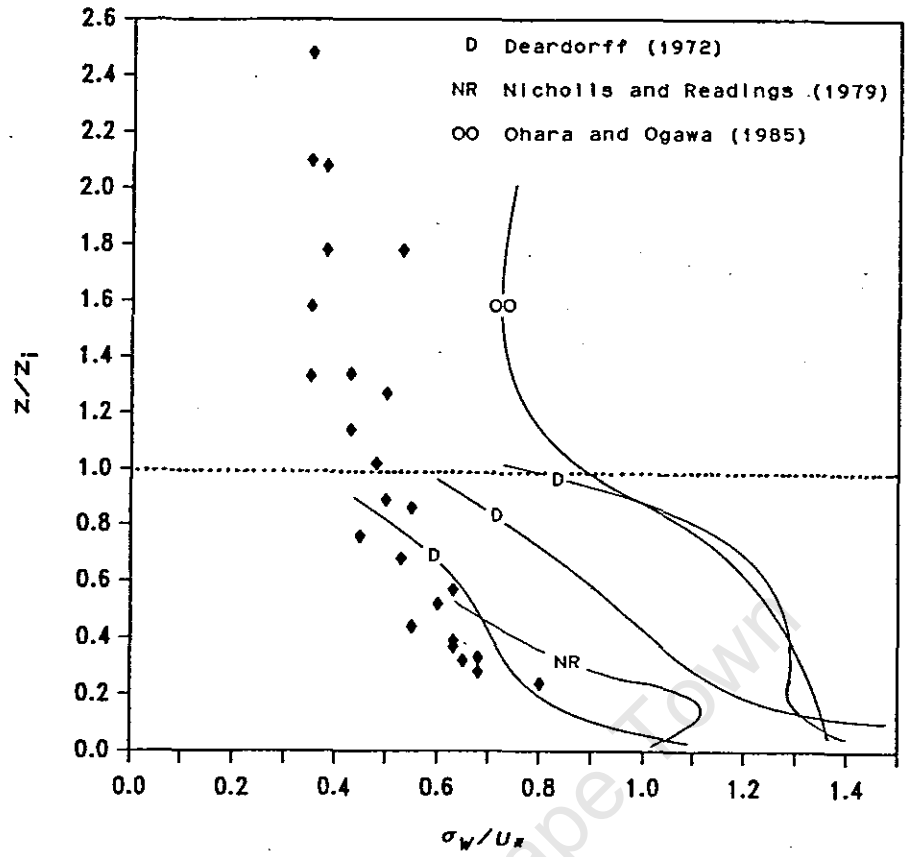


**Figure 19:** Vertical profiles of $\sigma_w$ normalised by surface layer scaling ($u_*$) as a function of non-dimensionalised height. Curves indicate data from other authors (see text).

Figures 19 and 20, with the associated curves indicating results from other authors. The data points were obtained from the same set of downwind distances and heights as used previously. Contrary to the heat flux data, the surface layer scaling by $u_*$ was a much better fit than the mixed layer scaling by $w_*$. The $u_*$ data followed a similar pattern to the TIBL data presented in Ohara and Ogawa (1985), although values were roughly half of the latter which were collected near the surface. In terms of magnitude, the data were similar to those of investigators concerned with the CBL (Deardorff, 1972; Nicholls and Readings, 1979), although not showing the more bowed pattern usually associated with the CBL, and instead displaying the generally smooth decrease of turbulence with height that seems to be typical of the TIBL. This echoes the earlier comments regarding the different profiles of turbulence found in the two boundary layers.

The values obtained from $w_*$ scaling were lower than other studies (Willis and Deardorff, 1974; Caughey and Palmer, 1979; Sun and Ogura, 1980; Ohara and Ogawa, 1985; Ogawa *et al*, 1985), although the latter data taken at the same scale in the TIBL were in fairly good agreement in the upper half of the TIBL, while the Ohara and Ogawa (1985) results taken at a smaller scale in the TIBL were conversely much greater. It should be borne in mind that the CBL data are centred

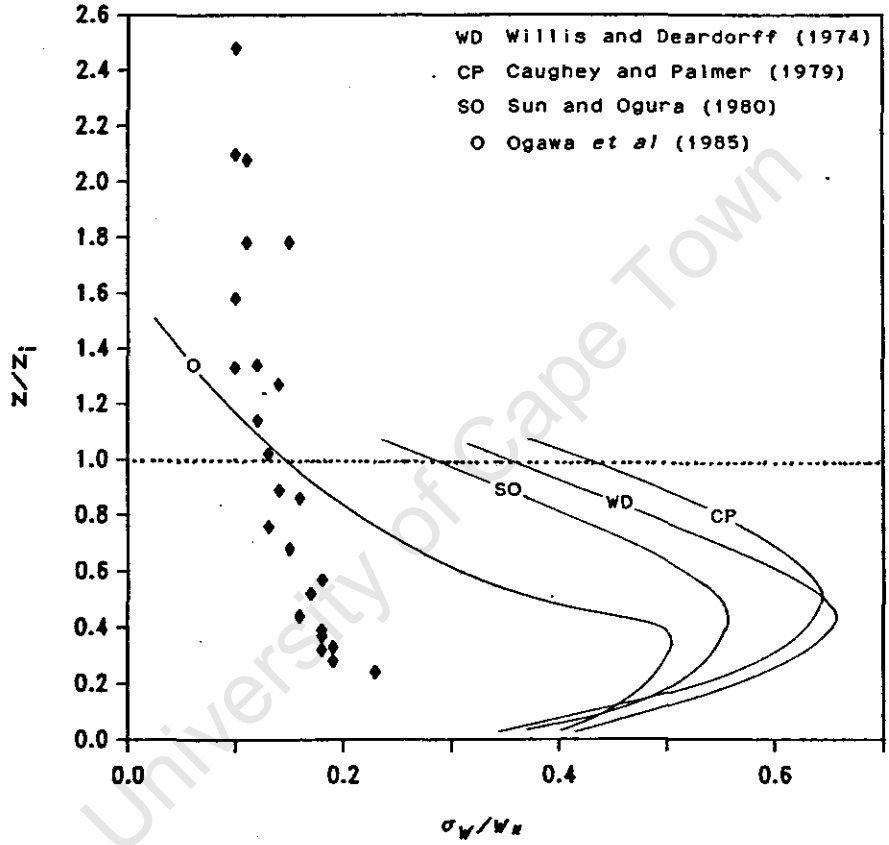




**Figure 20:** Vertical profiles of $\sigma_w$ normalised by mixed layer scaling ($w_*$) as a function of non-dimensionalised height. Curves indicate data from other authors (see text).

around a free convection prediction and, considering the earlier comments on enhanced stability, that convective activity was not necessarily as well developed as in the CBL, even though the TIBL formed a mixed layer. Few data and no predictions existed for regions higher than $z/z_i$ = 1. The observed values of 0.1 to 0.2 fell in the expected range, and were of similar value to the small amount of other data available.

## SUMMARY AND CONCLUSIONS

This paper has examined the mesoscale turbulence structure of the TIBL under conditions of stable onshore flow. Airborne measurements spanning the length and height of the TIBL were made, from which a detailed analysis of selected flow characteristics, fluxes and standard deviations was performed. From the data considered, this study has found that :

1) Wind profiles of speed and direction displayed a strong sea breeze influence. The TIBL was located slightly higher than the wind speed maximum, and was associated with the layer of relatively constant wind direction found near the surface.

2) The TIBL developed as a neutral and unstable layer from the initially stable onshore flow. Stability persisted aloft but decreased in the entrainment region at the upper boundary of the TIBL, where the first changes in temperature occurred.

3) The TIBL was characterised by increased values and variations in temperature and vertical velocity, the latter exhibiting the greater clarity. Fluctuations were most regular near the surface, and became intermittent higher up in the entrainment region. The behaviour of all raw and calculated values was subject to dampening under conditions of increased stability.

4) Sensible heat flux was minimal outside the TIBL, and slightly negative in its upper regions. Further below, a convoluted deeper layer of more moderate heatflux than found in the CBL was formed, which was subject to penetration by thermal convective elements. A lot of variation in heat flux occurred in the mixed layer, and a slightly negative bias to the normalised data was found. These were attributed to the

relatively neutral stability, in contrast to the unstable surface layer where heat flux was strongly positive.

5) Patterns of $\sigma_T$ were complex and particularly susceptible to the influence of stability and convective motions, with the greatest values occurring in the TIBL. In contrast to the CBL, $\sigma_T$ in the TIBL decreased smoothly with non-dimensional height, with generally larger levels and only a marginal increase in turbulence near $z/z_i = 1$.

6) The TIBL was denoted by strong increases in $\sigma_w$, patterns of which displayed close agreement with the observed TIBL height. The upper boundary of the TIBL was associated with a change to moderate values of $\sigma_w$, which resulted from the intermittent turbulence of the entrainment region. Non-dimensionalised $\sigma_w$ profiles of the TIBL exhibited low values for mixed layer scaling, partly attributed to stability, while surface layer scaling by $u_*$ provided values close to other data. Both profiles were distinctly different from the CBL profile in shape, and revealed the characteristic smooth decrease with height identified for other parameters in the TIBL.

This analysis of the mesoscale turbulent structure of the TIBL has highlighted many similarities found in both small scale turbulent studies and in larger scale studies of the CBL. However, certain features were particularly characteristic of the TIBL. A complex turbulent structure denoted by a variety of parameters has been shown to develop, as relatively stable marine air becomes modified to a well mixed layer over the land.



## REFERENCES

André, J.C., 1983: Planetary boundary layer parameterization and turbulence closure. In Lilly, D.K. and Gal-Chen, T. (eds.): Mesoscale meteorology - theories, observations and models, D. Reidel, 651-669.

Betts, A.K., 1973: Non precipitating cumulus convection and its parameterization. *Quart. J. Roy. Meteorol. Soc.*, 99, 170-196.

Carson, D.J., 1973: The development of a dry inversion capped convectively unstable boundary layer. *Quart. J. Roy. Meteorol. Soc.*, 99, 450-467.

Caughey, S.J. and Palmer, S.G., 1979: Some aspects of turbulence structure through the depth of the convective boundary layer. *Quart. J. Roy. Meteorol. Soc.*, 105, 811-827.

Collins, G.F., 1971: Predicting sea breeze fumigation from tall stacks at coastal sites. *Nuclear Safety*, 8, 490-499.

Comrie, A.C., 1988: Meteorological characteristics of thermal internal boundary layers. Chapter 2, unpublished M.Sc thesis, Dept. of Environ. and Geogr. Sci., Univ. of Cape Town.

Deardorff, J.W., 1972: Numerical investigation of neutral and unstable planetary boundary layers. *J. Atmos. Sci*, 29, 91-115.

Echols, W.T. and Wagner, N.K., 1972: Surface roughness and internal boundary layer near a coastline. *J. Appl. Meteorol.*, 11, 658-662.

Elliot, W.P., 1958: The growth of the atmospheric internal boundary layer. *Trans. Amer. Geophys. Union*, 39, 1048-1054.

Fiedler, F. and Panofsky, H.A., 1972: The geostrophic drag coefficient and the 'effective' roughness length. *Quart. J. Roy. Meteorol. Soc.*, 98, 213-220.

Gamo, M., Yamomoto, S. and Yokoyama, O., 1982: Airborne measurements of the free convective internal boundary layer during the sea breeze. *J. Meteorol. Soc. Japan*, 60, 1284-1298.

Kaimal, J.C., Wyngaard, J.C., Haugen, D.A., Coté, O.R., Izumi, Y., Caughey, S.J. and Readings, C.J., 1976: Turbulence structure in the convective boundary layer. *J. Atmos. Sci.*, 33, 2152-2169.

Kerman, B.R., Mickle, R.E., Portelli, R.V., Trivett, N.B., and Misra, P.K., 1982: The Nanticoke shoreline diffusion experiment, June 1978-II: Internal boundary layer structure. *Atmos. Environ.*, 16, 423-437.

Lenschow, D.H., 1970: Airplane measurements of planetary boundary layer structure. *J. Appl. Meteorol.*, 9, 874-884.

Lumley, J.L. and Panofsky, H.A., 1964: The structure of atmospheric turbulence. J. Wiley and Sons, New York.

Lyons, W.A. and Cole, H.S., 1973: Fumigation and plume trapping on the shores of Lake Michigan during stable onshore flow. *J. Appl. Meteorol.*, 12, 494-510.

Misra, P.K. and Onlock, S., 1982: Modelling continuous fumigation of Nanticoke generating station plume. *Atmos. Environ.*, 16, 479-489.

Nicholls, S. and Readings, C.J., 1979: Aircraft observations of the structure of the lower boundary layer over the sea. *Quart. J. Roy. Meteorol. Soc.*, 105, 785-802.

Ogawa, Y. and Ohara, T., 1985: The turbulent structure of the internal boundary layer near the shore - Part 1: Case study. *Boundary-Layer Meteorol.*, 31, 369-384.

Ogawa, Y., Ohara, T., Wakamatsu, S., Diosey, P.G. and Uno, I., 1985: Observation of lake breeze penetration and subsequent development of the thermal internal boundary layer for the Nanticoke II shoreline diffusion experiment. *Boundary-Layer Meteorol.*, 32, 207-230.

Ohara, T. and Ogawa, Y., 1985: The turbulent structure of the internal boundary layer - Part 2: Similarity and energy budget analysis. *Boundary-Layer Meteorol.*, 32, 39-56.

Peters, L.K., 1975: On the criteria for the occurrence of fumigation inland from a large lake. *Atmos. Environ.*, 9, 809-816.

Portelli, R.V., 1982: The Nanticoke shoreline diffusion experiment, June 1978-I: Experimental design and program overview. *Atmos. Environ.*, 16, 413-421.

Prophet, D.T., 1961: Survey of available information pertaining to the transport and diffusion of airborne material over ocean and shoreline complexes. Tech. Report 89, Aerosol Lab., Stanford Univ., 53pp.

Raynor, G.S., SethuRaman, S. and Brown, R.M., 1979: Formation and characteristics of coastal internal boundary layers during onshore flows. *Boundary-Layer Meteorol.*, 16, 487-514.

SethuRaman, S., Brown, R.M., Raynor G.S. and Tuthill, W.A., 1979: Calibration and use of a sailplane variometer to measure vertical velocity fluctuations. *Boundary-Layer Meteorol.*, 16, 99-105.

Smedman, A-S. and Högström, U., 1983: Turbulent characteristics of a shallow convective internal boundary layer. *Boundary-Layer Meteorol.*, 25, 271-287.

Sun, W.Y. and Ogura, Y., 1980: Modeling the evolution of the convective planetary boundary layer. *J. Atmos. Sci.*, 37, 1558-1572.

Van der Hoven, I., 1967: Atmospheric transport and diffusion at coastal sites. *Nuclear Safety*, 8, 490-499.

Venkatram, A., 1986: An examination of methods to estimate the height of the coastal internal boundary layer. *Boundary-Layer Meteorol.*, 34, 149-156.

Wyngaard, J.C., 1983: Lectures on the planetary boundary layer. In Lilly, D.K. and Gal-Chen, T. (eds.): Mesoscale meteorology - theories, observations and models, D. Reidel, 603-650.

Wyngaard, J.C., Coté, O.R. and Izumi, Y., 1971: Local free convection, similarity, and the budgets of shear stress and heat flux. *J. Atmos. Sci.*, 28, 1171-1182.

CHAPTER 4

# AN EVALUATION OF THERMAL INTERNAL BOUNDARY LAYER EQUATIONS

The performance of eight selected Thermal Internal Boundary Layer (TIBL) height equations was tested against a recently collected independent data set, and evaluated by means of statistical summary and difference measures. The equations of Plate (1971), Steyn and Oke (1982) and Gamo *et al* (1983) displayed the best overall performance, and were collectively ranked in highest position. These equations were theoretically derived from mixed-layer thermodynamics, and made direct use of a heat flux parameter. They possessed a high degree of accuracy, with low mean and model-oriented errors, and biases close to zero. Also well ranked was the empirical equation of Raynor *et al* (1975), which had a high potential accuracy, but which resulted in a greater variability of actual prediction. In general, the TIBL height predictions slightly underestimated both the gradient and height of the TIBL.

## INTRODUCTION

The increase in the number of air pollution sources located in shoreline environments has led to concern regarding air quality in these areas. The complex meteorology found in coastal regions has prompted the development of disperion models for planning and regulatory purposes, as well as for high dosage and emergency response forecasts. Models of this nature have been designed on a numerical, statistical and similarity basis (Lyons and Cole, 1973; Schuh, 1975; Anthes, 1978; Dobosy, 1979; Van Dop *et al*, 1979; Misra, 1980; Kerman, 1982), and take into account a wide range of specialised meteorological factors, including effects such as the mesoscale transport of pollutants under sea breeze or gradient wind conditions, and the possible extent of any fumigation zones.

An important characteristic under these circumstances is the formation of the Thermal Internal Boundary Layer (TIBL), which arises from an adjustment of the airflow to the changes in surface roughness and temperature that occur at the coastline. During conditions of onshore flow the TIBL is present as a convex mixed layer that increases in depth with distance inland, capped by a stable inversion layer. The juxtaposition of the modified and unmodified air results in the adjacent location of two entirely different dispersion regimes, within which pollutant behaviour differs greatly. Pollutants emitted into the TIBL are subject to limited vertical diffusion, especially near the shore, while emissions into the stable layer at higher levels may travel a considerable distance downwind with relatively little diffusion before fumigation occurs upon intersecting the TIBL (Figure 1). Naturally, this has serious implications for the prediction of ground level and elevated concentrations, making it important for models to include a module based on an accurate TIBL height formulation.

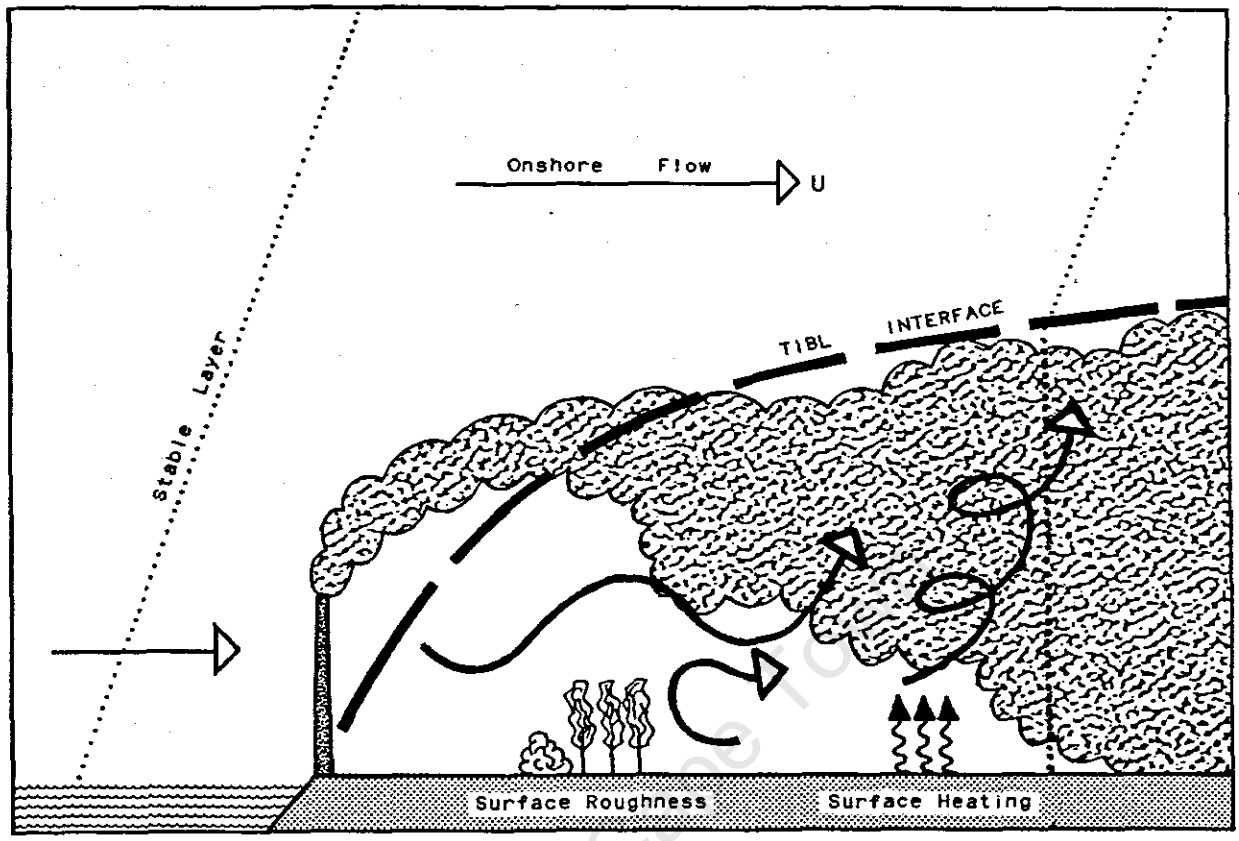


**Figure 1:** Schematic of TIBL formation and fumigation conditions during stable onshore flow.

Many of the TIBL height prediction formulae were developed in parallel with theoretical and empirical studies (an outline of their development appears in the next section), and few attempts have been made to independently assess their relative operational performance using other data sets. An important contribution was made by Stunder and SethuRaman (1985) who evaluated six TIBL equations using the Brookhaven (Raynor *et al*, 1979) and Kashimaura (Gamo *et al*, 1982) data bases, which possessed the complete sets of necessary input data. Some comments and examinations of data and equations were also made in Hsu (1986) and Venkatram (1986). Comparisons of predicted and observed data readily lend themselves to statistical evaluation, about which an extensive body of literature is in existence. Applications of statistics to meteorology and model evaluation have been made by Panofsky and Brier (1968), and more specifically by Fox (1981), Willmott (1982) and Hanna (1983).

It is the intention of this study to make use of a recently collected set of independent data to perform a comparative statistical evaluation of the performance of the TIBL height prediction equations. This will allow an assessment of their relative accuracy, sensitivity, applicability and potential for adaptation.

## DEVELOPMENT OF TIBL EQUATIONS

### Evaluation formulae

Although the TIBL height formulae can, as with most research, be classified along theoretical or empirical lines, a number of streams of thought exist in the literature on TIBL equations (Figure 2). Only the salient points with regard to operational usage of each equation are highlighted in the outline below, while for more detailed

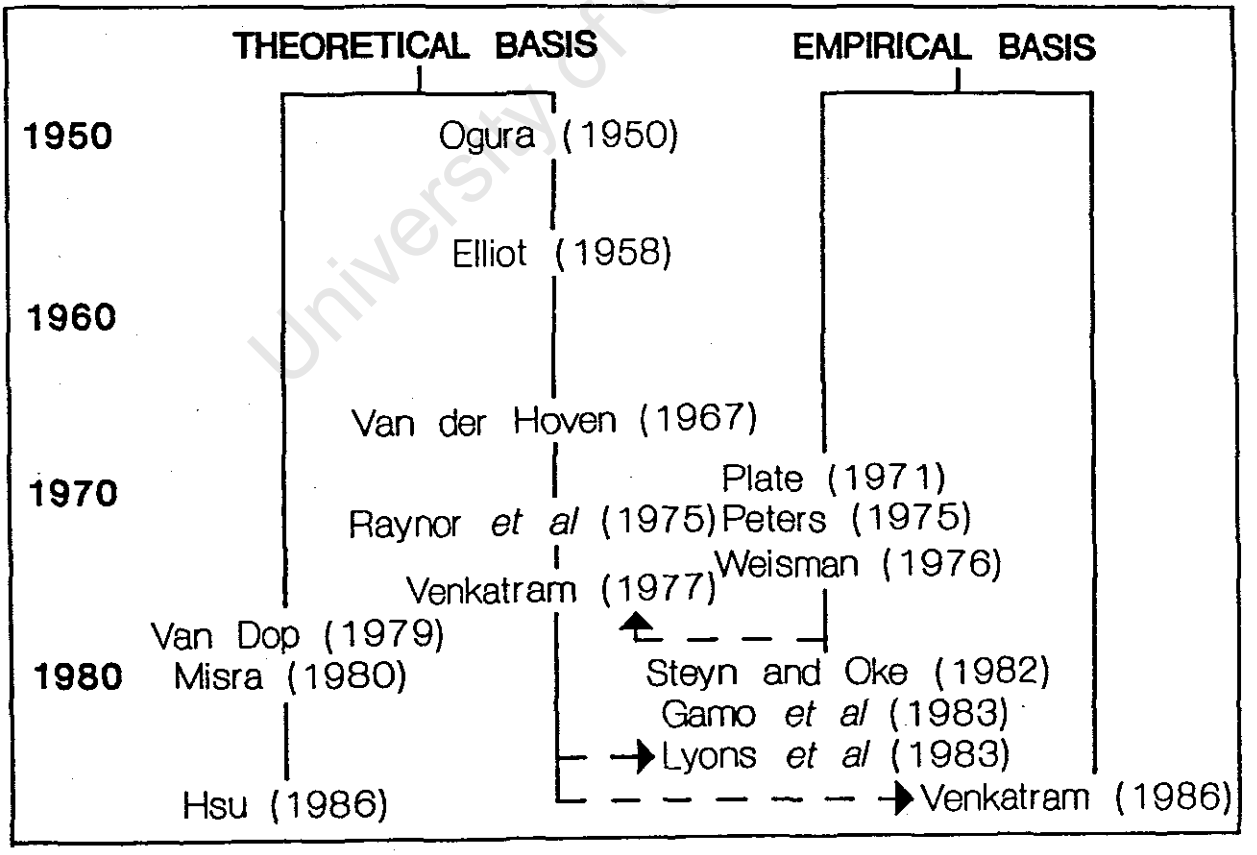


**Figure 2: Flow diagram of the development of TIBL equations illustrating main research streams (solid lines) and overlap of ideas (broken lines).**

derivations reference can be made either to the original authors or in some cases to Stunder and SethuRaman (1985).

In early work on boundary layers Elliot (1958) derived an internal boundary layer equation applicable for small fetch, essentially the same as that of Ogura (1950). In it was recognised the power dependence of internal boundary layer height on fetch, and the role of wind speed, stability and surface roughness, although the early equations made use of the unsatisfactory concept of eddy diffusivity which was avoided by later modellers. The first formulation that specifically dealt with the TIBL was that of Van der Hoven (1967). This empirical equation was presented graphically and was derived to fit the data of Prophet (1961) with the general form:

$$h = 8.8\left(\frac{x}{\bar{u}.\Delta\Theta}\right)^{1/2} \qquad (1)$$

where

$h$ = TIBL height (m)

$x$ = Distance inland (fetch) from shore (m)

$\bar{u}$ = Mean wind speed in TIBL ($m.s^{-1}$)

$\Delta\Theta$ = Vertical difference in potential temperature within overwater surface inversion layer (K).

Equation (1) contained the first parameterisations of wind speed and stability, but suffered from dimensional inhomogeneity. Nevertheless an important feature of this equation was the recognition of the square-root dependency on fetch, which has since been adopted in all other TIBL height prediction formulae.

Although the development of other formulations was evolving simultaneously, Raynor *et al* (1975) derived the following relationship of a similar style to equation (1) from physical and dimensional reasoning:

$$h = \frac{u_*}{\bar{u}_{10}} \cdot \left(\frac{x.|T_L - T_W|}{\beta}\right)^{1/2} \qquad (2)$$

where

$u_*$ = Land surface friction velocity ($m.s^{-1}$)

$\bar{u}_{10}$ = Mean wind speed near surface ($m.s^{-1}$)

$T_L$ = Land surface temperature (K)

$T_W$ = Water surface temperature (K)

$\beta$ = Overwater potential temperature lapse rate ($K.m^{-1}$).

This somewhat more sophisticated approach incorporated an allowance for surface roughness in the drag coefficient $u_*/\bar{u}_{10}$, as well as including the difference in surface temperatures as a relative measure of heat flux. As in most other formulae the initial lapse rate of the whole layer of onshore flow was used as a better indication of stability than the surface difference employed by Van der Hoven (1967).

Venkatram (1977) derived essentially the same equation on theoretical grounds from mixed layer theory, of the format:

$$h = \frac{u_*}{\bar{u}} \cdot \left(\frac{2.|T_L - T_W|.x}{\beta.[1-2F]}\right)^{1/2} \qquad (3)$$

where

$F$ = An entrainment fraction.

As a result of its mixed layer derivation, this model included the mean mixed layer wind $\bar{u}$ rather than the surface wind speed $\bar{u}_{10}$, and the entrainment parameter $2/1-2F$, while the surface temperature term was treated as a heat flux parameterisation. Equation (3) assumed that the TIBL was both buoyant and well-mixed, although a degree of stratification has sometimes been found to be present in wind speed and temperature profiles (Comrie, 1988).

In an alternative approach, Plate (1971) made the first use of mixed layer theory to estimate the height of the TIBL and

obtained a slightly different result. Using the work of Ball (1960) on the Convective Boundary Layer (CBL), Plate (1971) directly incorporated a heat flux term and the stability of the capping inversion layer, and obtained:

$$h = \left( \frac{4.H_O.x}{\rho.c_p.\beta.u} \right)^{1/2} \qquad (4)$$

where

$H_O$ = Surface heat flux over land ($W.m^{-2}$)

$\rho$ = Density of air ($\approx 1.2 * 10^3 g.m^{-3}$)

$c_p$ = Specific heat at constant pressure ($\approx 1.008 J.g^{-1}.K^{-1}$).

The major difference in equation (4) was the direct use of heat flux $H_O$, which is difficult to obtain for the bulk of meteorological observations. The difficulties with stratification mentioned above also apply.

Peters (1975) performed a theoretical energy balance derivation which resulted in a straight line boundary for the predicted TIBL. This formulation lacked the half-power relationship but included both heat flux in the numerator and surface temperature differences in the denominator. Its application was intended mainly for small $x$ as the monotonic increase in predicted TIBL height precluded the tendency towards an equilibrium height at large distances inland. A number of adaptations were made to Peters (1975) equation in Weisman (1976) where the following relationship was outlined:

$$h = \left( \frac{2.H_O.x}{\rho.c_p.\beta.u} \right)^{1/2} \qquad (5)$$

This was a parabolic extension to the straight line behaviour which recovered the more usual square root shape of the TIBL. It resulted in the same formula as Plate (1971) except for the coefficient in the numerator being halved.

Gamo *et al* (1983) also followed mixed layer theory, and made use of work on urban heat islands modified for the coastal atmosphere. An equation very similar to that of Weisman (1976) was derived, but with the incorporation of an entrainment factor as follows:

$$h = \frac{(2.[1+2F]H_Q.x)^{1/2}}{\rho.c_p.\beta.u} \qquad (6)$$

A full set of model equations was presented that allowed for both the distance and time dependence of the mixed layer, as well as for the prediction of certain variables downwind. The model was developed in conjunction with the Kashimaura data base, against which it was tested.

Steyn and Oke (1982) presented a model of the depth of the daytime mixed layer at the coast with similar provisions for the time and distance dependance of mixed layer height. This mathematical model was also based on the thermodynamic mixed-layer approach, and the resulting equation for TIBL height showed only minor differences to equation (6) above. TIBL height was expressed as:

$$h = h_s + \frac{(2.[1+F].H_Q.x)^{1/2}}{\rho.c_p.\beta.u} \qquad (7)$$

where

$h_s$ = Depth of the surface layer (m).

The inclusion of surface layer depth stemmed from a more precise consideration of the mixed layer as starting some distance above the surface, while differences in derivation caused a small change in the entrainment parameter.

Lyons *et al* (1983) extended the mixed layer concept by parameterising the heat flux term as a sinusoidal function dependent on time of day and solar insolation. This was an

attempt to circumvent the practical difficulties in measuring $H_O$ which resulted in the form:

$$h = h_O + \left(\frac{2.\Psi.H_C.\sin[\pi.t_S/D_L]}{\rho.c_p.\beta.u}\right)^{1/2} .(x-x_O)^N \qquad (8)$$

where

$h_O$ = Initial TIBL depth (m)

$\Psi$ = Solar insolation factor (between 0 and 1.0 for negligible to strong insolation)

$H_C$ = 272W.m$^{-2}$ = 20% of solar constant (Anthes, 1978)

$\pi$ = (in radians, alternatively 180·)

$t_S$ = Time since sunrise (hrs)

$D_L$ = Length of day (hrs)

$x_O$ = Correction distance for change in TIBL shape (m)

$N$ = Variable exponent.

This formulation was the first to specifically include the addition of the initial mixed layer where necessary, as well as allowing for correction distance if the coastline was characterised by more than one change in surface roughness. Also included was a variable exponent of $x$ which resulted in a best fit of 0.61 from the limited data of Lyons *et al* (1983). However, both theory and observations tend to support a value of 0.5 as employed in other formulations. Equation (8) can thus be rewritten in the same form as the previous equations with a single half-power exponent.

**Other approaches and comments**

Two recent formulae have adopted completely different approaches. Hsu (1986) followed Van Dop *et al* (1979) and Misra (1980) and simplified all the physics of the relationship into a standard simple format of the type:

$$h = Ax^{1/2} \qquad (9)$$

where the coefficient $A$ was determined theoretically or from a best fit to empirical data. Hsu (1986) using a small data set from France, Sweden and Japan found $A$ = 1.91 ± 0.38, but somewhat larger values as high as 5.7 (Misra and Onlock, 1980) have been found elsewhere. The large range of this factor make it fairly site and situation specific, and better suited to local empirical validation. Venkatram (1986) avoided describing the TIBL height itself, and eclipsed any use of terms such as heat flux by considering only the equilibrium height of the TIBL and the distance inland at which it was reached. This equates to the height of the inland mixed layer (CBL), of which it is currently possible to make reliable predictions or relatively easy measurements. The TIBL curve is then calculated to this height in the following manner:

$$h = (h_0^2 + [h_e^2 - h_0^2][1 - e^{-x/L}])^{1/2} \qquad (10)$$

where
$h_e$ = Equilibrium height (m)
$L$ = Relaxation distance ($L = Bh_e$, $B$ = empirically derived constant).

Estimates of $B$ are at present unavailable in the literature, although typical proportions seem to suggest a value of around 25. Both equations (9) and (10) hold promise for engineering and operational usage due to the minimal amount of sophisticated meteorological data required as input.

Many of the foregoing equations have common drawbacks. The use of a constant entrainment parameter $F$ is debatable, but given the present poor understanding of entrainment dynamics, the best operational estimate is the commonly used value of 0.2 (eg. Tennekes, 1973; Venkatram, 1977; Gamo *et al*, 1983). Fortunately, most formulations are relatively insensitive to changes in $F$ (Venkatram, 1977; Steyn and Oke, 1982). The assumption of constant heat flux or surface temperature difference in the horizontal, although resulting

in asymptotic behaviour, does not result in a final equilibrium height as is frequently observed in practice (Stunder and SethuRaman, 1985). Also, as mentioned earlier, assumptions of constant vertical profiles are not always satisfied, although their theoretical structure has been experimentally verified in the laboratory (Deardorff *et al*, 1969). Many of the TIBL predictions possess another operational problem due to the presence of $\beta$ in the denominator, namely the singularity of the solution as $\beta \longrightarrow 0$ in the presence of near neutral lapse rates.

## EXPERIMENTAL BACKGROUND AND EVALUATION METHODOLOGY

### Data acquisition

The database used in this study consisted of a range of TIBL measurements taken as part of a field study over a coastal area 30km to the north of Cape Town, near the tip of the Southern African subcontinent (Figure 3). The shoreline was approximately linear with a NNW to SSE alignment. The terrain sloped gently upward from the coast to about 100m at 20km inland, displaying little relief apart from a few small hills further to the south and north of the study area. Ground cover was mostly ploughed wheatfields, with some grass and bush areas nearer the coast. There were a number of small settlements and farms in the region, with the 2000MW Koeberg nuclear power station centrally located on the shoreline.

Data were collected via both airborne and surface measurements in a similar fashion to that collected at Brookhaven and Kashimaura (*ibid.*). An instrumented light aircraft provided information on temperature, humidity, turbulence and heat flux at different levels while surface temperatures, wind data, insolation and acoustic sounder traces were recorded on the ground. A more complete description of the experimental method may be found in

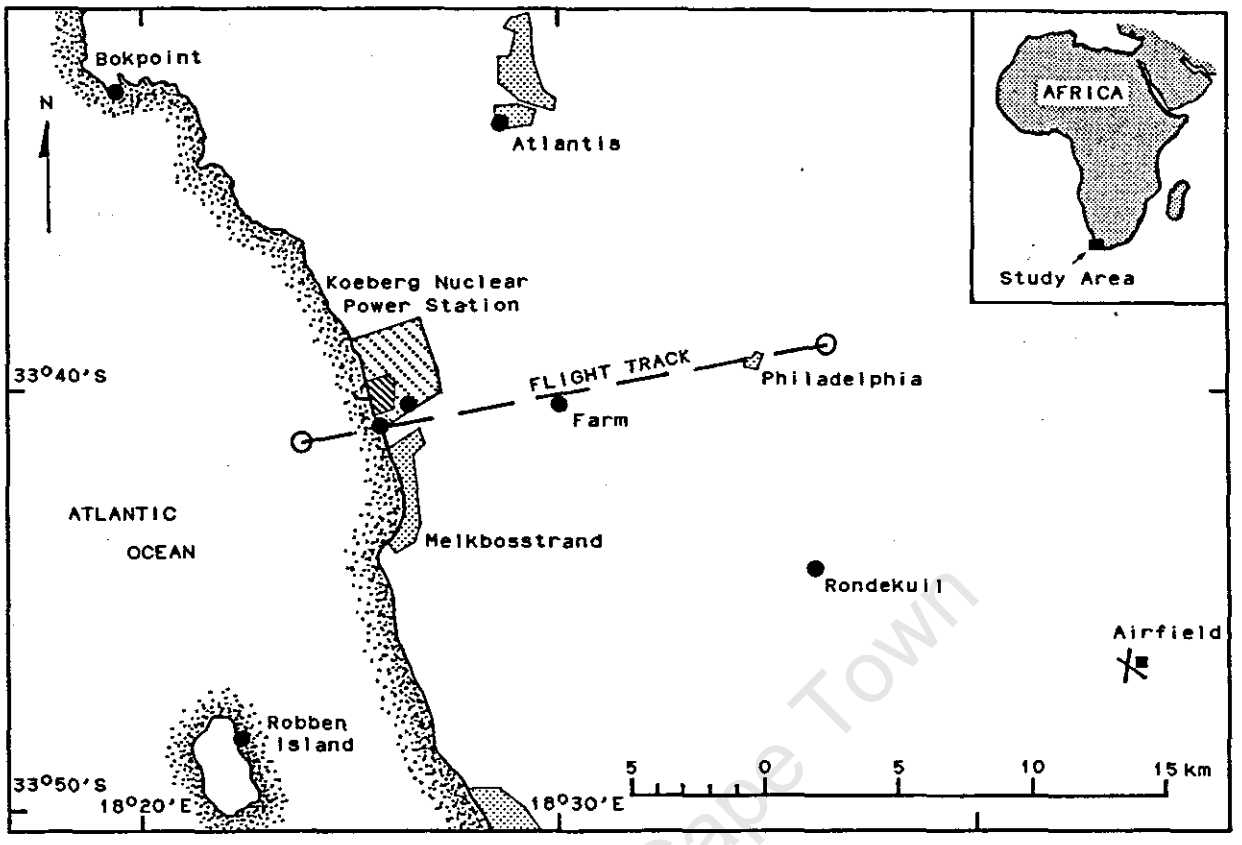


**Figure 3:** Location of the study area on the Southern African coastline showing instrument location (dots) and aircraft flight track (broken line).



Comrie (1988). The determination of TIBL height was made largely from the horizontal profiles of temperature, turbulent fluctuations and heat flux, with reference where necessary to the vertical temperature profiles and the acoustic sounder trace. It was thus possible to fix the TIBL boundary fairly precisely at numerous positions downwind, from which observed TIBL heights were determined at 1km intervals inland from the shore. The method of collection for the variables and constants in the various TIBL equations is provided in Table 1. A full tabulation of the corresponding data values can be found in Appendix 4.1.

TABLE 1
Input parameters and methods of data aquisition

| Parameter | Method |
|---|---|
| $H_O$ | $H_O$ = 0.39$S$ (Misra and Onlock, 1982; Venkatram, 1986) where $S$ = solar insolation from radiometer measurements |
| $\beta$ | Overwater aircraft temperature profiles |
| $\Delta\Theta$ | Overwater aircraft temperature profiles |
| $\bar{u}$ | Pilot balloon wind profiles |
| $\bar{u}_{10}$ | 10m meteorological masts |
| $T_L$ | Direct land surface thermistor readings |
| $T_W$ | Direct surf zone and water surface readings |
| $h_O$ | Overwater aircraft profiles of temperature and turbulence |
| $u_*$ | 0.4m.s$^{-1}$ from aircraft and surface measurements |
| $F$ | 0.2 (see text) |



## Statistical methods

A standardised methodology for the statistical evaluation of meteorological models was proposed by Fox (1981), and received general affirmation by Willmott (1982), who made a number of additional comments and modifications. Both emphasized that for one-dimensional scalar quantities a range of different measures should be computed to describe the relationships between observed and model-predicted variables. Willmott (1982) also stated that measures of the statistical significance of various correlation methods ought to be avoided as they are frequently misleading, and instead a complementary set of difference and summary univariate indices should be employed in a descriptive and informed approach to scientific model evaluation.

Statistical summary measures computed were firstly the mean observed and predicted values, $\bar{O}$ and $\bar{P}$, and secondly their standard deviations $\sigma_O$ and $\sigma_P$, which together generally

described the two variates. Also computed were the intercept and slope, $a$ and $b$, of the least squares regression $\hat{P}_i = a + b.O_i$, which outline the nature of the linear covariance between $\overline{O}$ and $\overline{P}$, and the coefficient of determination ($r^2$) or 'variance explained'. Difference measures used were the mean absolute error (MAE) and root mean square error (RMSE), both regarded as among the best measures of model performance as they summarised the mean differences in experimental units (metres). The mean bias error (MBE) was also computed as it provided a quick summary of over- or underprediction by the different models. Information on the nature of differences was obtained from the calculation of systematic (model oriented) and unsystematic (data oriented) errors and their relative proportions (potential accuracy), and on the relative size of the differences (actual accuracy) from $d$, the index of agreement. Computational formulae appear in Appendix 4.2, following the form of Fox (1981) and Willmott (1982).

It was decided not to adopt a scoring or weighting scheme to rank the various models, as any such scheme is by definition subjective and somewhat arbitrary in nature (Stunder and SethuRaman, 1985). Likewise, hypothesis tests such as the $F$ or $t$ tests are unreliable in model testing (Willmott, 1982) and can lead to confusion. Evaluation was based instead on knowledge both of the sensitivity of the above measures to the patterns and anomalies within the predicted and observed data, and of the models themselves, thus providing a comprehensive and in-depth assessment.



## RESULTS AND DISCUSSION

### Initial conditions

The observed data set was collected during the late southern summer in March and April 1987. A total of nearly 11 hours of complete TIBL data were taken over 8 different days

during this period, with measurements taken near midday when conditions were changing least. Each set of measurements provided around 5 to 10 TIBL height fixings, from which a total of 143 individual cases of observed TIBL height were obtained for analysis.

The TIBL height prediction formulae chosen for evaluation in this study comprised equations (1) through (8) inclusive. All inputs to these models were independent in nature, with no local empirical determinations required as in equations (9) and (10), which thus precluded the latter two equations from objective determination of TIBL height. Where a factor had an element of variability, the value suggested by the authors as typical or that most commonly indicated in the literature was used. All the equations except that of Lyons *et al* (1983) (equation (8)) assumed the existence of completely stable onshore flow, and therefore a modification was made to allow for the addition of the depth of an initial mixed layer ($h_O$) at the base of the TIBL. This modification allowed for the inclusion of Type A ($h_O > 0$) and Type B ($h_O = 0$) TIBLs (Comrie, 1988) in the evaluation, in a similar fashion to Stunder and SethuRaman (1985). In the evaluation which follows below, equations have been referred to by the name of their prime author.



**Typical Type A and B TIBLs**

Two typical examples of the evaluated TIBLs are presented here, Type A with an initial mixed layer, and Type B with completely stable upwind conditions. Run 413 is an example of TIBL Type A which had an initial mixed layer of 240m deep at the shoreline. Conditions were relatively clear and sunny, with a strong surface temperature differential and moderately strong wind speeds, as shown in Table 2. The initial height and relatively smooth TIBL profile that was observed can be seen in Figure 4. The TIBL grew steadily for about the first 15Km and reached to just below 900m height, beyond which TIBL growth levelled off to a more gradual rate

as the equilibrium height was approached. In this example the TIBL grew to a height greater than that predicted by any of the equations, although in the first half of its growth all were within 100m (about 20%) of the observed height except for Van der Hoven's formulation, which gave low values throughout. The best predictions for this selected

TABLE 2
Summary of meteorological parameters for two TIBL cases

| Parameter (units) | | Run 413 (Type A) | Run 421 (Type B) |
|---|---|---|---|
| $H_0$ | ($W.m^{-2}$) | 343 | 335 |
| #* | ($W.m^{-2}$) | 270 | 263 |
| $\beta$ | ($K.m^{-1}$) | 0.008 | 0.005 |
| $\Delta\theta$ | (K) | 8.7 | 3.2 |
| $\bar{u}$ | ($m.s^{-1}$) | 10.4 | 5.4 |
| $\bar{u}_{10}$ | ($m.s^{-1}$) | 7.8 | 4.2 |
| $T_L$ | (K) | 36.0 | 29.7 |
| $T_W$ | (K) | 11.6 | 13.4 |
| $h_0$ | (m) | 240 | 0 |

* $\# = \Psi H_C \sin(\pi t_S / D_L)$
(Lyons' equation)



case appeared to be those of Venkatram and Plate, as these deviated least from the observed height of the TIBL boundary.

Run 421 (Type B) took place under conditions of stable onshore flow and moderate wind speeds, with generally clear skies except for scattered small cumulus inland. The input set of initial meteorological conditions is also found in Table 2. Figure 5 illustrates the observed and predicted TIBL profiles, in which the TIBL grew fairly rapidly from

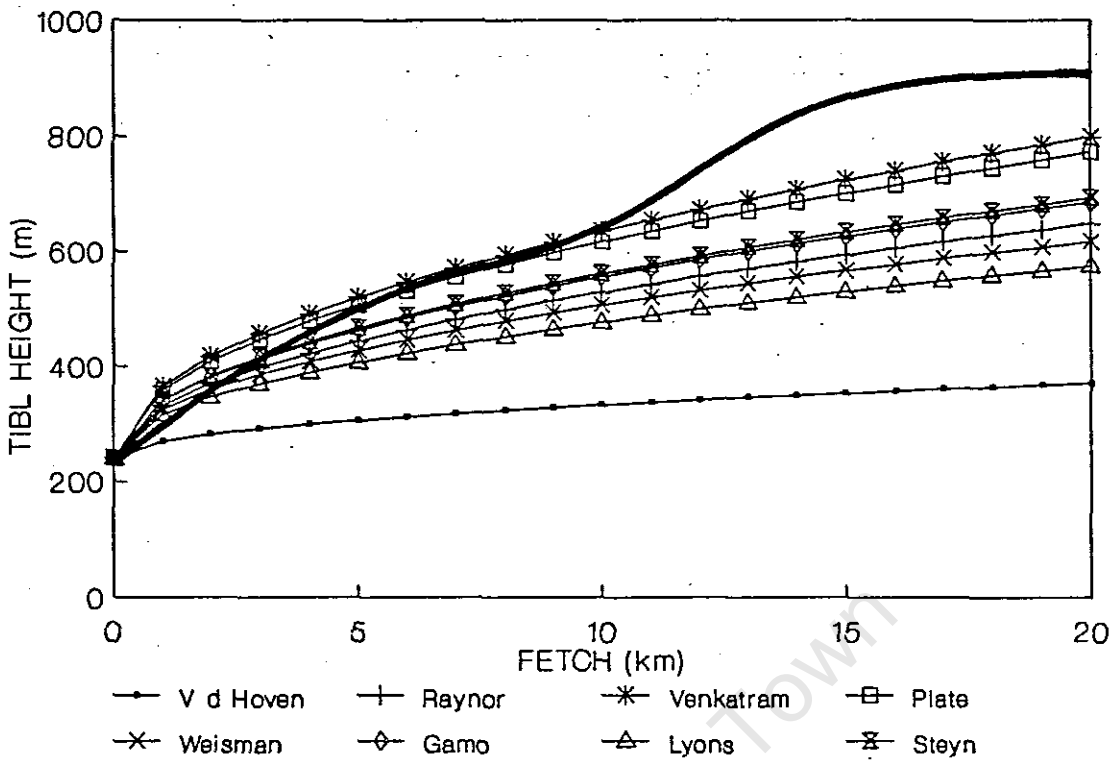


**Figure 4:** Observed (bold line) and predicted TIBL heights for Run 413, Type A.



ground level at the coastline to over 300m about 6km downwind. Over the next 2km a steep growth to about 550m due to convective activity caused a kink in the TIBL boundary, from which point a more gradual rate of increase was observed to just under 800m at 18km inland. The idealised smooth TIBL curves of the equations naturally could not precisely emulate the uneven pattern of the observed data, the accuracy of each model having to compromise on over- or underestimation at different points along the boundary. Only two of the eight chosen equations were strongly in error in this example, Van der Hoven's completely underpredicting, and Venkatram's completely overpredicting. Of the remaining formulae, that of Plate overpredicted by a factor of about 2 near the shore but by only a slight difference further inland, while those of Lyons and Weisman, although predicting well near the shore, generally underpredicted inland. The equations of Raynor, Gamo and Steyn all predicted within metres of each other, and supplied perhaps the best compromise by moderately overestimating TIBL height

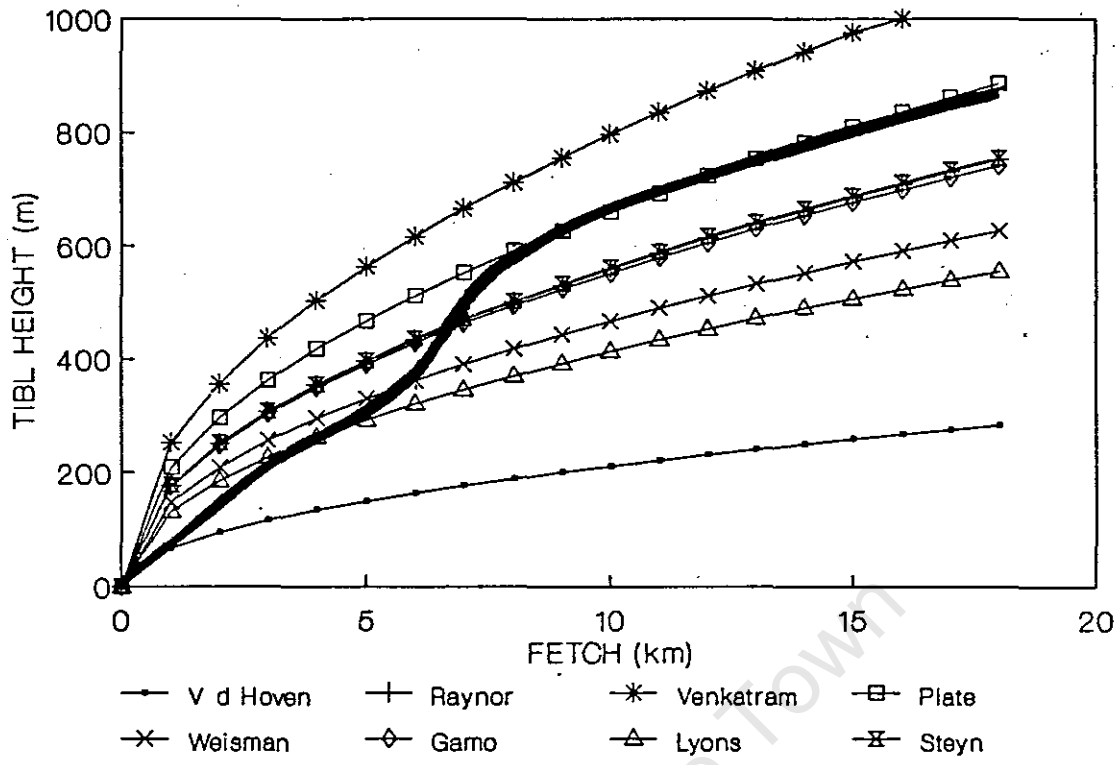


**Figure 5:** Observed (bold line) and predicted TIBL heights for Run 421, Type B.

nearer the coast, and moderately underestimating at greater distances downwind.

**Model performance - all data**

Statistical summary and difference measures were first calculated for all 143 cases of TIBL height (Appendix 4.3). The mean observed TIBL height for all cases was 622m, to which the closest approximations were the equations of Raynor and Steyn, both of which emerged with a mean predicted TIBL height of 600m (Figure 6). This slight underprediction was reflected in their MBEs of -22m, which were close to the observational error. Very near to this value was the equation of Gamo (-29m), while slightly higher was that of Plate, which on the average, overpredicted by 47m. Other formulations were in error, on the average, up to as much as -224m. It is of course desirable for a model to parallel any natural variations in the data, and the amount

of variability in the observed heights was described by a standard deviation of 281m (Figure 7). However, this measure can also be misleading in that an index of variance contains no guarantee of inherent accuracy. Thus although the formulae of Venkatram and Van der Hoven had the closest $\sigma_p$'s to the above value, not much was gleaned from this measure as all the values were within 10% of each other, and within 15% of the observed data.

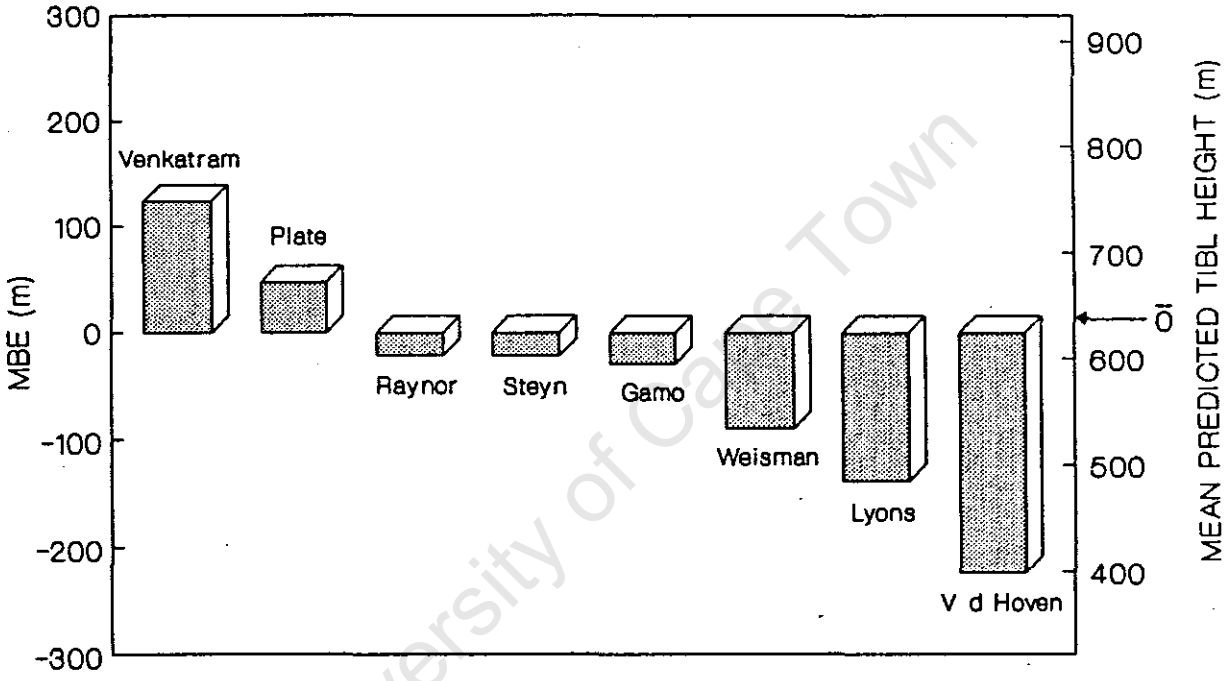


**Figure 6:** Mean bias errors and mean predicted TIBL heights for the eight selected equations (mean observed height = 622m).



At this point it is instructive to examine the regression parameters and scatterplots associated with some of the equations (Figure 8). Displays of this type can lead to great clarity between models as regards value, spread and bias of the data. Using the examples above it can be seen at a glance that, even though their means were the same, Steyn's equation was superior to Raynor's in terms of offset, gradient and variance. Likewise the plots for Van der Hoven's equation and Venkatram's equation showed the

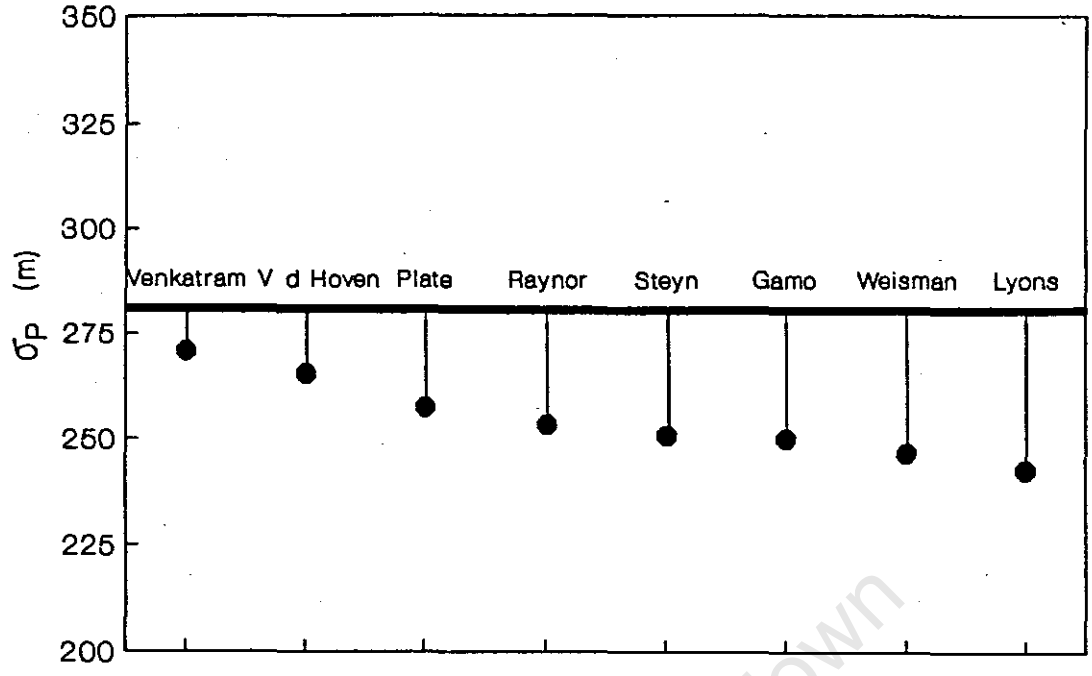


**Figure 7:** Standard deviations of predicted TIBL heights (dots) and observed TIBL heights (solid bold horizontal line).



respective performance below or above the observed data. In general, the larger values of *a* and smaller values of *b* suggested a systematic all round underestimate of both the TIBL gradient and height, as indicated earlier by the MBE. As regards the variance in $\overline{O}$ that is explained in $\overline{P}$ ($r^2$), Figure 9 reaffirms the above deductions, the equations of Plate, Gamo and Steyn having this proportion as high as 80%, and others dropping lower down to 55%.

For more precise distinctions between closely competing equations, use was made of two reliable measures of model performance, MAE and RMSE. Although MAE is intuitively more appealing due to its general expression of mean error in absolute terms, RMSE is also important as it is weighted more sensitively towards extreme values, thus incorporating a measure of consistency in the performance of a model (Willmott, 1982). Figure 10 illustrates the two respective sets of errors, which under the current assessment followed each other very closely. Ranking of the models by these

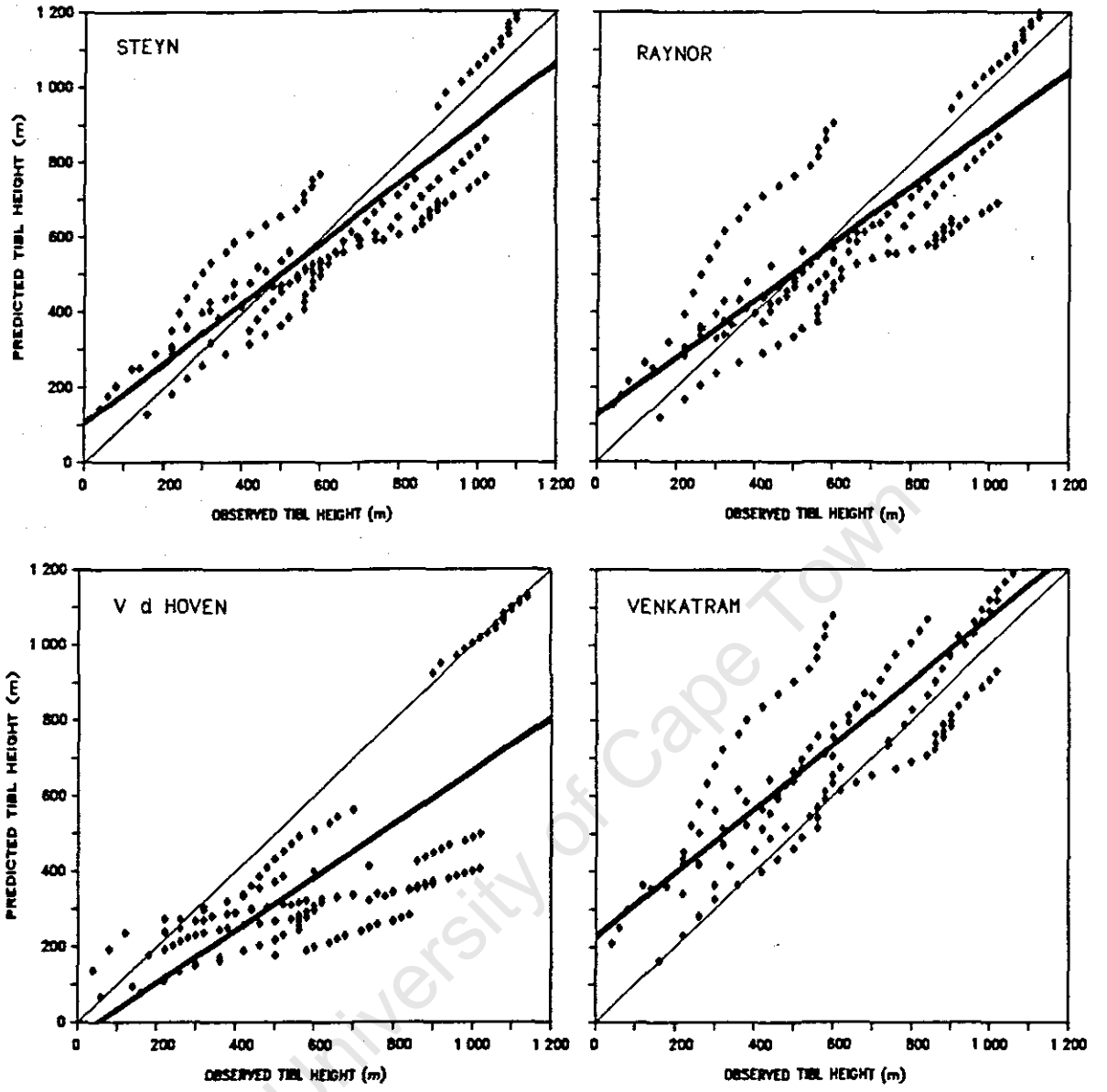




**Figure 8:** Regression lines (bold) and scatterplots for selected equations where regression formulae are: Steyn y=0.8x+102; Raynor y=0.75x+132; Van der Hoven y=0.7x-37; Venkatram y=0.84x+225. Feint diagonal lines represent *b* = 1 (predicted equals observed).

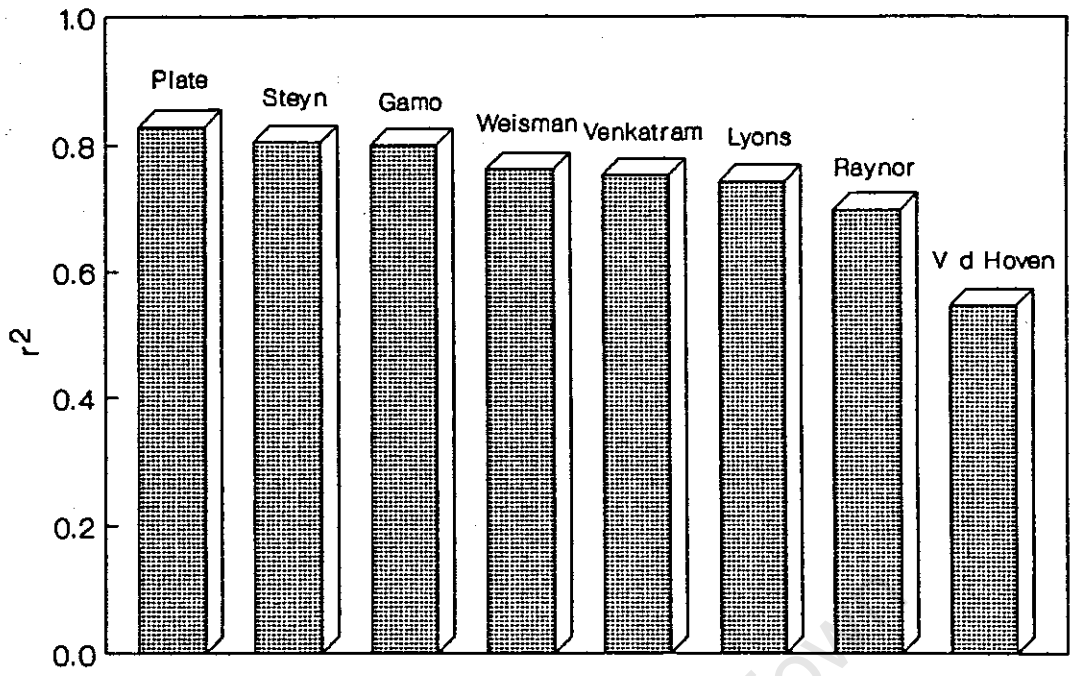


**Figure 9:** Correlation coefficients ($r^2$) or 'variance explained' for the eight selected equations.



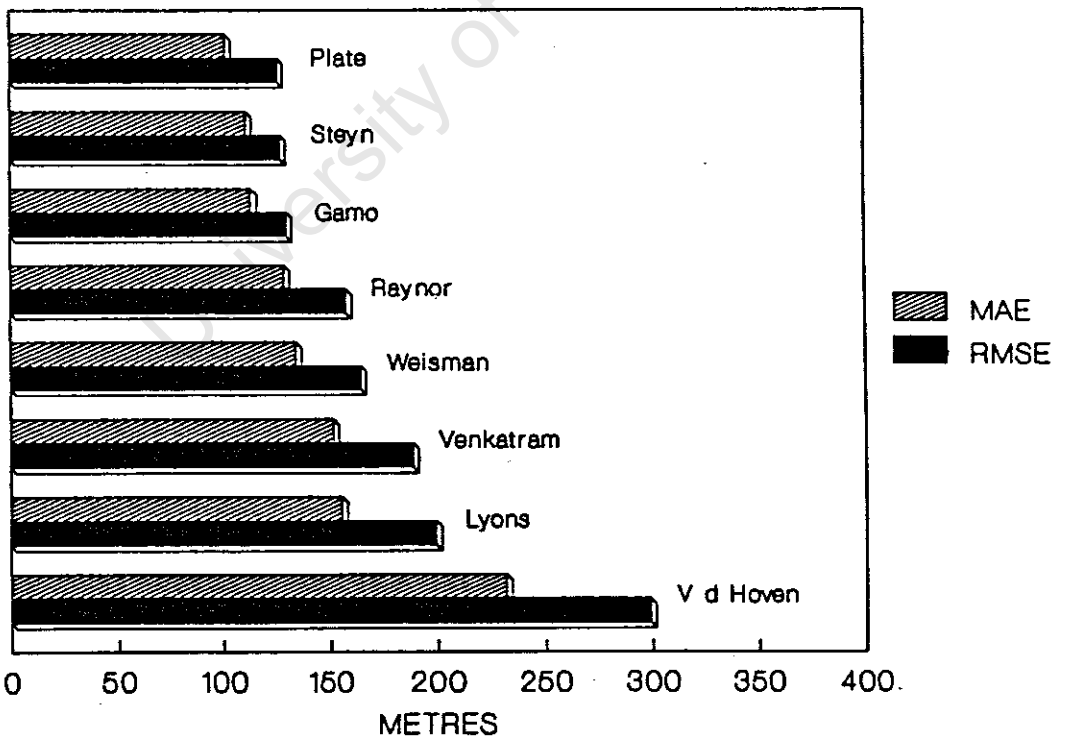


**Figure 10:** Mean absolute errors and root mean square errors of predicted TIBL height values.

methods was unanimous in each instance, with differences between the top three equations of Plate, Steyn and Gamo all within the observational error. The errors of the former two equations were practically identical, and constituted about 15% to 20% of the mean TIBL height.

Additional insight was gained from the complementary measures of systematic and unsystematic error. Considering the systematic or model-oriented error, Steyn's equation emerged with the lowest $RMSE_S$ of 60m, closely followed by Gamo, Plate and Raynor (Figure 11). When viewed as a proportion of systematic error ($MSE_S/MSE$) Raynor's equation in fact performed the best (0.21) due to its relatively smaller RMSE, with the next lowest being those of Steyn (0.23), Gamo (0.25) and Plate (0.28) (Figure 12). As this type of error can be described linearly, any adverse tendency of an equation may be damped out for operational use by making the appropriate adjustment. It is therefore also a measure of potential accuracy.



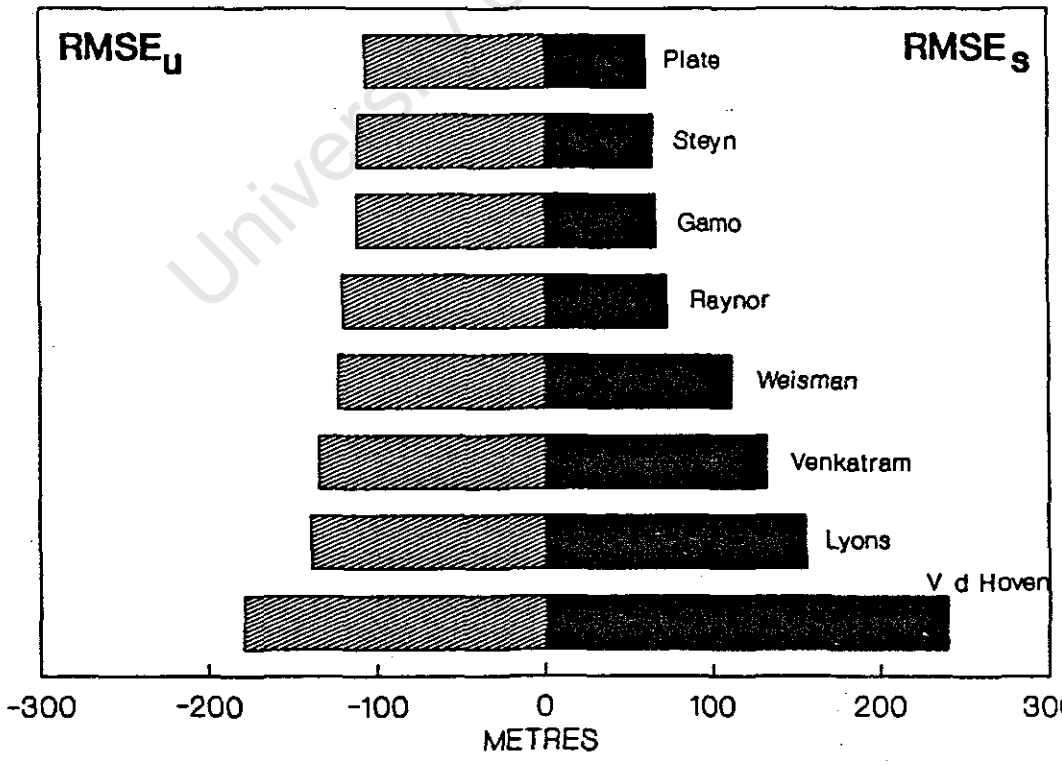


**Figure 11:** Systematic (model oriented) and unsystematic (data oriented) root mean square errors, which ranked the selected formulations in the same respective order.

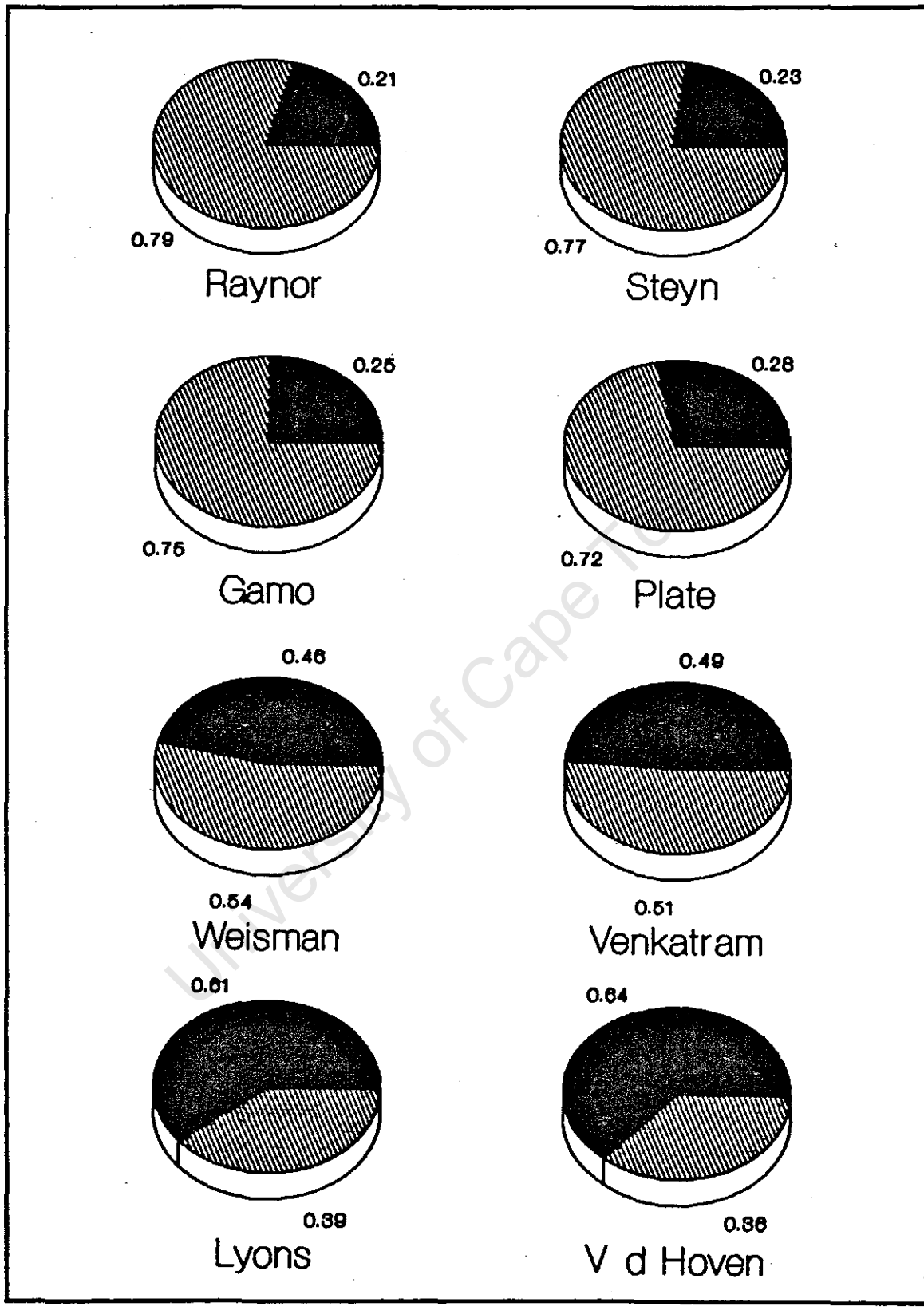




**Figure 12:** Proportions of systematic (model oriented - dark shading) and unsystematic (data oriented - light shading) error.

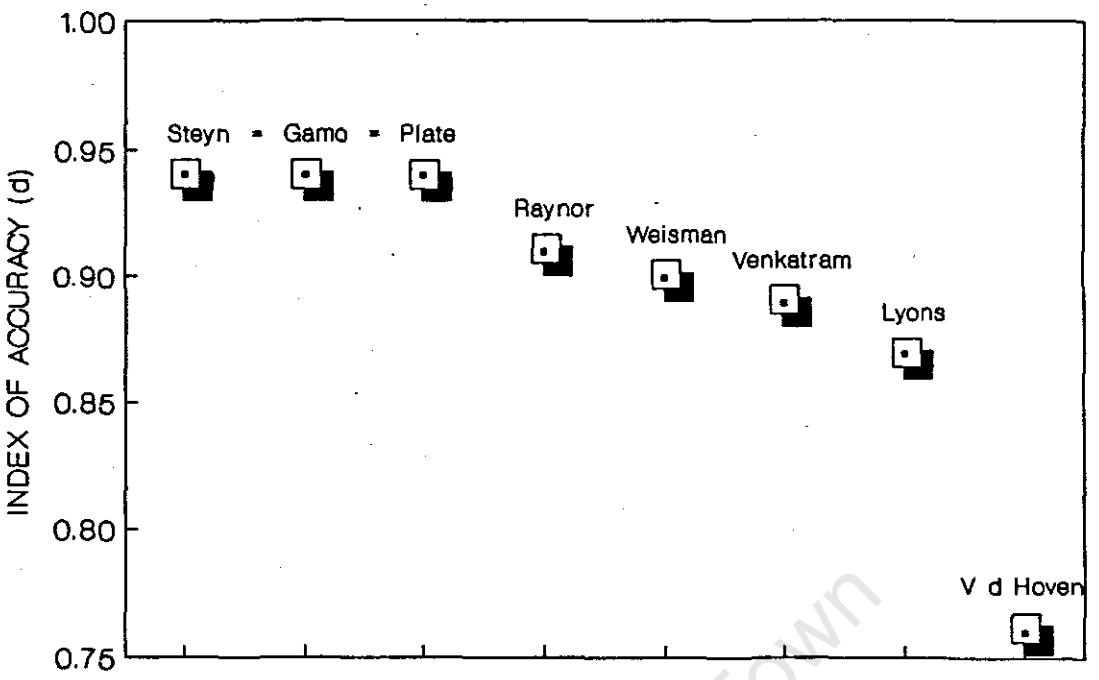


**Figure 13:** Indices of agreement (*d*) showing the equally well ranked equations of Steyn, Gamo and Plate.

A precise comparison of actual model accuracy is contained in the index of agreement (*d*) (Figure 13), which indicated that the equations of Steyn, Gamo and Plate all had an equally high level of accuracy (*d* = 0.94). These formulae were 3% more accurate than Raynor's equation, 4% more than Weisman's, 5% more than Venkatram's, and 7% more accurate than that of Lyons. Van der Hoven's equation was adjudged the least accurate of the prediction methods (*d* = 0.76).

**Model performance - categorised**

As the input data such as wind speed and stability did not show a great deal of variation, any categorisation of the data by these parameters would not have carried much meaning because of the small number of cases involved. However, classification into TIBL Types A (*n* = 91) and B (*n* = 52) provided sufficient cases in each type for additional insight to be gained from their seperate evaluation (Table 3).

TABLE 3
Statistical summary and difference measures for
Type A (N = 91) and Type B (N = 52)*

| | VdHoven | Raynor | Venkatram | Plate | Weisman | Gamo | Lyons | Steyn |
|---|---|---|---|---|---|---|---|---|
| TYPE A | | | | | | | | |
| $\bar{O}$ | 704 | 704 | 704 | 704 | 704 | 704 | 704 | 704 |
| $\bar{P}$ | 472 | 695 | 825 | 759 | 630 | 687 | 580 | 694 |
| $\sigma_O$ | 285 | 285 | 285 | 285 | 285 | 285 | 285 | 285 |
| $\sigma_P$ | 295 | 249 | 262 | 251 | 245 | 246 | 244 | 247 |
| *a* | -69 | 220 | 293 | 215 | 122 | 163 | 78 | 168 |
| *b* | 0.77 | 0.67 | 0.76 | 0.77 | 0.72 | 0.74 | 0.71 | 0.75 |
| MAE | 235 | 152 | 161 | 128 | 131 | 127 | 144 | 127 |
| MBE | -233 | -9 | 121 | 55 | -74 | -17 | -124 | -10 |
| RMSE | 312 | 183 | 204 | 147 | 172 | 146 | 201 | 144 |
| $RMSE_S$ | 242 | 93 | 140 | 85 | 109 | 75 | 149 | 73 |
| $RMSE_U$ | 197 | 157 | 149 | 120 | 133 | 125 | 135 | 124 |
| prop. | 0.60 | 0.26 | 0.47 | 0.33 | 0.40 | 0.26 | 0.55 | 0.26 |
| $r^2$ | 0.55 | 0.60 | 0.68 | 0.77 | 0.71 | 0.74 | 0.69 | 0.75 |
| *d* | 0.77 | 0.88 | 0.86 | 0.92 | 0.90 | 0.92 | 0.87 | 0.92 |
| TYPE B | | | | | | | | |
| $\bar{O}$ | 478 | 478 | 478 | 478 | 478 | 478 | 478 | 478 |
| $\bar{P}$ | 268 | 434 | 605 | 511 | 361 | 427 | 315 | 435 |
| $\sigma_O$ | 206 | 206 | 206 | 206 | 206 | 206 | 206 | 206 |
| $\sigma_P$ | 125 | 159 | 226 | 182 | 129 | 152 | 116 | 155 |
| *a* | 118 | 95 | 126 | 110 | 78 | 92 | 66 | 93 |
| *b* | 0.31 | 0.71 | 1.00 | 0.84 | 0.59 | 0.70 | 0.52 | 0.72 |
| MAE | 225 | 85 | 134 | 54 | 137 | 87 | 175 | 81 |
| MBE | -210 | -43 | 128 | 33 | -116 | -50 | -163 | -42 |
| RMSE | 274 | 97 | 157 | 74 | 149 | 93 | 195 | 87 |
| $RMSE_S$ | 253 | 74 | 128 | 47 | 143 | 79 | 190 | 72 |
| $RMSE_U$ | 106 | 63 | 92 | 58 | 41 | 48 | 45 | 49 |
| prop. | 0.85 | 0.58 | 0.66 | 0.40 | 0.92 | 0.73 | 0.95 | 0.68 |
| $r^2$ | 0.27 | 0.84 | 0.83 | 0.90 | 0.90 | 0.90 | 0.85 | 0.90 |
| *d* | 0.68 | 0.92 | 0.85 | 0.95 | 0.84 | 0.93 | 0.76 | 0.93 |

* All means, standard deviations and errors in metres.

The relative performance of the different equations was on the whole very similar for Type A and B, with much the same ranking as in the uncategorised evaluation. The $\overline{O}$, $\overline{P}$ and MBE values behaved as expected, as did the standard deviations which displayed only minor changes. In terms of MAE and RMSE, the equations of Steyn, Gamo and Plate ranked essentially equal for Type A, Steyn's being only marginally better than the others. In Type B, Plate's equation was somewhat better ranked than those of Steyn, Gamo or Raynor for both MAE and RMSE. The regression parameters also echoed their uncategorised behaviour, but reflected the same slight bias in Type A and Type B that was found in the mean errors. The lowest systematic error in Type A was for Steyn's model, and for Plate's model in Type B, where Raynor's equation also performed well. Conversely, the formulations of Steyn, Gamo and Raynor performed equally well for Type A TIBLs in terms of the proportion of systematic error (potential accuracy), while for Type B TIBLs Plate's equation clearly had the highest ranking. With reference to actual accuracy ($d$), in Type A the formulae of Steyn, Gamo and Plate were all equally high, while in Type B Plate's formula was 2% more accurate than those of Steyn and Gamo, and 3% more than Raynor's.

**Equation performance**

From the foregoing results it was possible to discern a generalised unscored ranking of the TIBL height predictions as outlined in Table 4 below. The first three formulations (Plate, Gamo and Steyn) all performed very close to one another throughout the statistical evaluation, with any differences between them consistently within the observational error. Depending on the measure employed they each had certain small benefits over one another, although when viewed in the context of the limited observational data set any further differentiation became meaningless. Raynor's equation was considered to be marginally less superior than

TABLE 4
Unscored ranking of TIBL height equations

| Rank | Model |
|---|---|
| } | Steyn |
| 1, 2 & 3 } | Plate |
| } | Gamo |
| 4 | Raynor |
| 5 | Weisman |
| 6 | Venkatram |
| 7 | Lyons |
| 8 | Van der Hoven |

those equally placed in top rank, but was the highest placed empirical equation. Its potential accuracy was in fact the most promising, but due to the greater scatter and variance of its predictions it received slightly lower rankings. The ranking of the lower four equations was consistent in all the statistical assessments.

Clearly the theoretically derived mixed-layer based models generally performed the best. The structure of these equations is essentially identical except for the choice of coefficient in the numerator, which for this data set ideally seemed to lie between a coefficient of 4 in equation (4) (Plate) and one of $2.[1+F] = 2.4$ in equation (6) (Gamo). This is reinforced in Stunder and SethuRaman (1985) who indicated Weisman's equation (the only equation of this type evaluated) to be the best. High ranking was also given to Raynor's equation with similar comments on correlation and scatter. Venkatram's equation was not highly ranked in Stunder and SethuRaman (1985), for the same reasons of overprediction as in this study. Although mixed-layer wind speed was incorporated, the entrainment parameter caused results to be consistently larger than the Raynor equation of similar format. As the Lyons equation also had the sound basis of the mixed-layer format, considerable potential would exist if the underprediction of the heat flux

parameterisation were to be counteracted. It was felt that the consistent underestimation was due to the low value of maximum heat flux ($272 W.m^{-2}$) contained in the parameterisation, for which a more realistic value closer to about $400 W.m^{-2}$ may provide improved results. This was in fact alluded to by Lyons *et al* (1983) for cases where actual measurements of maximum heat flux are available. Lyons' equation would then perform almost identically to that of Weisman. The poor ranking of the Van der Hoven equation was attributed to the inaccuracy of the $\Delta\Theta$ term in parameterising the upwind stability, the $\beta$ term in the other equations being far more appropriate as it comprised the whole depth of the TIBL. The systematic underestimation of TIBL height was also attributed to the size of the empirical coefficient of 8.8, which is by definition site-dependent.

## SUMMARY AND CONCLUSIONS

This paper has sought to evaluate the performance of the TIBL height prediction equations by means of a statistical comparison, in order to assess their relative accuracy, applicability and sensitivity. The evaluation was made via the application of a number of statistical summary and difference measures, using a recently collected independent data set. This study found, for the limited data and selected equations under consideration, that:

1) The equations of Plate (1971), Steyn and Oke (1982) and Gamo *et al* (1983) together received equally high ranking, and were judged to have the best overall performance. The equation of Raynor *et al* (1975) performed almost as well, but received a slightly lower ranking due to the greater variance of its predictions. The equations of Weisman (1976), Venkatram (1977), Lyons *et al* (1983) and Van der Hoven (1967) received sequentially lower ranking;

2) Models based on the thermodynamic principles of mixed-layer theory, and which included the direct use of surface heat flux, performed better in general than those equations that used other methods. The finer differences in prediction between equations of this type resulted from the relative sizes of the coefficient in the numerator;

3) Model performance using categorised (Type A and Type B) data was essentially the same as that using uncategorised data, with marginal changes generally favouring the equation of Steyn and Oke (1982) for Type A, and that of Plate (1971) for Type B;

4) The mean bias of the highest ranked equations fell within 50m above or below the observed TIBL height. The variance of all the equation predictions was slightly less than that of the observed data due to the idealised shape of the former. The calculated regression parameters suggested a generalised underestimation by a small magnitude of both TIBL gradient and height by the equations;

5) The mean errors of the highest ranked equations were all within metres of one another, constituting on average 15% to 20% of the observed TIBL height. These formulae all possessed a low proportion of model-oriented error and thus a high potential accuracy, the highest of which was the equation of Raynor *et al* (1975). The highest ranked equations also possessed the largest indices of agreement, with accuracies a number of percentage points above those of the other equations.

This evaluation has provided an independent assessment of the performance of TIBL height equations using a variety of different statistical techniques. In the interests of objectivity the formulations were tested as given in the literature, without the use of local correction factors as might well occur under operational conditions. In such circumstances the appropriate modifications would serve to

further improve the relative accuracy of the model concerned, facilitating reliable prediction of TIBL height and possible fumigation conditions.

## REFERENCES


Anthes, R.A., 1978: The height of the PBL and the production of circulation in a sea breeze model. *J. Atmos. Sci.*, 35, 1231-1239.

Ball, F.K., 1960: Control of inversion height by surface heating. *Quart. J. Roy. Meteorol. Soc.*, 86, 483-494.

Comrie, A.C., 1988: Meteorological characteristics of thermal internal boundary layers. Chapter 2, unpublished M.Sc thesis, Dept. of Environ. and Geogr. Sci., Univ. of Cape Town.

Deardorff, J.W., Willis, G.E. and Lilly, D.K., 1969: Laboratory investigation of non-steady penetrative convection. *J. Fluid Mech.*, 35, 7-31.

Dobosy, R., 1979: Dispersion of atmospheric pollutants in flow over the shoreline of a large body of water. *J. Appl. Meteorol.*, 18, 117-132.

Elliot, W.P., 1958: The growth of the atmospheric internal boundary layer. *Trans. Amer. Geophys. Union*, 39, 1048-1067.

Fox, D.G., 1981: Judging air quality model performance - a summary of the AMS workshop on dispersion model performance. *Bull. Amer. Meteorol. Soc.*, 62, 599-609.

Gamo, M., Yamamoto, S. and Yokoyama, O., 1982: Airborne measurements of the free convective internal boundary layer during the sea breeze. *J. Meteorol. Soc. Japan*, 60, 1284-1298.

Gamo, M., Yamamoto, S., Yokoyama, O. and Yoshikado, H., 1983: Structure of the free convective internal boundary layer above the coastal area. *J. Meteorol. Soc. Japan*, 61, 110-124.

Hanna, S.R., 1983: A simplified scoring system for air quality models. Paper 8336.6 presented at Annual Air Poll. Control Assoc. Meeting, Atlanta, Georgia.

Hsu, S.A., 1986: A note on estimating the height of the convective internal boundary layer near the shore. *Boundary-Layer Meteorol.*, 35, 311-316.

Kerman, B. R., 1982: A similarity model of shoreline fumigation. *Atmos. Environ.*, 16, 467-478.

Lyons, W.A. and Cole, H.S., 1973: Fumigation and plume trapping on the shores of Lake Michigan during stable onshore flow. *J. Appl. Meteorol.*, 12, 494-510.

Lyons, W.A., Keen, C.S. and Schuh, J.A., 1983: Modeling mesoscale diffusion and transport processes for releases within coastal zones during land/sea breezes. *United States Nuclear Regulatory Commission*, NUREG/CR3542.

Misra, P.K., 1980: Dispersion from tall stacks into a shoreline environment. *Atmos. Environ.*, 14, 396-400.

Misra, P.K. and Onlock, S, 1982: Modelling continuous fumigation of the Nanticoke generating station plume. *Atmos. Environ.*, 16, 479-489.

Ogura, Y., 1950: On the heat transfer in the lower layer of the atmosphere. *Geophys. Notes, Geophys. Inst., Tokyo Univ.*, 3, 27.

Panofsky, H.A. and Brier, G.W., 1968: Some applications of statistics to meteorology. Pennsylvania State University, 224pp.

Peters, L.K., 1975: On the criteria for the occurrence of fumigation inland from a large lake. *Atmos. Environ.*, 9, 809-816.

Plate, E.J., 1971: Aerodynamic characteristics of atmospheric boundary layers. United States Atomic Energy Commission, 190pp.

Raynor, G.S., Michael, P., Brown, R.M. and SethuRaman, S., 1975: Studies of atmospheric diffusion from a nearshore oceanic site. *J. Appl. Meteorol.*, 14, 1080-1094.

Raynor, G.S., SethuRaman, S. and Brown, R.M., 1979: Formation and characteristics of coastal internal boundary layers during onshore flows. *Boundary-Layer Meteorol.*, 16, 487-514.

Schuh, J.A., 1975: A mesoscale model of continuous shoreline fumigation and lid-trapping in a Wisconsin shoreline environment. *Special Report no. 27*, Center for Great Lakes Studies, Univ. of Wisconsin-Milwaukee, 107pp.

Steyn, D.G. and Oke, T.R., 1982: The depth of the daytime mixed layer at two coastal sites: a model and its validation. *Boundary-Layer Meteorol.*, 24, 161-180.

Stunder, M. and SethuRaman, S., 1985: A comparative evaluation of the coastal internal boundary-layer height equations. *Boundary-Layer Meteorol.*, 32, 177-204.

Tennekes, H., 1973: A model for the dynamics of the inversion above a convective boundary layer. *J. Atmos. Sci.*, 30, 558-567.

Van der Hoven, I., 1967: Atmospheric transport and diffusion at coastal sites. *Nuclear Safety*, 8, 490-499.

Van Dop, H., Steenkist, R. and Nieuwstadt, F.T.M., 1979: Revised estimates for continuous shoreline fumigation. *J. Appl. Meteorol.*, 18, 133-137.

Venkatram, A., 1977: A model of internal boundary layer development. *Boundary-Layer Meteorol.*, 11, 419-437.

Venkatram, A., 1986: An examination of methods to estimate the height of the coastal internal boundary layer. *Boundary-Layer Meteorol.*, 36, 149-156.

Weisman, B., 1976: On the criteria for the occurrence of fumigation inland from a large lake - a reply. *Atmos. Environ.*, 12, 172-173.

Willmott, C. J., 1982: Some comments on the evaluation of model performance. *Bull. Amer. Meteorol. Soc.*, 63, 1309-1313.

CHAPTER 5

# FORMATION, STRUCTURE AND HEIGHT OF THE THERMAL INTERNAL BOUNDARY LAYER - A CASE STUDY



A case study methodology was employed to provide an overall view of the Thermal Internal Boundary Layer (TIBL) as a dynamic mesoscale feature of the coastal atmosphere. The TIBL formed from morning convective conditions, and followed the same growth and decay pattern as the surface heating and the development of onshore flow. The initially irregular TIBL boundary became more uniform during the day, as a steady balance between wind speed and surface heating was achieved. Strong undulations in the TIBL were caused by eddies and thermal upcurrents, which were characterised by large fluctuations and increased values of vertical velocity, temperature and heat flux. TIBL height observations and predictions highlighted a nearshore region of complex and unpredictable TIBL formation, and an inland region of more regular TIBL formation where relatively accurate observation and prediction of TIBL height was possible.

## INTRODUCTION

The need for a greater understanding of atmospheric dynamics and dispersion in coastal regions has been a necessary consequence of industrial development in such areas. Petrochemical plants, fossil fuel and nuclear power generating facilities have increasingly been located in shoreline environments, giving rise to concern regarding coastal air quality. A wide range of research has in turn been stimulated in order to improve not only theoretical knowledge, but also operational expertise in planning, impact assessment and prediction with regard to the dispersion meteorology of the coastal zone.

The coastal zone is characterised by a complex meteorological environment, which exhibits a number of unique features that arise from the fundamental physical differences between the underlying marine and terrestrial surfaces. When fair weather conditions prevail, such effects include the development of the sea breeze, and the formation of the Thermal Internal Boundary Layer (TIBL).

The TIBL manifests itself as an adjustment of the atmospheric boundary layer to the surface discontinuities of temperature and roughness that occur at the interface between land and sea. During onshore flow, surface based turbulence penetrates upward giving rise to the convex upper boundary that characterises the TIBL, thereby separating the evolving mixed layer near the surface from the unmodified relatively stable air that overlies it. Two entirely different dispersion regimes are thus formed adjacent to each other, and a number of complications can result. Pollutants emitted within the TIBL may suffer severe vertical limitations on their dispersion, especially near the shore, whilst pollutants emitted into the stable layer aloft may travel some distance inland before intersecting the TIBL, at which point the still relatively concentrated

plume will fumigate downwards (Figure 1). Under both sets of circumstances the ground level concentrations may be far greater than those normally predicted. Also, as horizontal scales are of the order of kilometres, and the TIBL height only a few hundred metres, relatively small changes in the latter can drastically affect the pollutant concentrations and location of the fumigation zone. The accurate determination of TIBL height, theoretically or empirically, is therefore of great value.

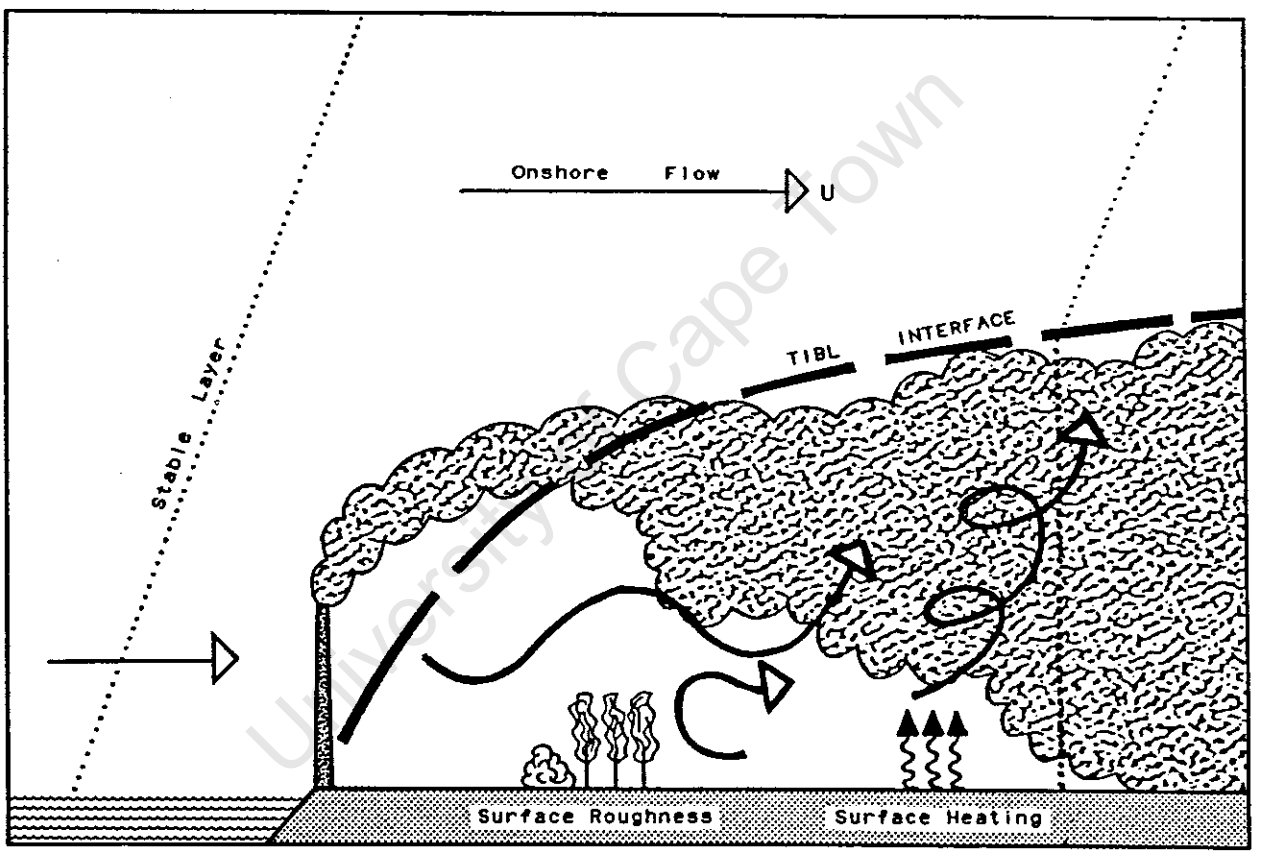




**Figure 1:** Schematic of TIBL formation and fumigation conditions during stable onshore flow.

Early knowledge on TIBLs was gained both from boundary layer and coastal air quality research, including Elliot (1958), Prophet (1961) and Van der Hoven (1967). Later studies covered the TIBL in more detail, with emphasis on fumigation, for example Collins (1971), Hewson and Olsson

(1967), Lyons and Cole (1973), Peters (1975) and Weisman and Hirt (1975). Only a small number of comprehensive field studies have been made due to the large resources required, with major contributions from Brookhaven, Long Island (Raynor *et al*, 1979), Nanticoke, Lake Erie (Portelli, 1982; Kerman *et al*, 1982) and Kashimaura in Japan (Gamo *et al*, 1982). Low level and nearshore turbulence measurements have also been performed, such as Echols and Wagner (1972), Smedman and Högström (1983), Ogawa and Ohara (1985) and Ogawa *et al* (1985). The prediction of TIBL height has also been included in numerous models, such as Raynor *et al* (1975), Venkatram (1977), Steyn and Oke (1982), Gamo *et al* (1983) and Lyons *et al* (1983).

Relatively few studies have sought to provide an overall view of the TIBL as a dynamic mesoscale feature of the coastal atmosphere. It is thus intended to provide a brief, yet sufficiently detailed, general coverage of the TIBL by means of a case study, encompassing its growth and decay, various structural and turbulent characteristics, and the observation and prediction of its height. The TIBL will thus be viewed within the context of not only its own properties, but also within that of the prevailing meteorology and the possible impact of its height on fumigation conditions.



## EXPERIMENTAL BACKGROUND AND DATA COLLECTION

### Study area

Figure 2 illustrates the location of the experimental site on the Atlantic coastline of Southern Africa, about 30km to the north of Cape Town. The shoreline was roughly linear and was aligned along a NNW to SSE axis. The terrain sloped gently upward from the coast to about 100m at 20km inland, displaying little relief except for a number of small hills further to the north and south of the study area. The land surface was covered mostly with ploughed wheatfields, with

some grass and low bush nearer the shore. There were a number of small settlements and farms in the region, with the 2000MW Koeberg nuclear power station centrally located on the shoreline.

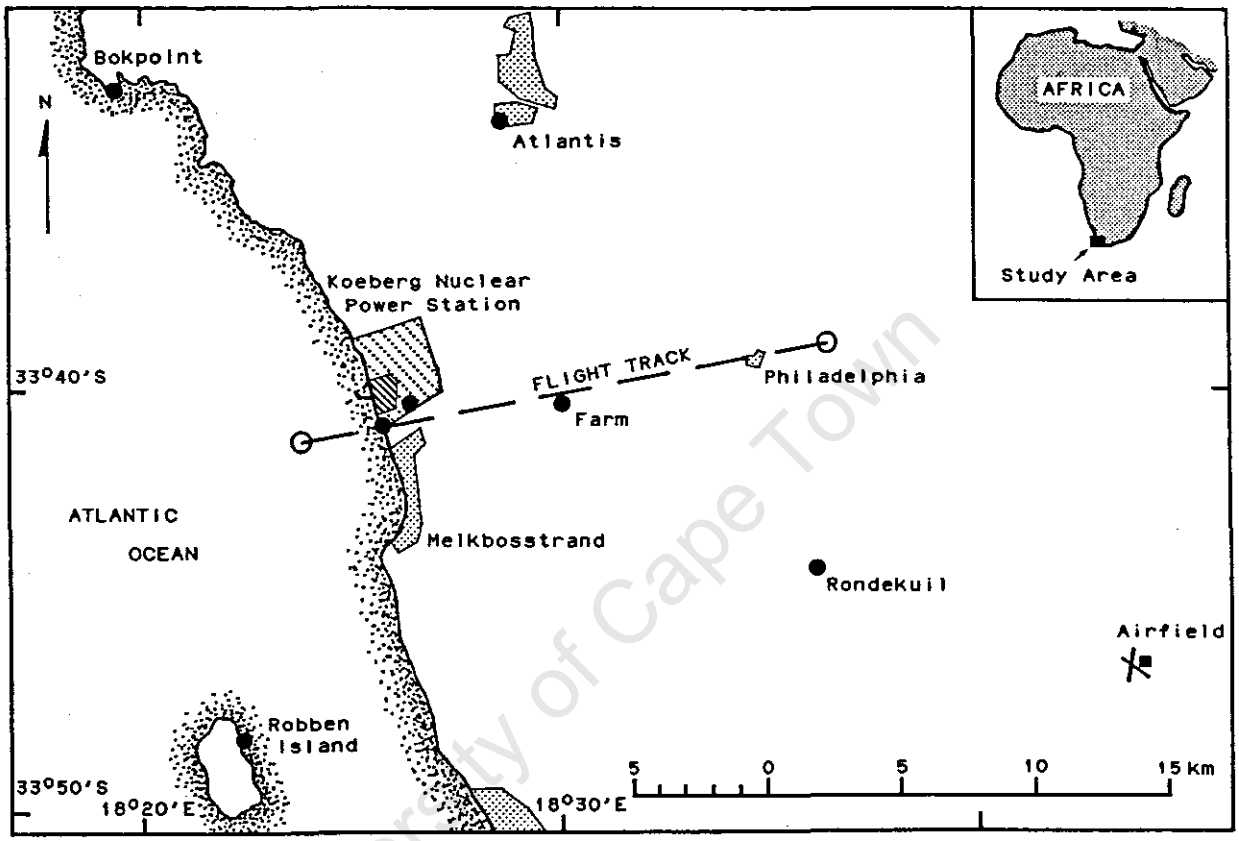


**Figure 2:** Location of the study area on the Southern African coastline showing instrument location (dots) and aircraft flight track (broken line).



## Instrumentation and data collection

Measurements of selected parameters were made via both airborne and surface sensors in a similar fashion to those collected at Brookhaven and Kashimaura (*ibid.*). This approach has proved to be the most effective method of obtaining a relatively complete data set over the time and distance scales required. Information on temperature, humidity, moisture content, turbulence and heat flux at

different levels of the atmosphere above the study region was provided by a light aircraft (Cessna 172) carrying computerised instrumentation. A selection of ground based measurements were also taken, with temperature, wind speed and direction available from a network of 10m masts, in addition to vertical pilot balloon wind profiles, land and sea surface temperatures, insolation and acoustic sounder measurements (Figure 2).

Surface data were acquired continuously throughout the day, including the acoustic sounder trace which was used to detail the constant changes in TIBL height, while the aircraft was flown in the middle of the day when conditions were fully developed and more constant over time. The data were calibrated and processed by microcomputer to provide horizontal and vertical profiles of the relevant parameters, from which composite two-dimensional cross-sections of the atmosphere were reconstructed. A more complete description of the experimental methodology may be found in Comrie (1988a).



## RESULTS AND DISCUSSION

### Synoptic conditions

The field experiments took place during March and April 1987, from which eight days of complete data resulted. The data set collected on Wednesday 1 April 1987 (Run 401) was selected for the current analysis as a typically representative and illustrative example of the conditions experienced. On this day the synoptic conditions were favourable for the development of onshore winds over the study region (Figure 3). A very weak ridge of high pressure extended over the area, separating two poorly developed cells of low pressure located W and SE of Cape Town. The study region was thus under the influence of a weak isobaric

pressure gradient, which provided gentle and generally westerly (onshore) winds within which more localised flow patterns were later to develop. Skies were clear except for a light scattering of fair weather cumulus inland from the study area.

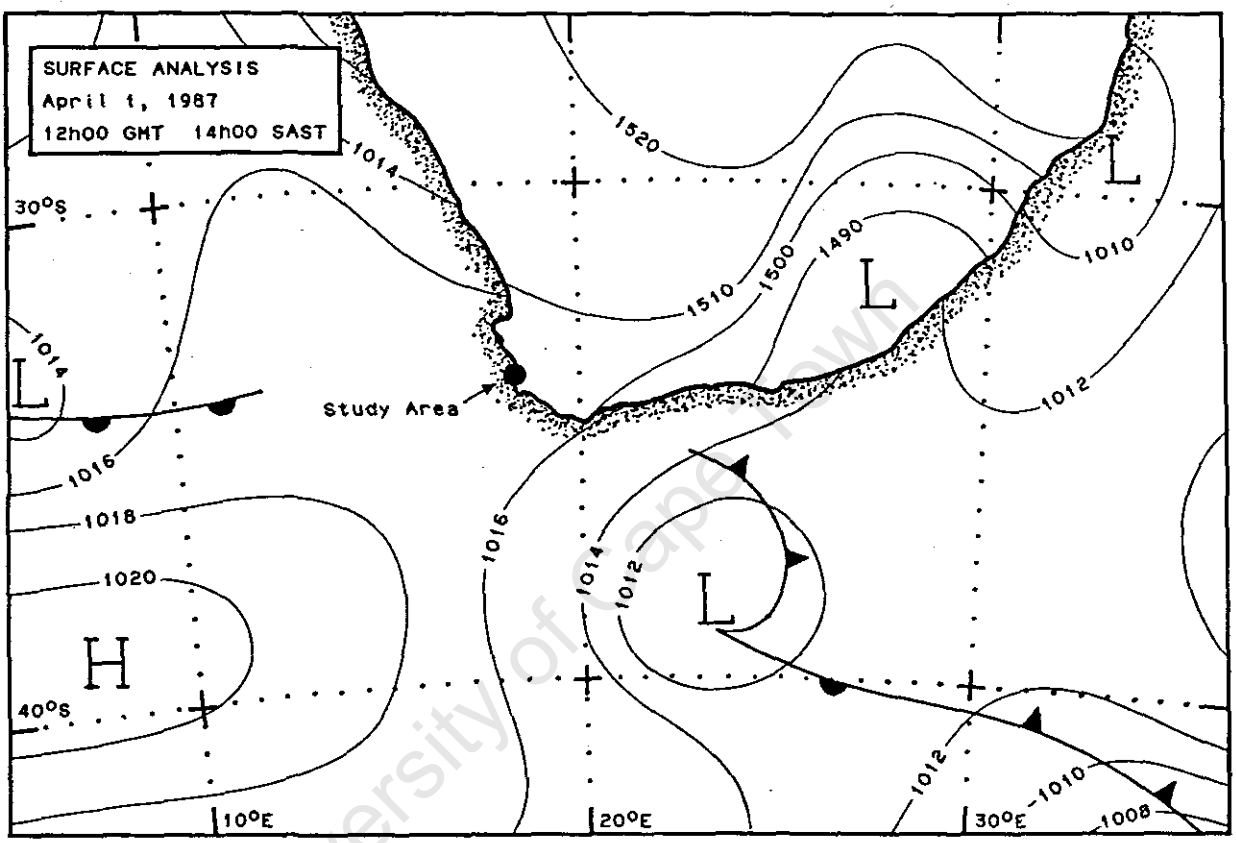


**Figure 3:** Synoptic surface pressure analysis (mB) over Southern Africa on 1 April 1987.



## Mesoscale wind field

The evolution of meteorological conditions during the day was revealed by the mesoscale surface (10m) data illustrated in Figure 4. At sunrise (07h00) a gentle drainage flow or land breeze was in progress over the study area. Wind directions displayed a northerly component throughout the region, with generally light wind speeds. The temperature of the drained air dropped by about 3°C or 4°C between 20km

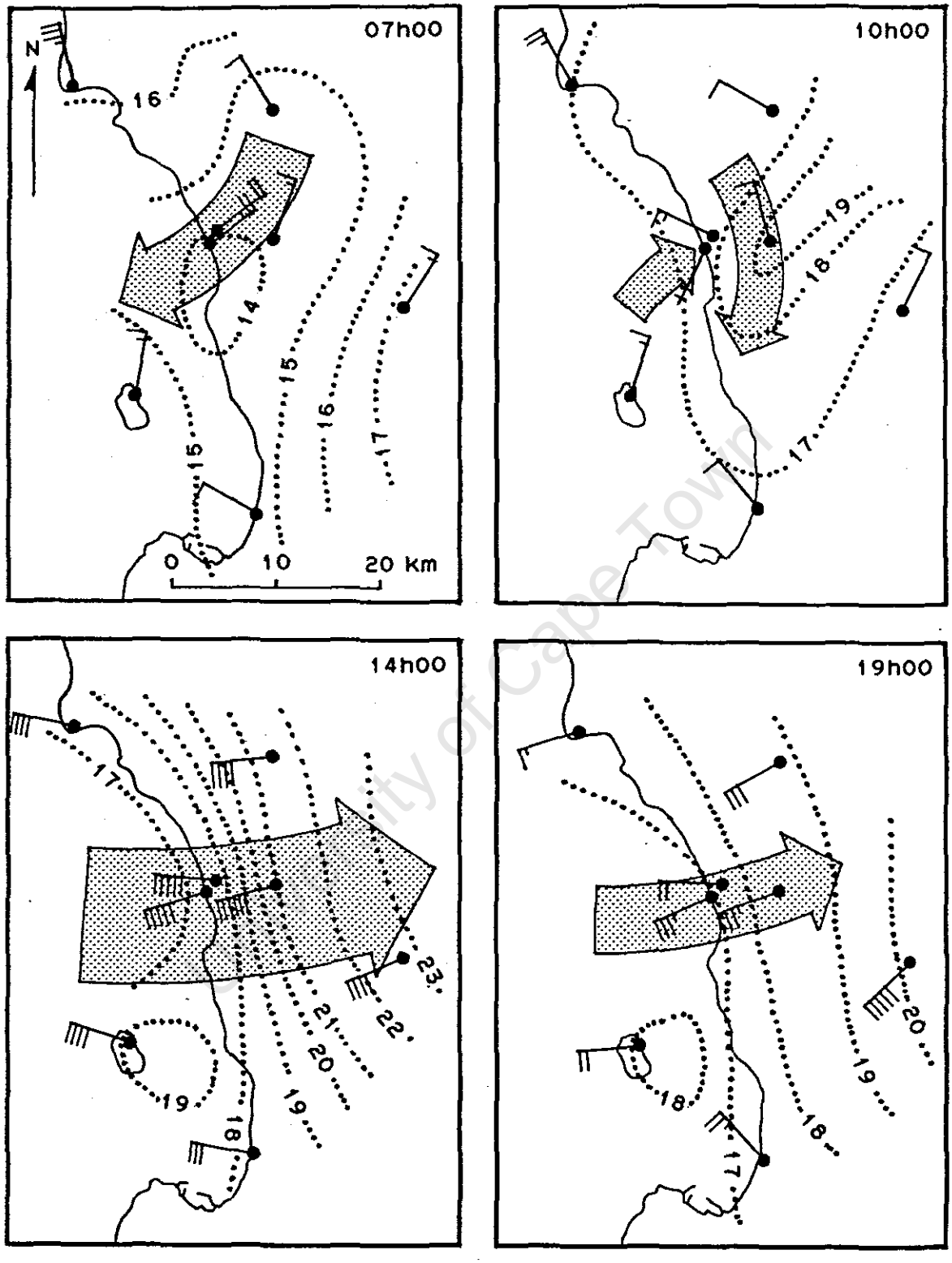


**Figure 4:** Evolution of surface (10m) meteorological conditions on 1 April 1987 (isotherms in $^{o}C$; one wind barb = $1m.s^{-1}$).

inland and the coast, where a minimum of about 13°C was recorded. Air temperatures over the sea were slightly warmer at about 15°C.

By 10h00 the northerly flow still persisted over much of the study area, but wind speeds had become almost calm as a result of the buildup of daytime conditions. This was especially notable in the temperature patterns which by this time had reversed, with temperatures inland about 2°C warmer than over the sea. This difference was sufficient to promote the onset of a sea breeze component over the study area, detected only at the coastal sites because its penetration had not yet extended more than a few kilometres inland.

As the day progressed, temperatures and wind speeds over the land continued to increase, while wind direction backed to westerly at all sites as the onshore component developed. At 14h00 just after solar noon the temperature differential was as much as 6°C, with relatively strong onshore winds of 4m.s$^{-1}$ to 6m.s$^{-1}$ over the study area. Solar radiation at this time was 850W.m$^{-2}$, with sea and land surface temperatures of 15.8°C and 37.9°C respectively. As the onshore flow moved inland, there was a tendency for the wind to back slightly and become directly perpendicular to the shoreline, due possibly to the thermal and frictional effects encountered over the land. These circumstances which arose during the day were suitable for the formation of a TIBL with the onset of a steady onshore flow out of the earlier calmer conditions. During the afternoon the WSW flow persisted, but wind speeds began to drop gradually towards the late afternoon with the corresponding decrease in the temperature differential. By sunset at 19h00 wind speeds had diminished to about 3m.s$^{-1}$, with a temperature differential of roughly 3°C.

**TIBL growth and decay**

The corresponding diurnal behaviour of the TIBL was recorded

by the acoustic sounder trace, illustrated in Figure 5, covering the same period of time from sunrise to sunset (07h00 to 19h00). The depth of the drainage flow at the sounder site 6km inland (Figure 2) was observed to decrease from about 150m to almost zero within the first hour after sunrise. A build up of thermal activity was detected by the acoustic sounder over the following two to three hours corresponding to the period of near calm discussed above. During the late morning the acoustic echoes clarified as wind speeds increased and thermal activity became smoothed. This period of transition during which convection over the land blended into the onset of onshore flow marked the start of TIBL formation. Hence in this example the TIBL did not increase in height from the ground upwards as might be expected, but was initiated from a turbulent layer a few hundred metres in depth.



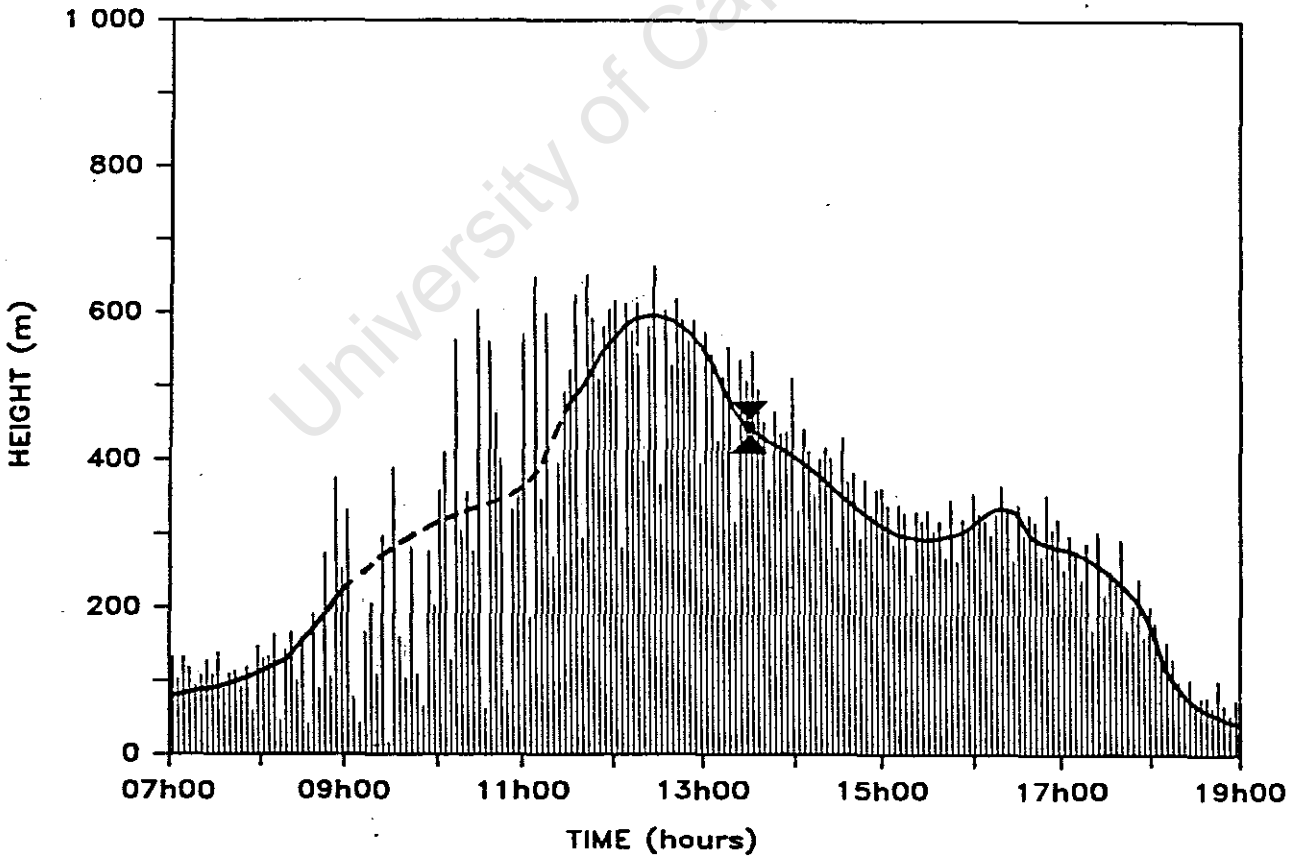


Figure 5: Facsimile of acoustic sounder trace showing observed height at 13h20 and inferred TIBL height during the day (solid line). The broken line represents unclear height definition due to convective activity.

The irregularity of the TIBL boundary until about noon indicated the intermittent nature of the turbulent mixing, due to the thermal activity and sporadic surges in wind flow that were occurring prior to the establishment of relatively steady conditions around 11h30. TIBL height peaked at around 500m to 600m near midday, and dropped off a little to about 400m during the early afternoon, coinciding with the airborne measurements which were taken simultaneously. During the course of the afternoon, TIBL height fluctuated by as much as 100m, due to the variability of the turbulent eddies associated with the TIBL. These oscillations of the TIBL boundary occurred at intervals of the order of approximately 5 minutes, with corresponding wavelengths of up to roughly a few kilometres. After about 16h30 the TIBL height decreased more rapidly to about 100m around sunset at 19h00. The acoustic sounder detected not only the TIBL boundary, but also the more intense turbulence nearer the surface, light turbulence at higher altitudes in the morning, and the evolution of a more stable layer above the TIBL in the evening. The growth and decay of the TIBL thus displayed many of the same characteristics as the mixing or convective boundary layer over the land, with relatively rapid growth before noon, a peak at the time of maximum heat flux followed by a gradual decrease during the afternoon, with further decreases towards evening as stable conditions developed.



**Vertical wind structure**

Comprehensive field measurements of TIBL structure were made between 13h00 and 14h00, during which time the TIBL height remained relatively constant. Vertical wind profiles (Figure 6) revealed the influence of the surface on the sea breeze component. This WSW flow occurred mainly in the lower 500m, above which the wind swung gently to a more westerly flow up to a height of about 1400m where direction became a constant 260$^{o}$. The wind speed profile revealed further distinctions between these three layers, with greatest wind

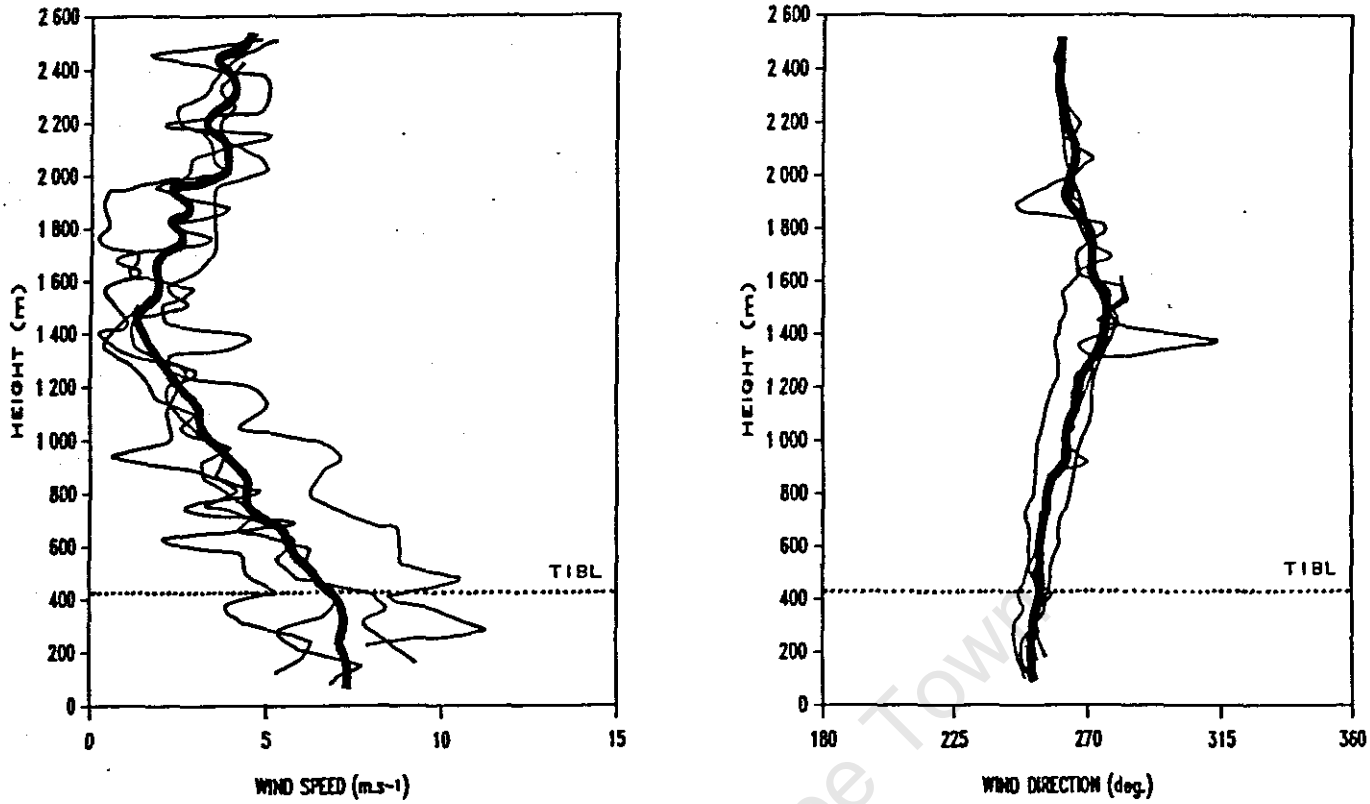


**Figure 6:** Vertical wind profiles showing mean wind speed and direction (bold lines) and individual profiles (feint lines), with the height of the TIBL boundary (dotted line).



speeds occurring below 500m, and which decreased to near calm around 1400m to 1500m. Above this height the gentle increase in wind speed corresponded to a different synoptic airflow in the atmosphere above the boundary layer. The TIBL itself was denoted by relatively uniform mean profiles of wind speed and direction up to 500m height.

### *Temperature and moisture structure*

Measurements by aircraft revealed a pattern of potential temperature which showed a stable onshore flow at the coastline which, during its passage inland, became eroded

from below by heating and mixing (Figure 7). Upon intersection with the TIBL, the isotherms bent downwards within the well mixed layer and displayed a constant potential temperature profile, which showed the characteristic increase in depth with distance downwind. A sharp increase in TIBL height was observed at 4km to 6km inland, beyond which the effects of TIBL growth were less sharp. At heights greater than about 1000m the isotherms remained relatively unaffected by any perturbations originating at the surface.

The increased temperatures within the TIBL (by about 4°C at the 200m level) had the consequence of reducing relative humidity in the TIBL, especially near the surface (Figure 8), thus facilitating the additional uptake of evaporative moisture off the land. The roughly 10% decrease in relative humidity was accompanied by an increase in moisture content of about 2.5g.kg$^{-1}$ between the coast and 16km inland at the 200m level (not illustrated).



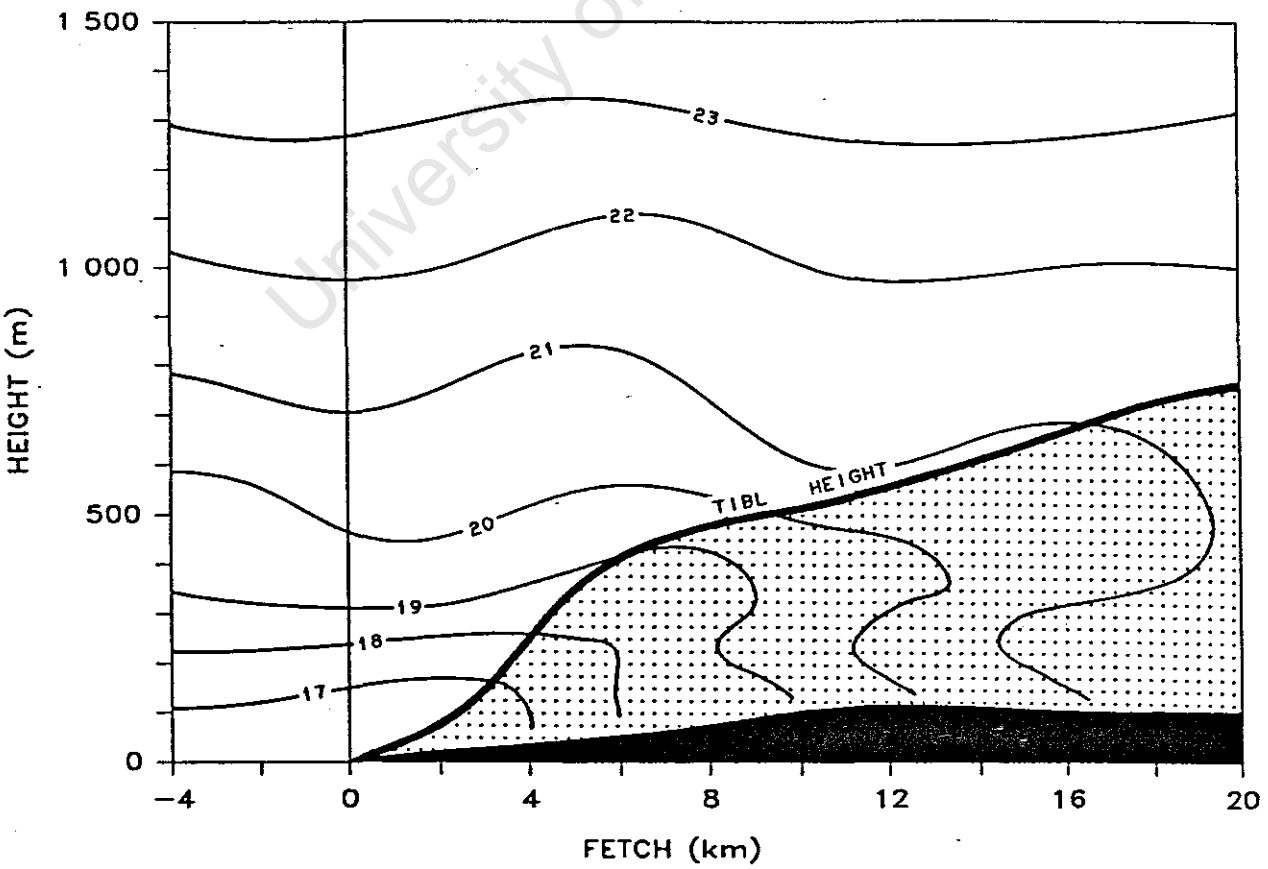


**Figure 7:** Cross-sectional pattern of potential temperature (°C) for Run 401.

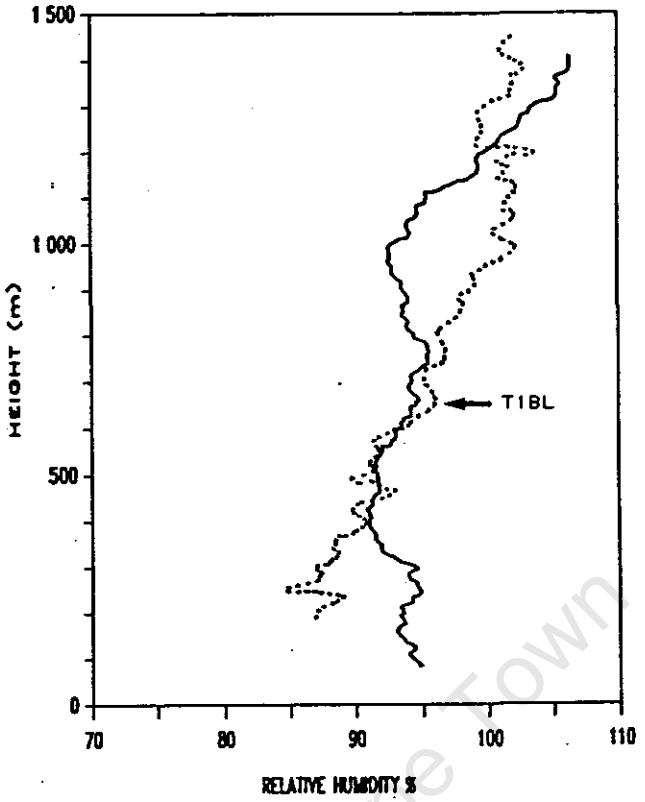


**Figure 8:** Vertical profiles of relative humidity (%) over the sea (solid line) and at 16km inland (dotted line) showing the decreased humidity within the TIBL.



## Turbulent structure

Cross-sections of the turbulent parameters $\sigma_w$ and $\sigma_T$ both displayed fairly similar structures associated with the TIBL (Figures 9 and 10). The slight persistence of low-level marine stability coupled with the occurrence of a thermal upcurrent produced a sharp rise in TIBL height near the 4km mark, with an associated bulge in the isopleths of both parameters. The nature of the aircraft flight pattern meant that the diminishing effect of the upcurrent was measured in successive horizontal runs as it moved upward. Undulations in the profile of the TIBL were also found further inland, for example at 12Km, but a generally steadier growth in the height of the turbulent region was found over the inland areas. Above the TIBL, loosely defined regions of low intensity turbulence were observed. Actual values of turbulent parameters increased two or threefold within the

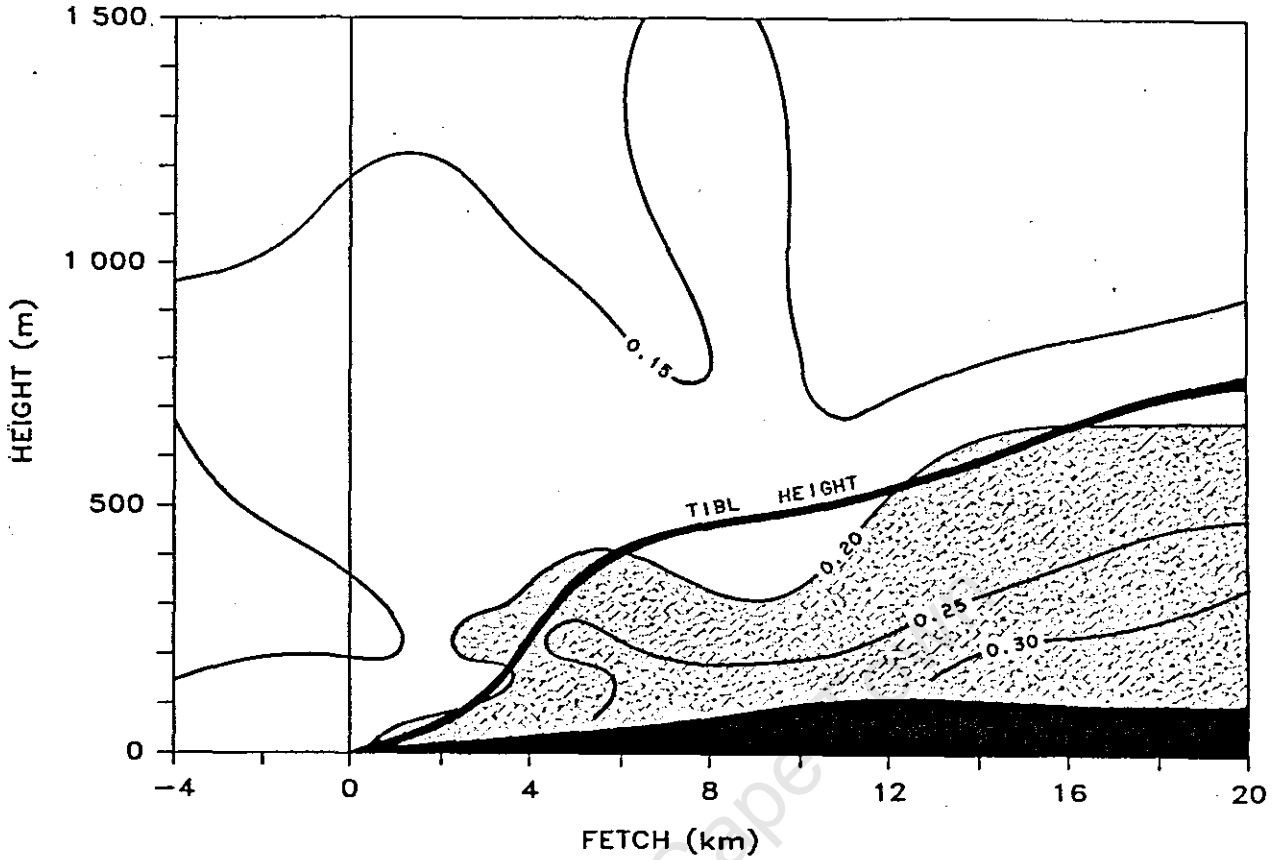


**Figure 9:** Cross-sectional pattern of $\sigma_w$ ($m.s^{-1}$) for Run 401.

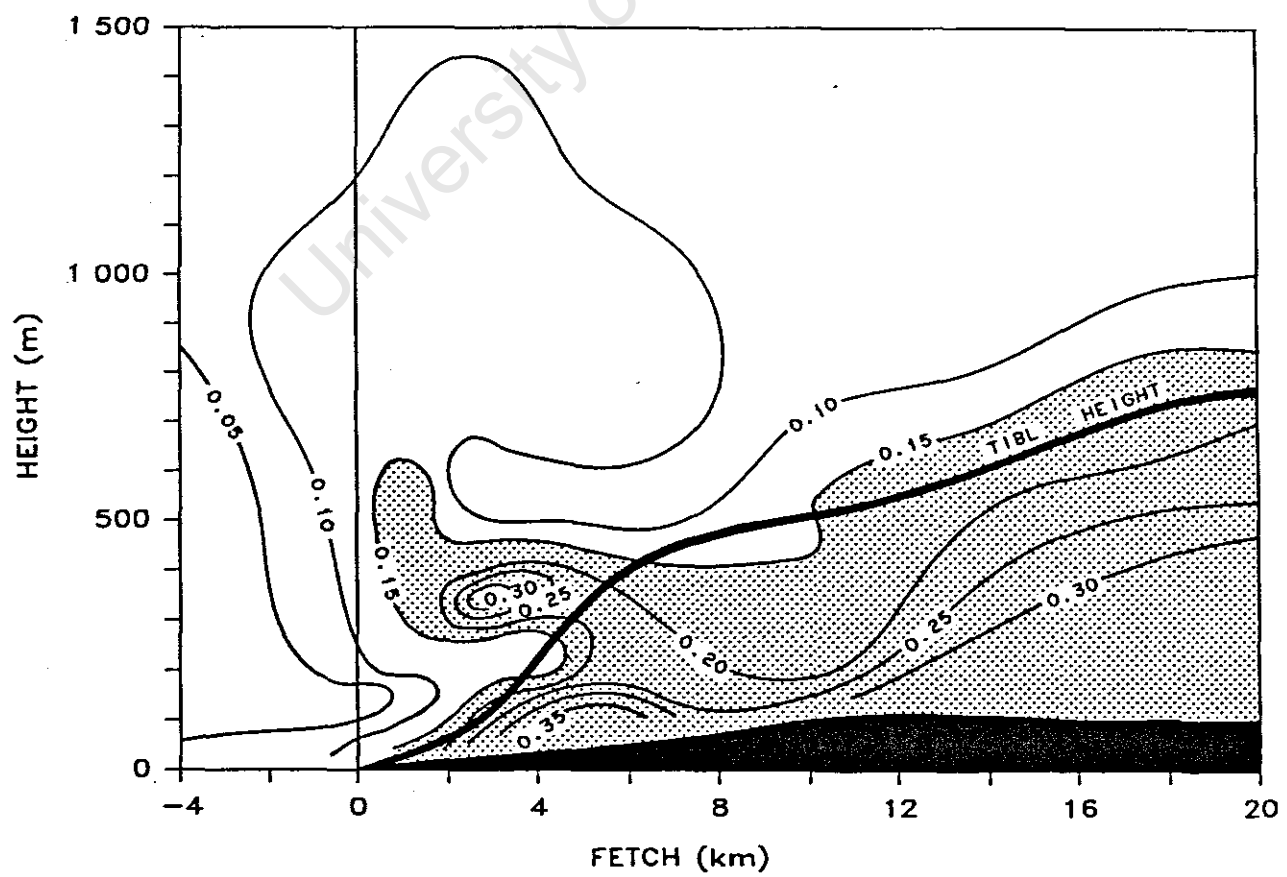


**Figure 10:** Cross-sectional pattern of $\sigma_T$ ($^0C$) for Run 401.

TIBL, with the strongest turbulence occurring near the surface.

**Heat flux structure**

Cross-sectional measurements of mean sensible heat flux ($\overline{w'\theta'}$) did not provide a clear definition of the TIBL height or shape, but the regions of more intense turbulence within and along the boundary of the TIBL were highlighted as areas of large heat flux (Figure 11). Heat flux was generally negligible outside the TIBL, but tenfold increases were found within the TIBL, especially in the lower regions associated with the surface boundary layer. Higher up, intense pockets of heat flux were more scattered and were associated with mixing and thermal activity, for example at the 4km to 6km marks and at 12km downwind. Some areas of relatively strong negative heat flux were also found, in many cases in close proximity to strongly positive regions.

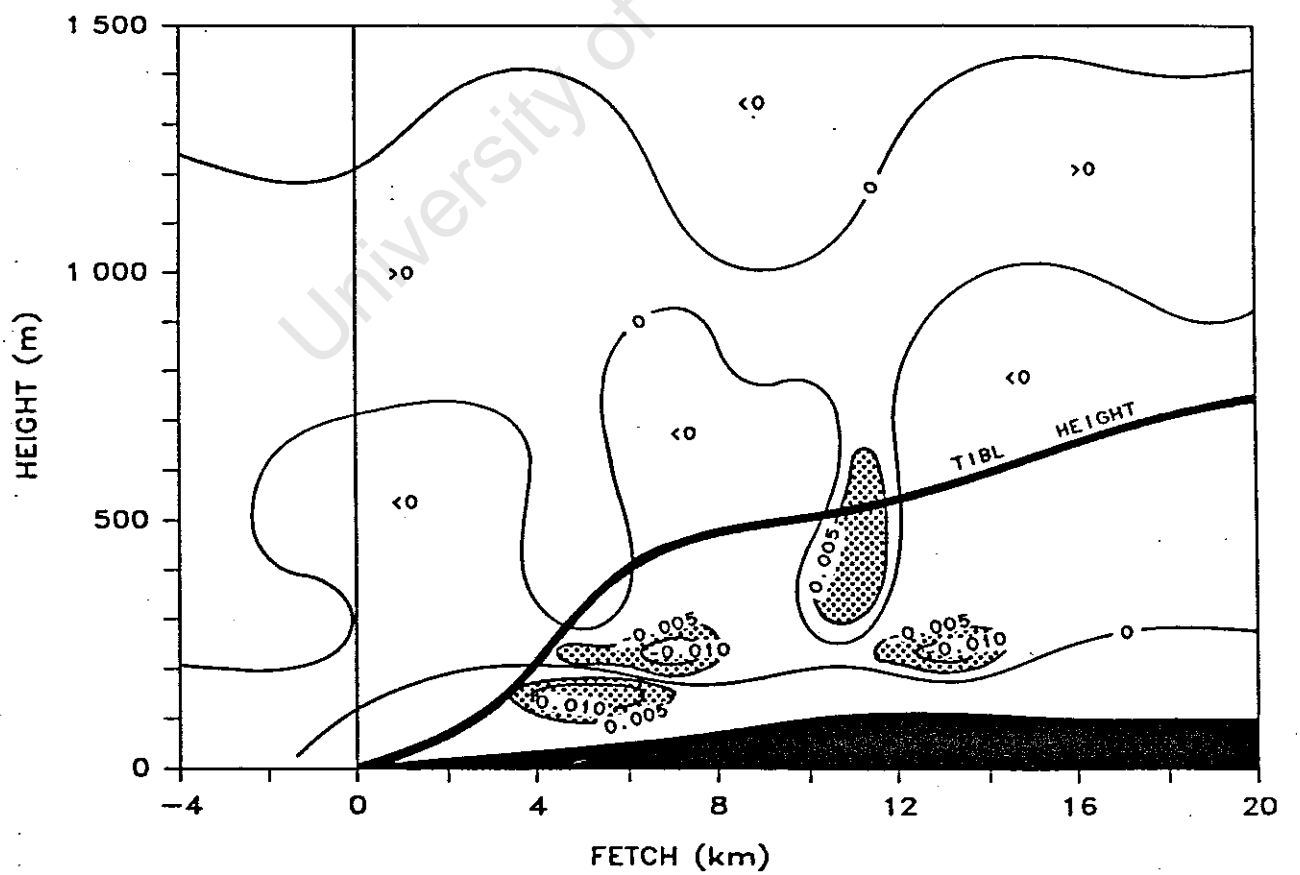


**Figure 11:** Cross-sectional pattern of mean sensible heat flux ($m.s^{-1}.K^{-1}$) for Run 401.

The isopleths of heat flux thus provided a fairly complex picture of the TIBL, with a contorted undulating boundary, although the latter was also partly due to the somewhat instantaneous nature of the measurements.

**Determination of TIBL height**

A range of methods were available for determining TIBL height from measured parameters, for example from the delimitation of the base of the stable layer in a vertical temperature profile (Raynor *et al*, 1979; Ogawa and Ohara, 1985), or from the maximum in the vector wind shear (Kerman *et al*, 1982). For the data presented above the observed TIBL height differed by as much as 20% to 30% depending on the parameter or definition followed. Gamo *et al* (1982) found similar discrepancies between TIBL height defined by temperature and turbulence. Intuitively, the definition of prime concern was that which described the height to which pollutants would diffuse within the TIBL. Unfortunately, no single parameter that could summarize this behaviour

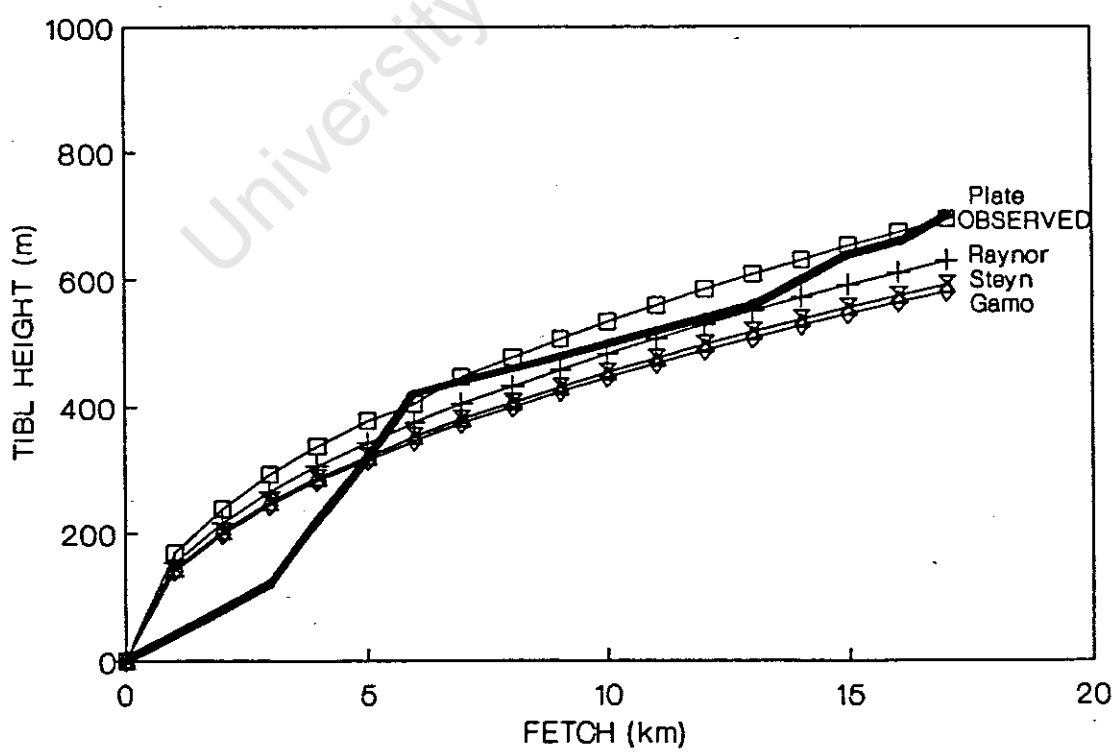


**Figure 12:** Observed (bold line) and predicted TIBL heights from the four selected equations for Run 401.

existed, and some preciseness was therefore lost when reference was made to a selection of parameters. Further complications in determining TIBL height resulted from spatial and temporal variation in the data, for example the transitory nature of eddies and thermals. The dynamic nature of the TIBL thus made definition of its shape somewhat akin to that of a developing cumulus cloud, especially in near-neutral conditions, and hence some form of averaging or approximation of the boundary was unavoidable.

For the present study, TIBL height was defined in a similar way to Gamo *et al* (1982), making use of horizontal transects of potential temperature, but also using vertical wind speed and heat flux transects where necessary. At the point of intersection with the TIBL, the boundary was denoted by increases both in in the value and variation of the parameter, which continued to increase and vary within the TIBL. Figure 12 illustrates the profile of observed TIBL height determined by this method. In it can be seen the relatively low TIBL height near the coast where stable conditions persisted, followed by a region of rapid growth associated with the presence of the thermal upcurrent, and further inland a large region of steadier and more gradual growth.



## TIBL height prediction

Also illustrated in Figure 12 are the TIBL height curves of four predictive equations (Plate, 1971; Raynor *et al*, 1975; Steyn and Oke, 1982; Gamo *et al*, 1983). These equations have been shown to perform relatively accurately under a range of similar conditions (Comrie, 1988c). The equations of TIBL height provided a smoothed profile of the TIBL due to the idealised assumptions that enabled their theoretical or empirical development. As the observed profile of the TIBL was irregular, the predictions were thus a compromise between over or under-estimation at different places along the TIBL boundary. Plate's (1971) equation was the highest

prediction, which overpredicted at all distances, although only minimally after the first 5km. The equations of Raynor *et al* (1975), Steyn and Oke (1982) and Gamo *et al* (1983) all overpredicted initially as well, but slightly underpredicted beyond the 5km mark, in the order given above. This distance coincided with the location of the thermal upcurrent observed in the data. For the 'average' TIBL the equations provided a reasonably good prediction, in this case to within 50m for most of the TIBL boundary, but accuracy was not as high near the coast where the more complex patterns of stability and semi-random turbulent motions occurred.

For the TIBL considered above, it was clear that changes in TIBL height as small as 100m, which occurred continuously throughout the day, might have affected the location of the fumigation zone by several kilometres. This effect would have been most marked over the inland areas where the TIBL gradient was most shallow, and would fortunately not have been as severe nearer the coast where the TIBL was less predictable. Inaccuracies under complex conditions such as those found in coastal areas therefore still leave much room for further examination.

Models of TIBL or mixed layer height are useful not only for purely predictive purposes, but also as a means of quantifying relationships between the wide range of input variables. Knowledge of the sensitivity of input variables under the prevailing meteorological conditions is important in operational surroundings where pollutant releases can be controlled, and where unfavourable dispersion conditions might be avoided by the monitoring of selected critical parameters.



## SUMMARY AND CONCLUSIONS

This study has sought to provide an overall view of the TIBL as a dynamic mesoscale feature of the coastal atmosphere.

This was achieved by means of a case study, making use of both surface and airborne measurements to provide coverage of TIBL growth and decay, structural and turbulent characteristics, and the observation and prediction of TIBL height. This case study of selected TIBL data has shown that:

1) A weak synoptic pressure gradient favoured the development of a localised onshore flow pattern over the study area. Early morning drainage flow off the land ceased 2 to 3 hours after sunrise with the increased surface heating, which promoted an onshore sea breeze component. Wind speeds strengthened until the mid afternoon when temperature contrasts were greatest, and then dropped slowly towards the evening. Vertical wind profiles revealed a surface based layer of uniform speed and direction that corresponded with the TIBL;

2) The diurnal behaviour of the TIBL corresponded well to the above pattern. The TIBL was formed out of convective conditions during the late morning, and its irregular upper boundary gradually became smoother as wind speed and surface heating achieved a steadier balance. Initial TIBL growth was rapid, peaking during the time of maximum heatflux near solar midday. Gradual decreases in height occurred until the late afternoon, when more rapid decay set in. Eddies and irregular pockets of turbulence caused fluctuations of up to 100m in TIBL height, with horizontal scales of up to a few thousand metres;

3) The potential temperature structure of the TIBL comprised a mixed layer of uniform profile that increased in depth with downwind distance, with entrainment activity causing bending of the isotherms at the TIBL boundary. Warmer temperatures within the TIBL reduced relative humidity, allowing the uptake of additional evaporative moisture;

4) The turbulent structure of the TIBL, as revealed by the standard deviations of vertical wind speed and temperature and the mean sensible heat flux, was characterised by strong increases in the values of these parameters within the TIBL. Localised pockets of intense turbulence, such as thermal upcurrents, resulted in strong undulations in the TIBL boundary, particularly in the more complex region of TIBL growth nearer the coast. Large heat fluxes were observed near the ground, with fluctuating positive and negative values occurring throughout the rest of the TIBL;

5) A considerable range of TIBL heights was obtained depending on the parameter or definition used, further complicated by the spatial and temporal variations in the data that resulted from its dynamic and irregular nature. The observed TIBL had a low initial height followed by a



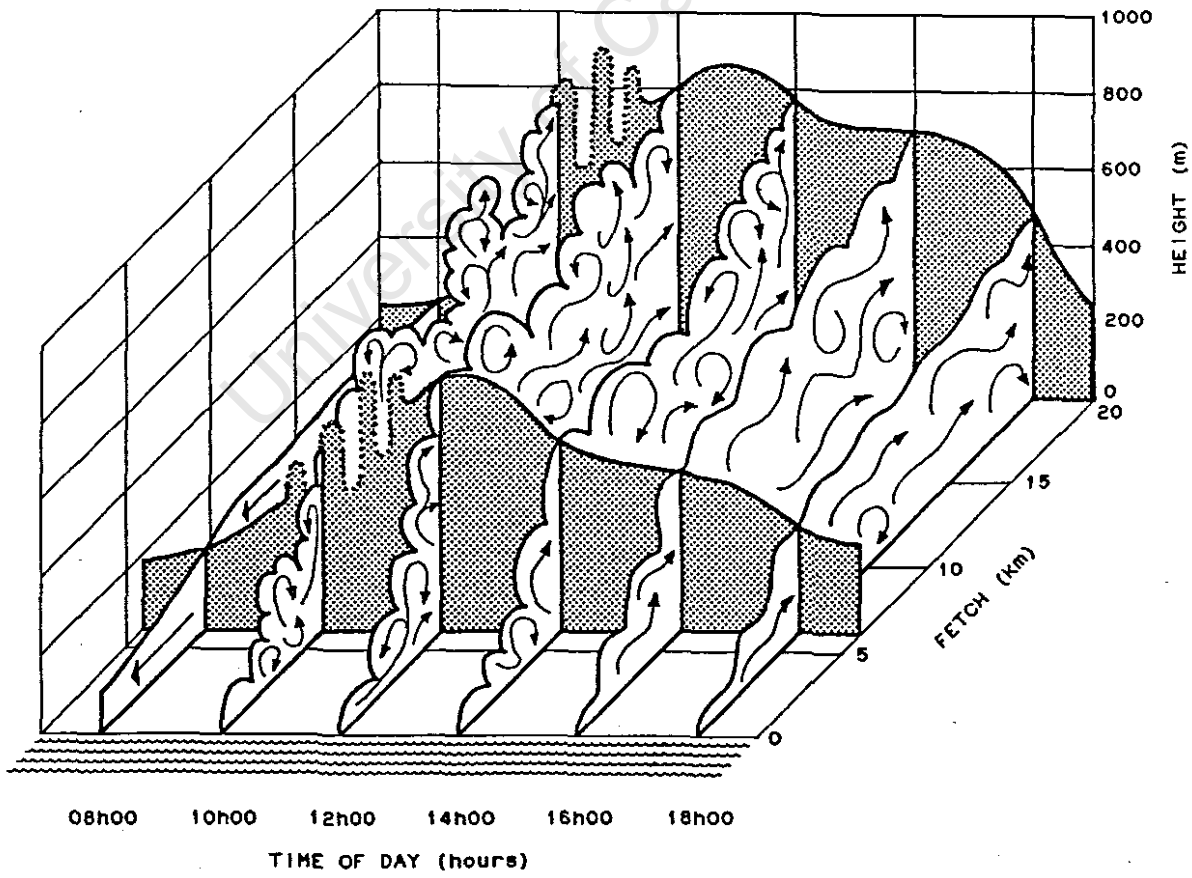


**Figure 13:** Composite schematic diagram of diurnal TIBL evolution and behaviour.

region of rapid growth (complex nearshore region), with a region of steadier and smoother growth further inland. The idealised profiles of TIBL height obtained from predictive equations provided a reasonable approximation of the observed data, especially inland, but did not account for the complex TIBL heights near the shore.

A composite schematic diagram summarising some of the above features of the TIBL and its evolution is illustrated in Figure 13. This particular case of the TIBL from the West Coast of Southern Africa on 1 April 1987 displayed many of the typical characteristics noted in Comrie (1988a; 1988b; 1988c). The relatively uniform shape of the TIBL boundary conveyed by the height prediction formulae was in reality far more complex. Different parameters outlined the constant variety of structure and temporal behaviour that characterised the TIBL as a dynamic and turbulent region of the coastal atmosphere.



## REFERENCES

Collins, G.F., 1971: Predicting sea breeze fumigation from tall stacks at coastal sites. *Nuclear Safety*, 8, 490-499.

Comrie, A.C., 1988a: Meteorological characteristics of thermal internal boundary layers. Chapter 2, unpublished M.Sc thesis, Dept. of Environ. and Geogr. Sci., Univ. of Cape Town.

Comrie, A.C., 1988b: The mesoscale turbulent structure of the thermal internal boundary layer. Chapter 3, unpublished M.Sc thesis, Dept. of Environ. and Geogr. Sci., Univ. of Cape Town.

Comrie, A.C., 1988c: An evaluation of thermal internal boundary layer equations. Chapter 4, unpublished M.Sc thesis, Dept. of Environ. and Geogr. Sci., Univ. of Cape Town.

Echols, W.T. and Wagner, N.K., 1972: Surface roughness and internal boundary layer near a coastline. *J. Appl. Meteorol.*, 11, 658-662.

Elliot, W.P., 1958: The growth of the atmospheric internal boundary layer. *Trans. Amer. Geophys. Union*, 39, 1048-1054.

Gamo, M., Yamamoto, S. and Yokoyama, O., 1982: Airborne measurements of the free convective internal boundary layer during the sea breeze. *J. Meteorol. Soc. Japan*, 60, 1284-1298.

Gamo, M., Yamamoto, S., Yokoyama, O. and Yoshikado, H., 1983: Structure of the free convective internal boundary layer above the coastal area. *J. Meteorol. Soc. Japan*, 61, 110-124.

Hewson, E.W. and Olsson, L.E., 1967: Lake effects on air pollution dispersion. *J. Air Poll. Control Assoc.*, 17, 757-761.

Kerman, B.R., Mickle, R.E., Portelli, R.V., Trivett, N.B. and Misra, P.K., 1982: The Nanticoke shoreline diffusion experiment, June 1978-II: Internal boundary layer structure. *Atmos. Environ.*, 16, 423-437.

Lyons, W.A. and Cole, H.S., 1973: Fumigation and plume trapping on the shores of Lake Michigan during stable onshore flow. *J. Appl. Meteorol.*, 12, 494-510.

Lyons, W.A., Keen, C.S. and Schuh, J.A., 1983: Modeling mesoscale diffusion and transport processes for releases within coastal zones during land/sea breezes. *United States Nuclear Regulatory Commission*, NUREG/CR3542.

Ogawa, Y. and Ohara, T., 1985: The turbulent structure of the internal boundary layer near the shore - Part 1: Case study. *Boundary-Layer Meteorol.*, 31, 369-384.

Ogawa, Y., Ohara, T., Wakamatsu, S., Diosey, P.G. and Uno, I., 1985: Observation of lake breeze penetration and subsequent development of the thermal internal boundary layer for the Nanticoke II shoreline diffusion experiment. *Boundary-Layer Meteorol.*, 32, 207-230.

Peters, L.K., 1975: On the criteria for the occurrence of fumigation inland from a large lake. *Atmos. Environ.*, 9, 809-816.

Plate, E.J., 1971: *Aerodynamic characteristics of atmospheric boundary layers*. United States Atomic Energy Commission, 190pp.

Portelli, R.V., 1982: The Nanticoke shoreline diffusion experiment, June 1978-I: Experimental design and program overview. *Atmos. Environ.*, 16, 413-421.

Prophet, D.T., 1961: Survey of available information pertaining to the transport and diffusion of airborne material over ocean and shoreline complexes. Tech. Report 89, Aerosol Lab., Stanford Univ., 53pp.

Raynor, G.S., Michael, P., Brown, R.M. and SethuRaman, S., 1975: Studies of atmospheric diffusion from a nearshore oceanic site. *J. Appl. Meteorol.*, 14, 1080-1094.

Raynor, G.S., SethuRaman, S. and Brown, R.M., 1979: Formation and characteristics of coastal internal boundary layers during onshore flows. *Boundary-Layer Meteorol.*, 16, 487-514.

Smedman, A-S. and Högström, U., 1983: Turbulent characteristics of a shallow convective internal boundary layer. *Boundary-Layer Meteorol.*, 25, 271-287.

Steyn, D.G. and Oke, T.R., 1982: The depth of the daytime mixed layer at two coastal sites: a model and its validation. *Boundary-Layer Meteorol.*, 24, 161-180.

Van der Hoven, I., 1967: Atmospheric transport and diffusion at coastal sites. *Nuclear Safety*, 8, 490-499.

VenKatram, A., 1977: A model of internal boundary layer development. *Boundary-Layer Meteorol.*, 11, 419-437.

Weisman, B. and Hirt, M.S., 1975: Dispersion governed by the thermal internal boundary layer. Presented at 68th Meeting, Air Poll. Control Assoc., Boston.

CHAPTER 6

# THESIS SUMMARY AND CONCLUSIONS

## SUMMARY AND CONCLUSIONS

This thesis has undertaken an empirical examination of the growth, structure and prediction of the Thermal Internal Boundary Layer (TIBL). The experimental methodology was designed to enable a comprehensive spatial and temporal data coverage. This was achieved using a specially instrumented light aircraft for transect flights over the entire length and height of the TIBL, together with a network of meteorological masts and surface instrumentation, including an acoustic sounder. The resulting data were investigated in terms of general meteorological characteristics, turbulent structure, and an evaluation of the TIBL height equations, while a synthesis of these approaches was provided by a case study. Each of these aspects of the study was reported in a separate chapter (paper). A number of the features identified in these studies have been incorporated into composite schematic diagrams illustrated in Figures 1 and 2. The overall conclusions reached in this thesis may be summarized as follows:

1) Localised onshore flow was promoted by a weak synoptic pressure gradient, frequently with favourable isobaric flow aloft. Thermal and frictional effects associated with the TIBL and the sea breeze component caused the oblique onshore flow to become more normal to the coastline, with significantly higher wind speeds inland, especially under less stable conditions. Large increases in low level turbulence were also found, and wind profiles revealed a surface based layer of relatively uniform speed and direction, with the TIBL interface occurring just above the velocity maximum.

2) The TIBL developed from the initially stable onshore flow as a neutral and slightly unstable layer within the sea breeze component. It grew rapidly from convective conditions in the morning, peaking at midday and decreasing slowly in the afternoon, following the same diurnal growth and decay

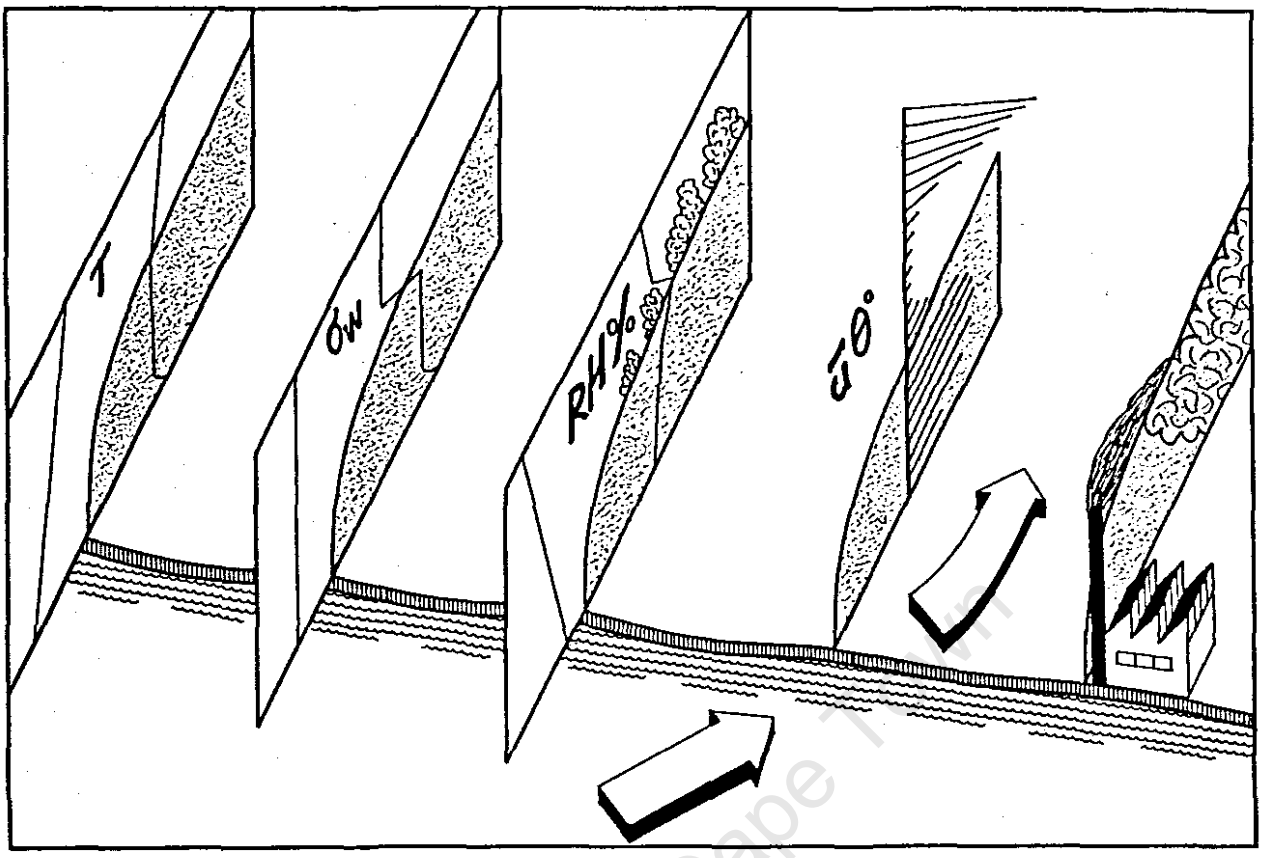


Figure 1: Composite summary schematic of selected meteorological characteristics of the TIBL.



pattern as the surface heating and the development of the onshore flow. TIBL buildup was strongly influenced by the overwater lapse rate and the presence of an initial mixed layer. The initially irregular TIBL boundary became more uniform during the day, as a steady balance between wind speed and surface heating was achieved.

3) Warmer temperatures occurred throughout the mixed layer, allowing slight increases of specific humidity by the uptake of evaporative moisture. Conversely, relative humidity decreased in the TIBL, with maxima of relative humidity associated with the entrainment region and the presence of scattered cloud. Temperature structure also strongly influenced the intensity of turbulence and the degree of entrainment into the TIBL aloft.

4) The patterns of the standard deviations of vertical velocity and temperature ($\sigma_w$ and $\sigma_T$) displayed strong increases in the TIBL, decreasing somewhat in the entrainment region as a result of intermittent turbulence. A turbulent similarity analysis of standard deviations for the TIBL and the Convective Boundary Layer (CBL) revealed a similar magnitude of data, but the increase in turbulence associated with the top of the CBL was not generally present, and instead a smooth decrease of turbulence with non-dimensional height was found in the TIBL.

5) Values of sensible heat flux ($\overline{w'\theta'}$) within the TIBL varied greatly, but were strongly positive in the surface layer, moderate to slightly negative within the mixed layer, and negligible outside the TIBL. Strong undulations in the structure of the TIBL were caused by transitory eddies and thermal upcurrents, which were characterised by large fluctuations and increased values of sensible heat flux.



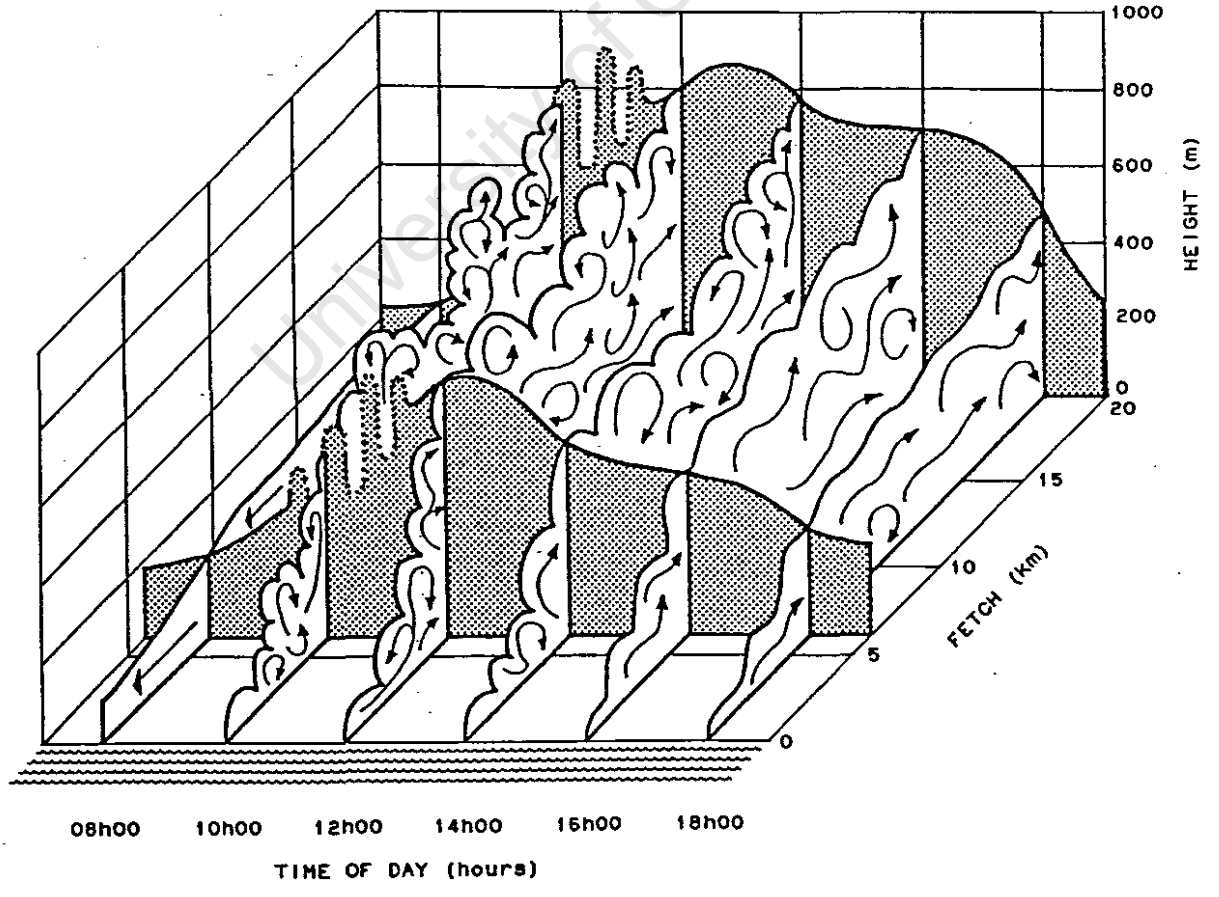


**Figure 2:** Composite schematic diagram of diurnal TIBL evolution and behaviour.

6) The theoretically based TIBL height equations of Plate (1971), Steyn and Oke (1982) and Gamo *et al* (1983) displayed the best overall performance, and were collectively ranked in highest position. They possessed a high degree of accuracy, with low mean and model-oriented errors, and biases close to zero. Also well ranked was the empirical equation of Raynor *et al* (1975), which although possessing a high potential accuracy, had a greater variability of actual prediction. In general, the TIBL height predictions slightly underestimated both the gradient and the height of the TIBL.

7) Observations of TIBL structure and height highlighted a nearshore region of complex and unpredictable TIBL formation, further complicated by vertical variations in stability. These continual dynamic adjustments to TIBL growth occurred within the first few kilometres of the shore, frequently comprising an initially slow and later rapid increase in height, followed by a region of more regular TIBL formation where relatively accurate observation and prediction of TIBL height was possible.

The overall conclusions of this thesis have confirmed many of the observations and findings noted in other studies, while producing new insights into certain aspects of mesoscale TIBL development. In particular, temporal analyses, combined with cross sections of the meteorological and turbulent properties of the TIBL, have elucidated aspects of the complex shape, structure and temporal behaviour of the TIBL. It has also been shown that the reliable prediction of TIBL height can be performed to some degree of accuracy. Evaluation of the impact of the TIBL on fumigation conditions and pollutant dispersion in shoreline environments will thus be benefitted by the additional understanding of the growth, structure and prediction of the TIBL provided by this thesis.

# REFERENCES

André, J.C., 1983: Planetary boundary layer parameterization and turbulence closure. In Lilly, D.K. and Gal-Chen, T. (eds.): Mesoscale meteorology - theories, observations and models, D. Reidel, 651-669.

Anthes, R.A., 1978: The height of the PBL and the production of circulation in a sea breeze model. *J. Atmos. Sci.*, 35, 1231-1239.

Ball, F.K., 1960: Control of inversion height by surface heating. Quart. *J. Roy. Meteorol. Soc.*, 86, 483-494.

Beran, D.W., Hooke, W.H. and Clifford, S.F., 1973: Acoustic echo sounding techniques and their application to gravity wave, turbulence and stability studies. *Boundary-Layer Meteorol.*, 4, 133-167.

Betts, A.K., 1973: Non precipitating cumulus convection and its parameterization. Quart. *J. Roy. Meteorol. Soc.*, 99, 170-196.

Bierly, E.W. and Hewson E.W., 1963: Atmospheric diffusion studies near a lakeshore. *J. Appl. Meteorol.*, 1, 390-396.

Bornstein, R.D., 1968: Observations of the urban heat island effect in New York City. *J. Appl. Meteorol.*, 7, 575-582.

Carson, D.J., 1973: The development of a dry inversion capped convectively unstable boundary layer. *Quart. J. Roy. Meteorol. Soc.*, 99, 450-467.

Caughey, S.J. and Palmer, S.G., 1979: Some aspects of turbulence structure through the depth of the convective boundary layer. *Quart. J. Roy. Meteorol. Soc.*, 105, 811-827.

Collins, G.F., 1971: Predicting sea breeze fumigation from tall stacks at coastal sites. *Nuclear Safety*, 8, 490-499.

Comrie, A.C., 1986: Thermal internal boundary layers in the South Western Cape - a report on the first field investigation. Unpublished Internal Report, Dept. of Environ. and Geog. Sci., Univ. of Cape Town, 15pp.

Comrie, A.C., 1988a: Meteorological characteristics of thermal internal boundary layers. Chapter 2, unpublished M.Sc thesis, Dept. of Environ. and Geogr. Sci., Univ. of Cape Town.

Comrie, A.C., 1988b: The mesoscale turbulent structure of the thermal internal boundary layer. Chapter 3, unpublished M.Sc thesis, Dept. of Environ. and Geogr. Sci., Univ. of Cape Town.

Comrie, A.C., 1988c: An evaluation of thermal internal boundary layer equations. Chapter 4, unpublished M.Sc thesis, Dept. of Environ. and Geogr. Sci., Univ. of Cape Town.

Deardorff, J.W., 1972: Numerical investigation of neutral and unstable planetary boundary layers. *J. Atmos. Sci.*, 29, 91-115.

Deardorff, J.W., Willis, G.E. and Lilly, D.K., 1969: Laboratory investigation of non-steady penetrative convection. *J. Fluid Mech.*, 35, 7-31.

Di Vecchio, R.A., Smith, D.B. and Martin, G., 1976: Performance of a recent formulation for rate of growth of boundary layers near shorelines. Presented at Conference on Coastal Meteorology, *Amer. Meteor. Soc.*, Virginia Beach.

Dobosy, R., 1979: Dispersion of atmospheric pollutants in flow over the shoreline of a large body of water. *J. Appl. Meteorol.*, 18, 117-132.

Dooley, J., 1976: Fumigation of power plant plumes in the lakeshore environment. The University of Wisconsin - Milwaukee, Wisconsin.

Echols, W.T. and Wagner, N.K., 1972: Surface roughness and internal boundary layer near a coastline. *J. Appl. Meteorol.*, 11, 658-662.

Elliot, W.P., 1958: The growth of the atmospheric internal boundary layer. *Trans. Amer. Geophys. Union*, 39, 1048-1054.

Fiedler, F. and Panofsky, H.A., 1972: The geostrophic drag coefficient and the 'effective' roughness length. *Quart. J. Roy. Meteorol. Soc.*, 98, 213-220.

Fox, D.G., 1981: Judging air quality model performance - a summary of the AMS workshop on dispersion model performance. *Bull. Amer. Meteorol. Soc.*, 62, 599-609.

Gamo, M., Yamamoto, S. and Yokoyama, O., 1982: Airborne measurements of the free convective internal boundary layer during the sea breeze. *J. Meteorol. Soc. Japan*, 60, 1284-1298.

Gamo, M., Yamamoto, S., Yokoyama, O. and Yoshikado, H., 1983: Structure of the free convective internal boundary layer above the coastal area. *J. Meteorol. Soc. Japan*, 61, 110-124.

Garratt, J.R., 1987: The stably stratified internal boundary layer for steady and diurnally varying offshore flow. *Boundary-Layer Meteorol.*, 38, 369-394.

Hanna, S.R., 1983: A simplified scoring system for air quality models. Paper 8336.6 presented at Annual Air Poll. Control Assoc. Meeting, Atlanta, Georgia.

Hewson, E.W. and Olsson, L.E., 1967: Lake effects on air pollution dispersion. *J. Air Poll. Control Assoc.*, 17, 757-761.

Hsu, S.A., 1983: On the growth of a thermally modified boundary layer by advection of warm air over a cooler sea. *J. Geophys. Res.*, 88, 771-774.

Hsu, S.A., 1986: A note on estimating the height of the convective internal boundary layer near the shore. *Boundary-Layer Meteorol.*, 35, 311-316.

Jury, M.R. and Mulholland, M., 1986: Coastal dispersion climatology near the SW tip of Africa - a system for evaluation and prediction. Dept. of Oceanography, Univ. of Cape Town, 23pp.

Kaimal, J.C., Wyngaard, J.C., Haugen, D.A., Coté, O.R., Izumi, Y., Caughey, S.J. and Readings, C.J., 1976: Turbulence structure in the convective boundary layer. *J. Atmos. Sci.*, 33, 2152-2169.

Keen, C.S., 1979: Air pollution survey of Greater Cape Town, Volume 4. Report for the Cape Town City Council, 146pp.

Keen, C.S., 1984: Sea breezes in the complex terrain of the Cape Peninsula. Postprints from the Third Conf. on Meteorology of the Coastal Zone, Miami, Florida, *Amer. Meteorol. Soc.*, Boston, 129-134.

Kerman, B. R., 1982: A similarity model of shoreline fumigation. *Atmos. Environ.*, 16, 467-478.

Kerman, B.R., Mickle, R.E., Portelli, R.V., Trivett, N.B., and Misra, P.K., 1982: The Nanticoke shoreline diffusion experiment, June 1978-II: Internal boundary layer structure. *Atmos. Environ.*, 16, 423-437.

Knox, N.E. and Lyons, W.A., 1975: The thermal internal boundary layer in a shoreline environment during summer fumigation episodes. Presented at the First Conf. on Regional and Mesoscale Analysis and Predictions, Las Vegas, Nevada, *Amer. Meteorol. Soc.*, Boston.

Lenschow, D.H., 1970: Airplane measurements of planetary boundary layer structure. *J. Appl. Meteorol.*, 9, 874-884.

Lenschow, D.H., 1976: Estimating updraft velocity from airplane response. *Mon. Wea. Rev.*, 104, 618-627.

Lilly, D.K., 1968: Models of cloud topped mixed layers under a strong inversion. *Quart. J. Roy. Meteorol. Soc.*, 94, 292-309.

Lumley, J.L. and Panofsky, H.A., 1964: The structure of atmospheric turbulence. J. Wiley and Sons, New York.

Lyons, W.A. and Olsson, L.E., 1972: Mesoscale air pollution transport in the Chicago lake breeze. *J. Air Poll. Control Assoc.*, 22, 876-881.

Lyons, W.A. and Cole, H.S., 1973: Fumigation and plume trapping on the shores of Lake Michigan during stable onshore flow. *J. Appl. Meteorol.*, 12, 494-510.

Lyons, W.A., 1975: Turbulent diffusion and pollutant transport in shoreline environments. Lectures on air pollution and environmental impact analysis, Workshop on Meteorology and Environmental Assessment, *Amer. Meteorol. Soc.*, Boston, 136-208.

Lyons, W.A., Keen, C.S. and Schuh, J.A., 1983: Modeling mesoscale diffusion and transport processes for releases within coastal zones during land/sea breezes. *United States Nuclear Regulatory Commission*, NUREG/CR3542.

Meroney, R.W., Cermak, C.E. and Yang, B.T., 1975: Modelling of atmospheric transport and fumigation at shoreline sites. *Boundary-Layer Meteorol.*, 9, 69-90.

Misra, P.K. and Onlock, S, 1982: Modelling continuous fumigation of the Nanticoke generating station plume. *Atmos. Environ.*, 16, 479-489.

Misra, P.K., 1980: Dispersion from tall stacks into a shoreline environment. *Atmos. Environ.*, 14, 396-400.

Moroz, W.J., 1967: A lake breeze on the eastern shore of Lake Michigan - observations and model. *J. Atmos. Sci.*, 24, 337-355.

Nicholls, S. and Readings, C.J., 1979: Aircraft observations of the structure of the lower boundary layer over the sea. Quart. *J. Roy. Meteorol. Soc.*, 105, 785-802.

Ogawa, Y. and Ohara, T., 1985: The turbulent structure of the internal boundary layer near the shore - Part 1: Case study. *Boundary-Layer Meteorol.*, 31, 369-384.

Ogawa, Y., Ohara, T., Wakamatsu, S., Diosey, P.G. and Uno, I., 1985: Observation of lake breeze penetration and subsequent development of the thermal internal boundary layer for the Nanticoke II shoreline diffusion experiment. *Boundary-Layer Meteorol.*, 32, 207-230.

Ogura, Y., 1950: On the heat transfer in the lower layer of the atmosphere. Geophys. Notes, Geophys. Inst., Tokyo Univ., 3, 27.

Ohara, T. and Ogawa, Y., 1985: The turbulent structure of the internal boundary layer - Part 2: Similarity and energy budget analysis. *Boundary-Layer Meteorol.*, 32, 39-56.

Panofsky, H.A. and Brier, G.W., 1968: Some applications of statistics to meteorology. Pennsylvania State University, 224pp.

Peters, L.K., 1975: On the criteria for the occurrence of fumigation inland from a large lake. *Atmos. Environ.*, 9, 809-816.

Peterson, E.W., 1969: Modification of mean flow and turbulent energy by a change in surface roughness under conditions of neutral stability. *Quart. J. Roy. Meteorol. Soc.*, 95, 561-575.

Pielke, R.A., 1974: A three-dimensional numerical model of the sea breeze over south Florida. *Mon. Wea. Rev.*, 102, 115-139.

Plate, E.J., 1971: Aerodynamic characteristics of atmospheric boundary layers. United States Atomic Energy Commission, 190pp.

Portelli, R.V., 1982: The Nanticoke shoreline diffusion experiment, June 1978-I: Experimental design and program overview. *Atmos. Environ.*, 16, 413-421.

Prophet, D.T., 1961: Survey of available information pertaining to the transport and diffusion of airborne material over ocean and shoreline complexes. Tech. Report 89, Aerosol Lab., Stanford Univ., 53pp.

Rao, K.S., Wyngaard, J.C. and Cotè, O.R., 1974: The structure of a two-dimensional internal boundary layer over a sudden change of surface roughness. *J. Atmos. Sci.*, 31, 738-746.

Raynor, G.S., Michael, P., Brown, R.M. and SethuRaman, S., 1975: Studies of atmospheric diffusion from a nearshore oceanic site. *J. Appl. Meteorol.*, 14, 1080-1094.

Raynor, G.S., SethuRaman, S. and Brown, R.M., 1979: Formation and characteristics of coastal internal boundary layers during onshore flows. *Boundary-Layer Meteorol.*, 16, 487-514.

Schuh, J.A., 1975: A mesoscale model of continuous shoreline fumigation and lid-trapping in a Wisconsin shoreline environment. Special Report no. 27, Center for Great Lakes Studies, Univ. of Wisconsin-Milwaukee, 107pp.

SethuRaman, S., (ed.), 1984: A Summary of the Brookhaven *Workshop on Coastal Atmospheric Transport Processes*. Postprints from the Third Conference on Meteorology of the Coastal Zone, Miami, Florida, *Amer. Meteorol. Soc.*, Boston, 121-128.

SethuRaman, S., Brown, R.M., Raynor, G.S. and Tuthill, W.A., 1979: Calibration and use of a sailplane variometer to measure vertical velocity fluctuations. *Boundary-Layer Meteorol.*, 16, 99-105.

Shir, C.C., 1972: A numerical computation of air flow over a sudden change of surface roughness. *J. Atmos. Sci.*, 29, 304-310.

Smedman, A-S. and Högström, U., 1983: Turbulent *characteristics of a shallow convective internal* boundary layer. *Boundary-Layer Meteorol.*, 25, 271-287.

Steyn, D.G. and Oke, T.R., 1982: The depth of the daytime mixed layer at two coastal sites: a model and its validation. *Boundary-Layer Meteorol.*, 24, 161-180.

Stull, R.B., 1976: Mixed-layer depth model based on turbulence energetics. *J. Atmos. Sci.*, 33, 1268-1278.

Stunder, M. and SethuRaman, S., 1985: A comparative *evaluation of the coastal internal boundary-layer* height equations. *Boundary-Layer Meteorol.*, 32, 177-204.

Sun, W.Y. and Ogura, Y., 1980: Modeling the *evolution of the* convective planetary boundary layer. *J. Atmos. Sci.*, 37, 1558-1572.

Taylor, P.A., 1970: A model of airflow above changes in surface heat flux, temperature and roughness for neutral and unstable conditions. *Boundary-Layer Meteorol.*, 1, 18-39.

Tennekes, H., 1973: A model for the dynamics of the inversion above a convective boundary layer. *J. Atmos. Sci.*, 30, 558-567.

Tennekes, H., 1974: The atmospheric boundary layer. *Physics Today*, 27, 52-63.

Tennekes, H. and Driedonks, A.G.M., 1981: Basic entrainment equations for the atmospheric boundary layer. *Boundary-Layer Meteorol.*, 20, 515-531.

Van der Hoven, I., 1967: Atmospheric transport and diffusion at coastal sites. *Nuclear Safety*, 8, 490-499.

Van Dop, H., Steenkist, R. and Nieuwstadt, F.T.M., 1979: Revised estimates for continuous shoreline fumigation. *J. Appl. Meteorol.*, 18, 133-137.

Venkatram, A., 1977: A model of internal boundary layer development. *Boundary-Layer Meteorol.*, 11, 419-437.

Venkatram, A., 1986: An examination of methods to estimate the height of the coastal internal boundary layer. *Boundary-Layer Meteorol.*, 36, 149-156.

Weisman, B. and Hirt, M.S., 1975: *Dispersion governed by the* thermal internal boundary layer. Presented at 68th Meeting, Air Poll. Control Assoc., Boston.

Weisman, B., 1976: On the criteria for the occurrence of fumigation inland from a large lake - a reply. *Atmos. Environ.*, 12, 172-173.

Willmott, C. J., 1982: Some comments on the evaluation of model performance. *Bull. Amer. Meteorol. Soc.*, 63, 1309-1313.

Wyngaard, J.C., 1983: Lectures on the planetary boundary layer. In Lilly, D.K. and Gal-Chen, T. (eds.): Mesoscale meteorology - theories, observations and models, D. Reidel, 603-650.

Wyngaard, J.C., Coté, O.R. and Izumi, Y., 1971: Local free convection, similarity, and the budgets of shear stress and heat flux. *J. Atmos. Sci.*, 28, 1171-1182.

## APPENDIX 2

### 2.1: Abbreviations and symbols

| | | |
|---|---|---|
| $\sigma_u$ | $m.s^{-1}$ | Standard deviation of horizontal wind velocity |
| $\sigma_w$ | $m.s^{-1}$ | Standard deviation of vertical wind velocity |
| $\sigma_\theta$ | $^o$ | Standard deviation of wind direction |
| $\sigma_T$ | $^o$C | Standard deviation of temperature |
| $T$ | $^o$C | Dry bulb temperature |
| $T_w$ | $^o$C | Wet bulb temperature |

### 2.2: Date and Run number for the eight test days

| Date | Run Number |
|---|---|
| 18 March 1987 | 318 |
| 19 March 1987 | 319 |
| 27 March 1987 | 327 |
| 30 March 1987 | 330 |
| 31 March 1987 | 331 |
| 1 April 1987 | 401 |
| 13 April 1987 | 413 |
| 21 April 1987 | 421 |

# APPENDIX 3

## 3.1: Abbreviations and symbols

| | | |
|---|---|---|
| $L$ | m | Monin-Obukhov length |
| $Q_0$ | $m.s^{-1}.K^{-1}$ | Surface sensible heat flux |
| $S$ | $W.m^{-2}$ | Solar radiation |
| $T$ | K | Temperature |
| $T'$ | K | Instantaneous temperature fluctuation |
| $T_*$ | K | Surface scaling temperature |
| $\sigma_T$ | K | Standard deviation of temperature |
| $u$ | $m.s^{-1}$ | Horizontal wind speed |
| $u'$ | $m.s^{-1}$ | Instantaneous wind speed fluctuation |
| $u_*$ | $m.s^{-1}$ | Surface scaling velocity |
| $w$ | $m.s^{-1}$ | Vertical wind velocity |
| $w'$ | $m.s^{-1}$ | Instantaneous vertical velocity fluctuation |
| $w_*$ | $m.s^{-1}$ | Mixed layer scaling velocity |
| $\overline{u'w'}$ | $m^2.s^{-2}$ | Momentum flux |
| $z$ | m | Height above ground |
| $z_i$ | m | Boundary layer height |
| $\theta_*$ | K | Mixed layer scaling temperature |
| $\overline{w'\theta'}$ | $m.s^{-1}.K^{-1}$ | Sensible heat flux |

## APPENDIX 4

4.1: Input values of TIBL height equation parameters for the eight TIBLs evaluated.

| Input Parameter | | Run 318 | 319 | 327 | 330 | 331 | 401 | 413 | 421 |
|---|---|---|---|---|---|---|---|---|---|
| $H_Q$ | ($W.m^{-2}$) | 355 | 369 | 335 | 363 | 324 | 332 | 343 | 335 |
| #* | ($W.m^{-2}$) | 236 | 263 | 205 | 270 | 216 | 270 | 270 | 263 |
| $\beta$ | ($K.100m^{-1}$) | 1.33 | 0.51 | 0.48 | 0.50 | 0.58 | 0.56 | 0.77 | 0.47 |
| $\Delta\Theta$ | (K) | 2.3 | 1.4 | 7.4 | 4.5 | 1.6 | 0.6 | 8.7 | 3.2 |
| $\bar{u}$ | ($m.s^{-1}$) | 8.2 | 8.6 | 7.6 | 6.8 | 8.1 | 6.9 | 10.4 | 5.4 |
| $\bar{u}_{10}$ | ($m.s^{-1}$) | 6.2 | 6.8 | 5.1 | 5.1 | 6.1 | 5.2 | 7.8 | 4.2 |
| $T_L$ | (K) | 35.1 | 36.8 | 39.9 | 35.4 | 33.6 | 37.9 | 36.0 | 29.7 |
| $T_W$ | (K) | 12.2 | 13.4 | 14.5 | 13.9 | 14.5 | 15.8 | 11.6 | 13.4 |
| $h_Q$ | (m) | 860 | 160 | 140 | 200 | 0 | 0 | 240 | 0 |

* $\# = \Psi.H_C.\sin(\pi t_S/D_L)$
Lyons *et al* (1983) heat flux parameterisation

4.2: Computational formulae for the statistical summary and difference measures following the form of Fox (1981) and Willmott (1982).

$$MAE = n^{-1} \sum_{i=1}^{n} |P_i - O_i| \quad (11)$$

$$MBE = n^{-1} \sum_{i=1}^{n} (P_i - O_i) \quad (12)$$

$$RMSE = [n^{-1} \sum_{i=1}^{n} (P_i - O_i)^2]^{0.5} \quad (13)$$

$$RMSE_s = [n^{-1} \sum_{i=1}^{n} (\hat{P}_i - O_i)^2]^{0.5} \quad (14)$$

$$RMSE_u = [n^{-1} \sum_{i=1}^{n} (P_i - \hat{P}_i)^2]^{0.5} \quad (15)$$

$$d = 1 - [\sum_{i=1}^{n} (P_i - O_i)^2 / \sum_{i=1}^{n} (|P'_i| + |O'_i|)^2] \quad (16)$$

where $n$ = number of cases, $\overline{P}$ = predicted and $\overline{O}$ = observed, and where $0 \leq d \leq 1$, $P'_i = P_i - \overline{O}$ and $O'_i = O_i - \overline{O}$.

4.3: Statistical summary and difference measures for the eight TIBL equations for 143 cases (means, standard deviations and errors in metres).

| | VdHoven | Raynor | Venkatram | Plate | Weisman | Gamo | Lyons | Steyn |
|---|---|---|---|---|---|---|---|---|
| $\overline{O}$ | 622 | 622 | 622 | 622 | 622 | 622 | 622 | 622 |
| $\overline{P}$ | 398 | 600 | 745 | 669 | 532 | 593 | 484 | 600 |
| $\sigma_O$ | 281 | 281 | 281 | 281 | 281 | 281 | 281 | 281 |
| $\sigma_P$ | 265 | 254 | 271 | 258 | 247 | 250 | 243 | 251 |
| $a$ | -37 | 132 | 225 | 150 | 56 | 97 | 21 | 102 |
| $b$ | 0.70 | 0.75 | 0.84 | 0.83 | 0.77 | 0.80 | 0.74 | 0.80 |
| MAE | 231 | 128 | 151 | 101 | 133 | 113 | 155 | 111 |
| MBE | -224 | -21 | 123 | 47 | -89 | -29 | -138 | -22 |
| RMSE | 299 | 157 | 188 | 125 | 164 | 129 | 199 | 126 |
| $RMSE_S$ | 240 | 73 | 132 | 66 | 111 | 64 | 156 | 60 |
| $RMSE_U$ | 178 | 139 | 135 | 106 | 120 | 112 | 124 | 111 |
| prop. | 0.64 | 0.21 | 0.49 | 0.28 | 0.46 | 0.25 | 0.61 | 0.23 |
| $r^2$ | 0.55 | 0.70 | 0.75 | 0.83 | 0.76 | 0.80 | 0.74 | 0.80 |
| $d$ | 0.76 | 0.91 | 0.89 | 0.94 | 0.90 | 0.94 | 0.87 | 0.94 |

## 4.4: Abbreviations and symbols

| | |
|---|---|
| $\bar{O}$ | Mean observed TIBL height |
| $\bar{P}$ | Mean predicted TIBL height |
| $\sigma_O$ | Standard deviation of observed TIBL heights |
| $\sigma_P$ | Standard deviation of predicted TIBL heights |
| $a$ | y - intercept of least squares regression |
| $b$ | x coefficient of least squares regression |
| MAE | Mean absolute error |
| MBE | Mean bias error |
| RMSE | Root mean square error |
| $MSE_S$ | Systematic error |
| $MSE_U$ | Unsystematic error |
| prop. | Proportion of systematic error |
| $r^2$ | Correlation coefficient |
| $d$ | Index of accuracy |

# APPENDIX 5

## 5.1: Abbreviations and symbols

| | | |
|---|---|---|
| $\sigma_w$ | (m) | Standard deviation of vertical velocity |
| $\sigma_T$ | (K) | Standard deviation of temperature |
| $\overline{w'\theta'}$ | ($m.s^{-1}.K^{-1}$) | Mean sensible heat flux |